INFORMATION TO USERS

This reproduction was made from a copy of a document sent to us for microfilming. While the most advanced technology has been used to photograph and reproduce this document, the quality of the reproduction is heavily dependent upon the quality of the material submitted.

The following explanation of techniques is provided to help clarify markings or notations which may appear on this reproduction.

1. The sign or "target" for pages apparently lacking from the document photographed is "Missing Page(s)". If it was possible to obtain the missing page(s) or section, they are spliced into the film along with adjacent pages. This may have necessitated cutting through an image and duplicating adjacent pages to assure complete continuity.

2. When an image on the film is obliterated with a round black mark, it is an indication of either blurred copy because of movement during exposure, duplicate copy, or copyrighted materials that should not have been filmed. For blurred pages, a good image of the page can be found in the adjacent frame. If copyrighted materials were deleted, a target note will appear listing the pages in the adjacent frame.

3. When a map, drawing or chart, etc., is part of the material being photographed, a definite method of "sectioning" the material has been followed. It is customary to begin filming at the upper left hand corner of a large sheet and to continue from left to right in equal sections with small overlaps. If necessary, sectioning is continued again—beginning below the first row and continuing on until complete.

4. For illustrations that cannot be satisfactorily reproduced by xerographic means, photographic prints can be purchased at additional cost and inserted into your xerographic copy. These prints are available upon request from the Dissertations Customer Services Department.

5. Some pages in any document may have indistinct print. In all cases the best available copy has been filmed.

University Microfilms International
300 N. Zeeb Road
Ann Arbor, MI 48106

Order Number 1332312

Design of a digital tracking control system for optical disk drive applications

Kadlec, Ronald James, M.S.

The University of Arizona, 1987

U·M·I

300 N. Zeeb Rd.
Ann Arbor, MI 48106

PLEASE NOTE:

In all cases this material has been filmed in the best possible way from the available copy. Problems encountered with this document have been identified here with a check mark ✓.

1. Glossy photographs or pages _____
2. Colored illustrations, paper or print _____
3. Photographs with dark background _____
4. Illustrations are poor copy _____
5. Pages with black marks, not original copy _____
6. Print shows through as there is text on both sides of page _____
7. Indistinct, broken or small print on several pages ✓
8. Print exceeds margin requirements _____
9. Tightly bound copy with print lost in spine _____
10. Computer printout pages with indistinct print _____
11. Page(s) _____ lacking when material received, and not available from school or author.
12. Page(s) _____ seem to be missing in numbering only as text follows.
13. Two pages numbered _____. Text follows.
14. Curling and wrinkled pages _____
15. Dissertation contains pages with print at a slant, filmed as received _____
16. Other _____

_____

_____

DESIGN OF A DIGITAL TRACKING CONTROL SYSTEM FOR OPTICAL DISK DRIVE APPLICATIONS

by

Ronald James Kadlec

A Thesis Submitted to the Faculty of the

DEPARTMENT OF ELECTRICAL AND COMPUTER ENGINEERING

In Partial Fulfillment of the Requirements
For the Degree of

MASTER OF SCIENCE
WITH A MAJOR IN ELECTRICAL ENGINEERING

In the Graduate College

THE UNIVERSITY OF ARIZONA

1 9 8 7

STATEMENT BY AUTHOR

This thesis has been submitted in partial fulfillment of requirements for an advanced degree at the University of Arizona and is deposited in the Departmental Library to be made available to borrowers under rules of the Library.

Brief quotations from this report are allowable without special permission, provided that accurate acknowledgment of source is made. Requests for permission for extended quotation from or reproduction of this manuscript in whole or in part may be granted by the head of the major department or the Dean of the Graduate College when in his or her judgment the proposed use of the material is in the interest of scholarship. In all other instances, however, permission must be obtained from the author.

SIGNED: Ronald James Kadlec

APPROVAL BY THESIS DIRECTOR

This thesis has been approved on the date shown below:

Dr. M. K. SUNDARESHAN
Professor of Electrical
and Computer Engineering

11/24/87
Date

TABLE OF CONTENTS

		Page
	LIST OF ILLUSTRATIONS	v
	LIST OF TABLES	vii
	ABSTRACT	viii
1.	INTRODUCTION	1
	Optical Disk Drives and Controls	1
	Problem Description	5
	Dynamic Simulation Language Description	10
	Outline of the Thesis	10
2.	DEVELOPMENT OF THE DIGITAL SYSTEM	13
	Continuous System Model Development	13
	Mechanical Analysis	13
	Power Amplifier	23
	Electronic Compensation	27
	Mapping to the Z Domain	31
	DSL Frequency Domain Program	33
	DSL Program Input	35
	DSL Program Algorithm	35
	Program Output	36
3.	MODEL VALIDATION	57
	Technique	57
	HP3562A Dynamic System Analyzer	57
	DSL - HP3562A Comparisons	58
4.	CONTROLLER DEVELOPMENT AND PERFORMANCE ANALYSIS	71
	DSL Time Domain Program Structure	71
	Initial Segment	71
	Derivative Segment	72
	Sample Segment	72
	Dynamic Segment	73
	Terminal Segment	73
	Quantization Model	73
	Computation Delay Model	75
	Time Domain Simulation Output	83

TABLE OF CONTENTS--Continued

Page

45 Degree Phase Margin System - F_s=10 KHZ 84
45 Degree Phase Margin System - F_s=15 KHZ 84
45 Degree Phase Margin System - F_s=30 KHZ 86
10 Degree Phase Margin System - F_s=30 KHZ 87
10 Degree Phase Margin System - F_s=60 KHZ 87

5. CONCLUSIONS 105

Contributions of this Thesis 105
Suggestions for Further Studies 107

APPENDIX A: DSL FREQUENCY DOMAIN PROGRAM FOR THE FINE ACTUATOR 108

APPENDIX B: DSL FREQUENCY DOMAIN PROGRAM FOR THE COARSE ACTUATOR 113

APPENDIX C: DSL TIME DOMAIN PROGRAM 119

LIST OF REFERENCES 130

LIST OF ILLUSTRATIONS

Figure		Page
1.	Dual Actuator Mechanical System	2
2.	Analog Servo Block Diagram	7
3.	Digital Servo Block Diagram	9
4.	Dual Actuator Force Diagram	14
5.	Fine Actuator Free Body Diagram	16
6.	Coarse Actuator Free Body Diagram	19
7.	Power Amplifier Block Diagram	24
8.	Power Amplifier Schematic	26
9.	Bode Plot of the Fine Actuator and Sensor	40
10.	Bode Plot of the Fine Actuator Servo Compensation for 45 Degree Phase Margin.	41
11.	Bode Plot of the Fine Actuator Servo Open Loop Transfer Function (45 Degree Phase Margin)	42
12.	Bode Plot of the Fine Actuator Servo Closed Loop Transfer Function (45 Degree Phase Margin)	43
13.	Bode Plot of the Fine Actuator Servo Compensation for 10 Degree Phase Margin	44
14.	Bode Plot of the Fine Actuator Servo Open Loop Transfer Function (10 Degree Phase Margin)	45
15.	Bode Plot of the Fine Actuator Servo Closed Loop Transfer Function (10 Degree Phase Margin)	46
16.	Bode Plot of the Coarse Actuator and Sensor	47
17.	Bode Plot of the Coarse Actuator Servo Compensation for 45 Degree Phase Margin	48
18.	Bode Plot of the Coarse Actuator Servo Open Loop Transfer Function (45 Degree Phase Margin)	49
19.	Bode Plot of the Coarse Actuator Servo Closed Loop Transfer Function (45 Degree Phase Margin)	50
20.	Bode Plot of the Coarse Actuator Servo Compensation for 10 Degree Phase Margin	51
21.	Bode Plot of the Coarse Actuator Servo Open Loop Transfer Function (10 Degree Phase Margin)	52
22.	Bode Plot of the Coarse Actuator Servo Closed Loop Transfer Function (10 Degree Phase Margin)	53
23.	Bode Plot of the Fine Actuator and Sensor	61
24.	Bode Plot of the Fine Actuator Servo Compensation for 45 Degree Phase Margin	62
25.	Bode Plot of the Fine Actuator Servo Open Loop Transfer Function (45 Degree Phase Margin)	63

LIST OF ILLUSTRATIONS--Continued

Figure Page

26. Bode Plot of the Fine Actuator Servo Compensation for 10 Degree Phase Margin 64
27. Bode Plot of the Fine Actuator Servo Open Loop Transfer Function (10 Degree Phase Margin) 65
28. Bode Plot of the Coarse Actuator and Sensor 66
29. Bode Plot of the Coarse Actuator Servo Compensation for 45 Degree Phase Margin 67
30. Bode Plot of the Coarse Actuator Servo Open Loop Transfer Function (45 Degree Phase Margin) 68
31. Bode Plot of the Coarse Actuator Servo Compensation for 10 Degree Phase Margin 69
32. Bode Plot of the Coarse Actuator Servo Open Loop Transfer Function (10 Degree Phase Margin) 70
33. Analog Compensator I/O for the Fine Servo - PM=45 76
34. Analog Compensator I/O for the Fine Servo - PM=10 77
35. Analog Compensator I/O for the Coarse Servo - PM=45 78
36. Analog Compensator I/O for the Coarse Servo - PM=10 79
37. Quantization Effects 80
38. Computation Delay 82
39. Tracking Error of 45 Degree Phase Margin System With F_s=10KHZ. 89
40. Tracking Error of 45 Degree Phase Margin System With F_s=15KHZ. 90
41. Positional Error Between the Fine and the Coarse Actuator for 8,12, and 16-Bit Digital Servo. 91
42. Tracking Error for 1 nsec and 3.3 microsec Computation Delays. 92
43. Positional Error Between the Fine and the Coarse Actuator. . 93
44. Tracking Error for 16.5 and 29.5 microsec Computation Delays 94
45. Tracking Error of 45 Degree Phase Margin System With F_s=30KHZ. 95
46. Positional Error Between the Fine and the Coarse Actuator. . 96
47. Tracking Error for Different Computation Delays. 97
48. Tracking Error Blowup Near Zero Time. 98
49. Positional Error Between the Fine and the Coarse Actuator. . 99
50. Tracking Error of 10 Degree Phase Margin System With F_s=30KHZ. 100
51. Tracking Error of 10 Degree Phase Margin System With F_s=60KHZ. 101
52. Tracking Error Over an Expanded Time Scale. 102
53. Tracking Error for Different Computation Delays. 103
54. Tracking Error Over an Expanded Time Scale. 104

LIST OF TABLES

Table		Page
1.	Frequency Domain Specifications to be Used in Present Designs	28
2.	Analog Compensation - Gain, Pole, and Zero Values	37
3.	Digital Compensation for the Fine Actuator Servomechanism . .	55
4.	Digital Compensation for the Coarse Actuator Servomechanism .	56
5.	Computation Time Delay Study	83

ABSTRACT

A large spectrum of new technologies are being explored in the optical disk drive systems. Optics, lasers, media, and servomechanisms are a few examples. This thesis will be directed to the study of a servomechanism used in a majority of the optical disk drives, commonly referred to as the tracking servomechanism. The tracking servomechanism, consisting of a fine and a coarse actuator, is mechanically analyzed by the use of free body diagrams. A transfer function for each actuator is derived. Analog compensators are designed to achieve specific phase and gain margin requirements. A digital compensator is derived from the analog compensator by the use of a mapping technique. Major contributions of this thesis include studies to determine an acceptable sampling rate, number of bits, and computation delay associated with the implementation of a digital servo controller in a tracking servomechanism.

CHAPTER 1

INTRODUCTION

Optical Disk Drives and Controls

The optical disk drive is a new technology being developed to allow large amounts of computer data to be stored in an efficient way. The storage capabilities of the optical disk is one to two orders of magnitude greater than the currently popular magnetic disk. The ability to store large amounts of data in an efficient manner is the primary attribute of the optical disk drive system. The overall objective of the optical disk drive is to reliably provide quick access to large amounts of data for the host computer at a cost competitive with the magnetic storage devices.

The major components that make up an optical disk drive are the laser, optics, controller, media, and servomechanisms. Figure 1 illustrates the physical relationship of a few of these major components. The optical disk rotates about an axis. The fine actuator is mounted on top of the coarse actuator. A high-power single-mode laser diode is generally used as the laser source [1] . Exposing the optical disk to the laser light will produce a change in the optical disk's reflectivity. The intensity of the laser light received by the detector determines if the bit of data is a one or a zero.

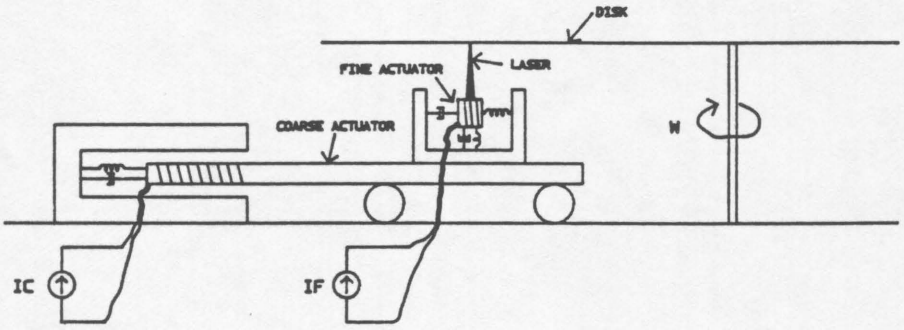

Figure 1. Dual Actuator Mechanical System

The optics unit consists of several elements (prisms, beam splitters, refractors, etc.) whose function is to direct the laser in the desired direction [2] .

The controller has several functions. The primary function is to interface the disk drive to the host computer. This involves receiving commands from the host computer and providing current status back. Typically, error correction code is located in the controller to enhance the reliability of the system.

The optical disk currently appears to be the focus of attention in the optical disk drive development. The ability to develop an erasable media with long life characteristics at an economical price is a major technical challenge being faced [3] . There are currently two popular types of media being used in optical disk drive systems - phase change and magneto-optic media [4] . Phase change medium deals with changing the atomical structure of the material. Initially, the disk has an amorphous film. A heat treatment changes the medium to crystalline for higher reflectivity. During a write procedure, a short laser beam pulse and rapid cooling converts the written spot from a crystalline state to an amorphous state. The highly ordered crystalline state has high reflectivity whereas the disordered amorphous state has low reflectivity. Reading the stored information is a matter of identifying the different reflectivities. A longer pulse from a slightly defocused laser followed by a slow cooling reverses the process, allowing information to be erased.

The writing on a magneto-optic medium is done thermomagnetically. Irradiation by the laser beam causes a change in the coercivity of the magneto-optic film so that the magnetization can be changed by an external field. Only the heated film experiences a change in magnetization. Thus, writing requires heat from the laser and a bias field. Erasing and re-writing is accomplished by the same process with the applied field reversed. The plane of polarization of the laser light is rotated as a result of passing through the magnetized film. An analyzer and photodetector identify the polarization of the transmitted light.

The optical disk drive has three major servomechanisms. A velocity controlled servomechanism is used to control the angular velocity of the optical disk. The objective of this servo is to prevent the angular velocity from deviating from the desired operating speed. A position controlled servomechanism is used in controlling the focus actuator. The objective of this servomechanism is to focus the energy of the laser beam onto the optical disk surface as the disk rotates.

The tracking servomechanism will be the focal point of this thesis report. As illustrated in Figure 1, this servomechanism is comprised of a coarse and a fine actuator. Both actuators are electromechanically equivalent to voice coil motors. The tracking servomechanism is a position controlled system. The objective of the tracking servomechanism is to maintain the laser light on the center of the data track as the disk rotates. This is accomplished by the fine and the coarse actuators. This

combination of two actuators is commonly referred to as a dual actuator. The laser and the fine actuator are mechanically mounted on the coarse actuator. The light from the laser is directed from the coarse actuator by the use of several optical elements to a single optical element located in the fine actuator. The fine actuator provides motion to this optical element. The motion of this optical element provides a means of directing the laser light onto the center of the data track. The coarse actuator servomechanism's objective is to sense the displacement of the optical element relative to the fine actuator and attempt to minimize this displacement. The result of minimizing this displacement allows the laser to pass through the center of the optical elements. The optical elements are most effective when the laser light passes through their center as opposed to near their edges.

The optical disk drive systems are currently in an early stage of development and there does not exist extensive published literature on these systems. In particular, there does not appear to be any previous work in the analysis and design of the dual actuator tracking system that is of interest to us in this thesis.

Problem Description

The tracking servomechanism, consisting of a fine and a coarse actuator, will be mechanically analyzed by the use of free body diagrams. A transfer function for each actuator will be derived. Analog

compensators will be designed to provide a specified phase and gain margin. A digital compensator will be derived from the analog compensator by the use of a mapping technique. The interest in the digital compensator is stimulated by the recent advancements in digital signal processors. Analog compensation is implemented by the use of discrete resistors, capacitors, analog switches, and operational amplifiers. The tolerances of the passive components and the input offset voltage and current of the operational amplifier can cause difficulties in designing a high volume manufacturable product. The replacement of the analog compensator by a digital compensator can remedy these problems by eliminating a majority of the analog components.

The architecture of the analog tracking servomechanism is derived from the configuration of the given plant (mechanics) and the control objective. The plant consists of two voice coil motors that require current inputs and provide voltage outputs proportional to displacement. The objective of the servomechanism is for the fine actuator to follow the center of the data track on the disk and for the coarse actuator to follow the fine actuator. Therefore, a positional servomechanism is appropriate in this application. A block diagram of the analog servo to be studied is shown in Figure 2.

The fine and the coarse actuator blocks represent the electromechanical properties of the fine and the coarse actuators respectively. The power amplifier blocks represent transconductance amplifiers. This type of amplifier produces a current output that is proportional to the voltage

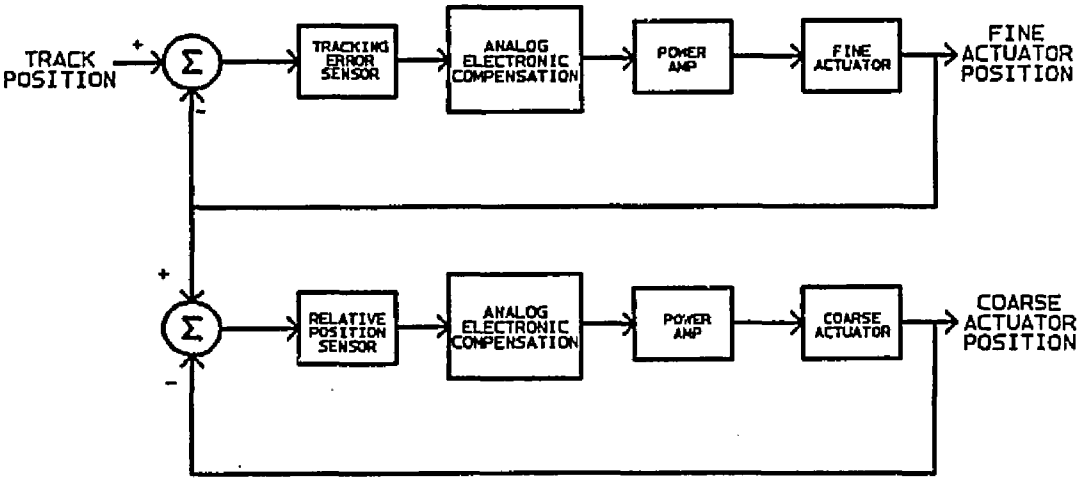

Figure 2. Analog Servo Block Diagram

applied at the input. The analog electronic compensation block represents the portion of the servo that provides the required phase and gain margins to assure system stability. The tracking error sensor block represents the sensitivity of the sensor in volt/meter. The position of the laser light relative to the data track on the disk is sensed by the tracking error sensor [5] . The relative position sensor block represents the sensitivity of the relative position sensor. The displacement of the fine actuator's optical element relative to the coarse actuator is sensed by the relative position sensor.

Figure 3 is a block diagram of the digital servo. This block diagram is equivalent to the block diagram of the analog servo (Figure 2) except for the replacement of the analog compensators with the digital compensators. The digital compensators are each represented by four blocks. The analog-to-digital and digital-to-analog converters are required to implement the digital controller design. They provide the conversion between the analog voltages and digital words. The block labeled clocks represents the required sequencing of the analog voltage sampling, machine computation, and the conversion from a digital word to analog voltage. The block labeled computer can represent a microprocessor, digital signal processor, or a large computer.

This study will determine requirements on the digital servo such that the dynamic performance of the digital servo is comparable to the analog servo for both a high (45 degrees) and a low (10 degrees) phase

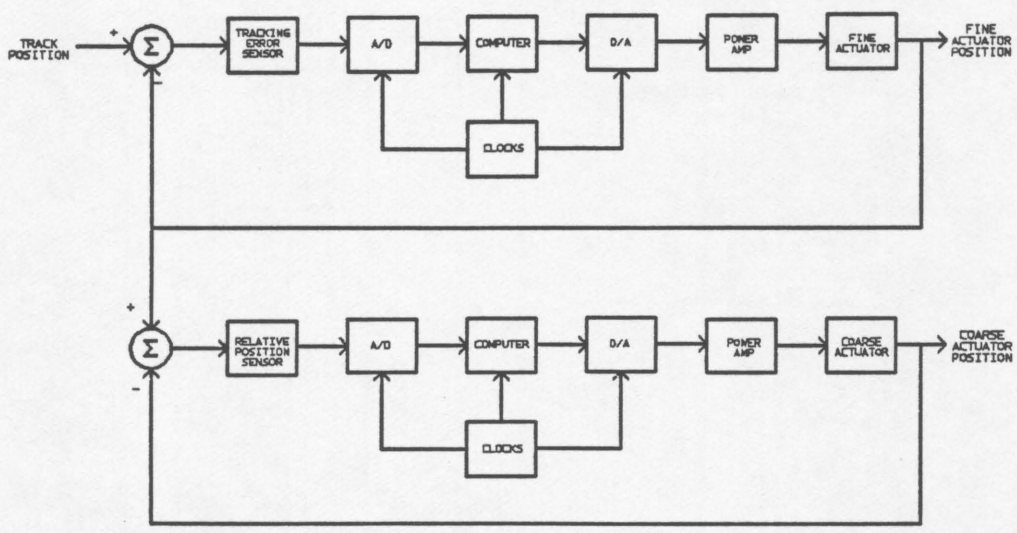

Figure 3. Digital Servo Block Diagram

margin system. The primary parameters of interest are the sampling rate, computation delay, and the effects of quantization on the dynamic performance of the servo.

Dynamic-Simulation Language Description

The study of this dual actuator system will be accomplished by computer simulations. The computer language that has been chosen is called Dynamic Simulation Language (DSL) [6] . This is an IBM developed and supported language that is available to the public. The language is Fortran based. DSL lends itself well to the modelling of continuous dynamic systems. The user is supplied with a library of DSL functions from which a physical system can be modelled. This library is augmented by the FORTRAN library functions. Users may create their own functions by using macros or procedures. A DSL program is made up of five segments: Initial, Derivative, Dynamic, Sample, and Terminal segments. The use of these 5 segments are illustrated in the programs that are used in the simulation of this thesis topic.

Outline of the Thesis

The principal objectives of this study are to determine requirements on the digital compensator. In Chapter 2, mathematical expressions that describe the dynamic characteristics of the servo system are derived. The mechanical forces on the actuators are quantitatively defined. The

equations describing the mechanical forces are transformed into transfer functions. The power amplifier stage is analyzed and mathematical equations describing it are derived. Equations for the analog and digital compensators are derived. A DSL frequency domain program that designs the analog and digital compensations is described. This chapter concludes with designed analog and digital compensators and the Bode plots of the servomechanisms. Two designs are performed. One design is for a servomechanism with 10 degrees of phase margin. The other design is for a 45 degree phase margin system. The two different systems are studied so that the influence of phase margin on the digital controller design can be determined.

In Chapter 3, a validation of the model is conducted using the DSL frequency domain program. A HP3562A Dynamic Signal Analyzer is used to synthesize the transfer functions developed in the previous chapter. The synthesized Bode plots are compared to the DSL generated Bode plots in order to verify that the DSL frequency domain program has no errors.

In Chapter 4, the performance of the analog and the digital servomechanisms is analyzed by simulation studies. The time domain simulations study the influence of sampling time, quantization, and computation delay on the dynamic performance of the digital servo system relative to the analog servo system.

Finally, Chapter 5 contains some statements outlining conclusions of the study and suggestions for further studies on this servo system.

CHAPTER 2

DEVELOPMENT OF THE DIGITAL SYSTEM

Continuous System Model Development

The continuous system model is developed by analyzing the mechanics and the electronics of the system. This involves several steps. The mechanical free body diagram for the actuators must be constructed and analyzed. The power amplifier design must be determined and analyzed. This will complete the description of the plant to be controlled. Finally, the electronic compensation that enables the servomechanism to meet bandwidth, phase margin, and gain margin requirements will be designed.

Mechanical Analysis

The actuator mechanics will be modelled as a spring, mass, viscous damper system. The composite portrait of these elements is in Figure 4.

Fine Actuator. The free body diagram for the fine actuator can now be studied as in Figure 5. The input force to the fine actuator is the result of forcing a current through the coil. This current creates a magnetic field of flux, such that when combined with an existing magnetic field

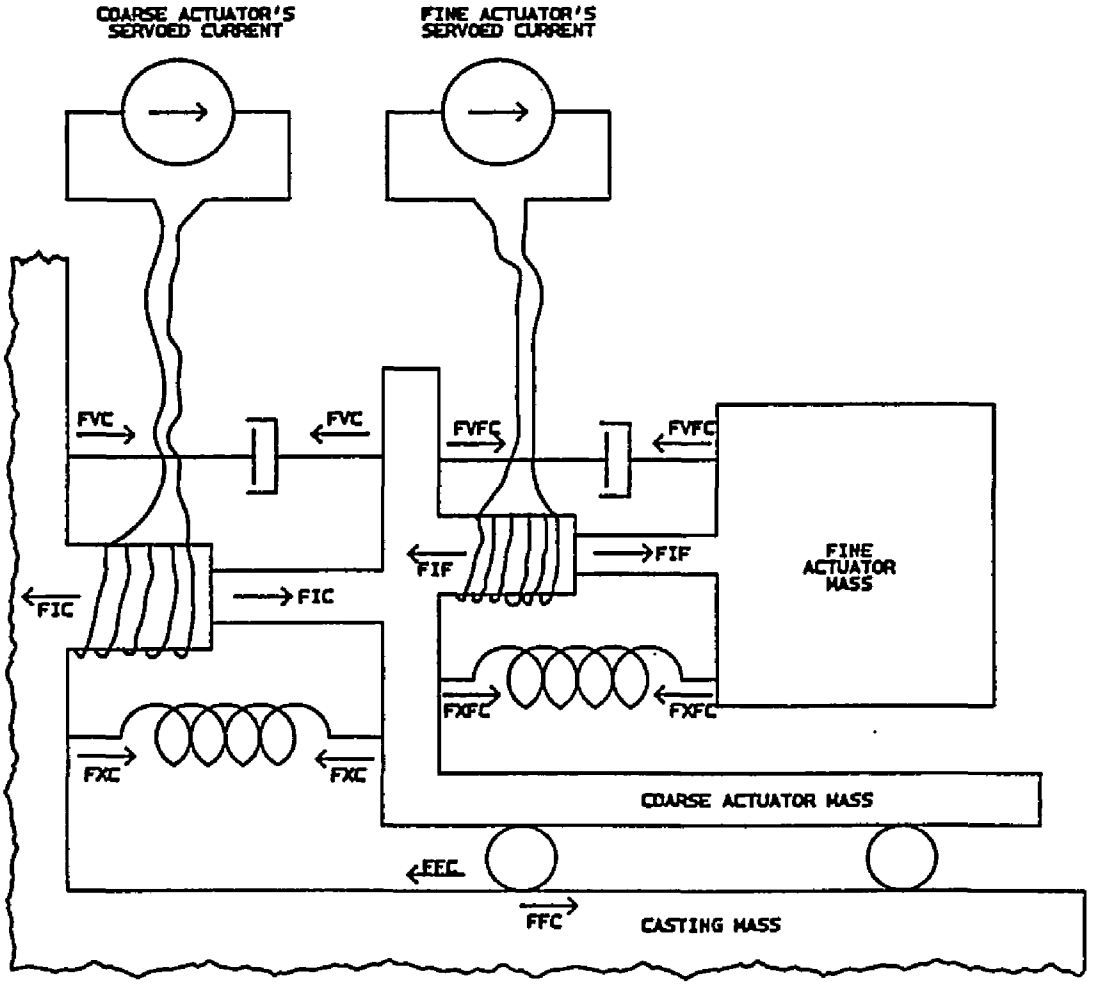

Figure 4. Dual Actuator Force Diagram

from a nearby permanent magnet, a force is exerted on the actuator proportional to the amount of current passed through the coil. Thus,

$$f_{if}=k_{ff}i_f \tag{1}$$

where

f_{if}: is the force due to the current (Newtons),

k_{ff}: is the force constant (Newtons/Amp),

and i_f: is the coil current (Amps).

The fine actuator is naturally centered in the unenergized state by the mechanical suspension. There are many ways in which this suspension can be created. One common way is to use two leaf springs. This provides a force opposite the displacement from the equilibrium position as,

$$f_{xfc}=k_{xcf}(x_f-x_c) \tag{2}$$

where

f_{xcf}: is the force due to the spring (Newtons),

k_{xcf}: is the spring force constant (Newtons/Meter),

x_c: is the coarse actuator position relative to the casting (Meters),

and x_f: is the fine actuator position relative to the casting (Meters).

The viscous force is a result of air resistance and/or due to the technique implemented in the mechanical suspension of the actuator and is given by

$$f_{vfc}=k_{vcf}(v_f-v_c) \tag{3}$$

where

f_{vfc}: is the force due to the viscous damping

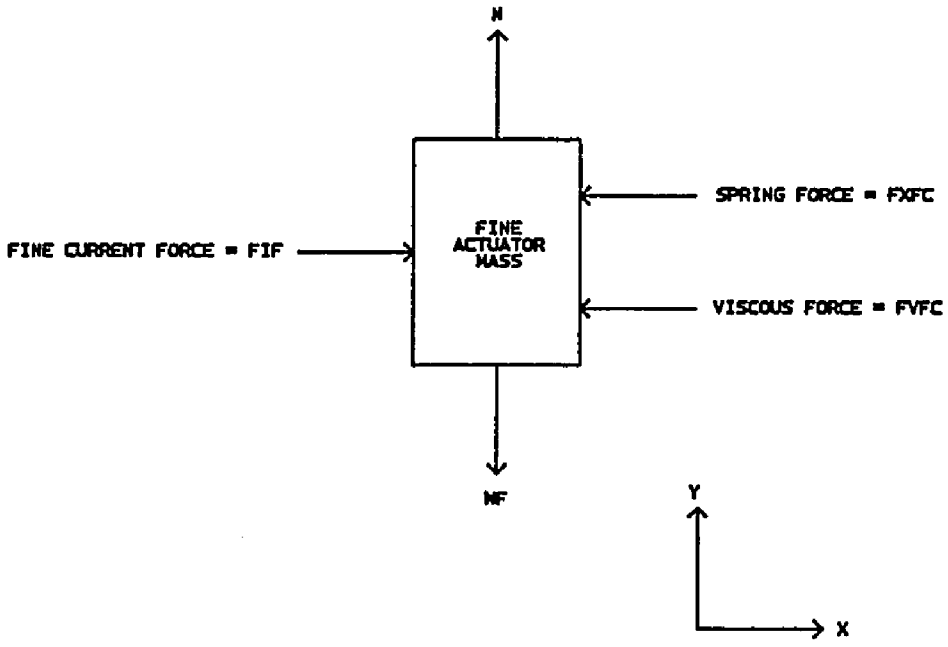

Figure 5. Fine Actuator Free Body Diagram

k_{vcf}: is the viscous damping constant (Newtons/Meter/Sec),

v_c: is the coarse actuator velocity relative to the casting (Meters/Sec),

and v_f: is the fine actuator velocity relative to the casting (Meters/Sec).

The result of summing the forces in the x-direction provides:

$$f_{if}-f_{xfc}-f_{vfc}=m_f a_f \tag{4}$$

where

m_f: is the mass of the fine actuator (Kilograms),

and a_f: is the fine actuator acceleration (Meter/Sec/Sec).

Therefore:

$$a_f=(f_{if}-f_{xfc}-f_{vfc})/m_f, \tag{5}$$

$$=(k_{ff}i_f-k_{xcf}(x_f-x_c)-k_{vcf}(v_f-v_c))/m_f \tag{6}.$$

The velocity v_f and position x_f of the fine actuator can be derived from the acceleration by integrations.

$$v_f=\int a_f \, dt \tag{7}$$

$$x_f=\int v_f \, dt \tag{8}$$

Coarse Actuator. The nature of the forces acting upon the coarse actuator are similar to those acting upon the fine actuator. The forces due to the coil current, spring and viscous damping of the mechanical suspension are present (Figure 6). The coarse actuator also has the fine actuator's reactionary forces as a result of the fine actuator being mounted on top of the coarse actuator. The static and kinetic frictional forces on the

coarse actuator are typically small. The force due to current is described by,

$$f_{ic}=k_{fc}i_c \tag{9}$$

where

f_{ic}: is the force due to the current (Newtons),

k_{fc}: is the force constant (Newtons/Amp),

and i_c: is the coil current (Amps).

The spring force is:

$$f_{xc}=k_{xc}x_c \tag{10}$$

where

f_{xc}: is the force due to the spring (Newtons),

k_{xc}: is the spring force constant (Newtons/Meter),

and x_c: is the coarse actuator position relative to the casting (Meters).

The viscous force is:

$$f_{vc}=k_{vc}v_c \tag{11}$$

where

f_{vc}: is the force due to the viscous damping (Newtons),

k_{vc}: is the viscous damping constant (Newtons/Meter/Sec),

and v_c: is the coarse actuator velocity relative to the casting (Meters/Sec).

The frictional force is:

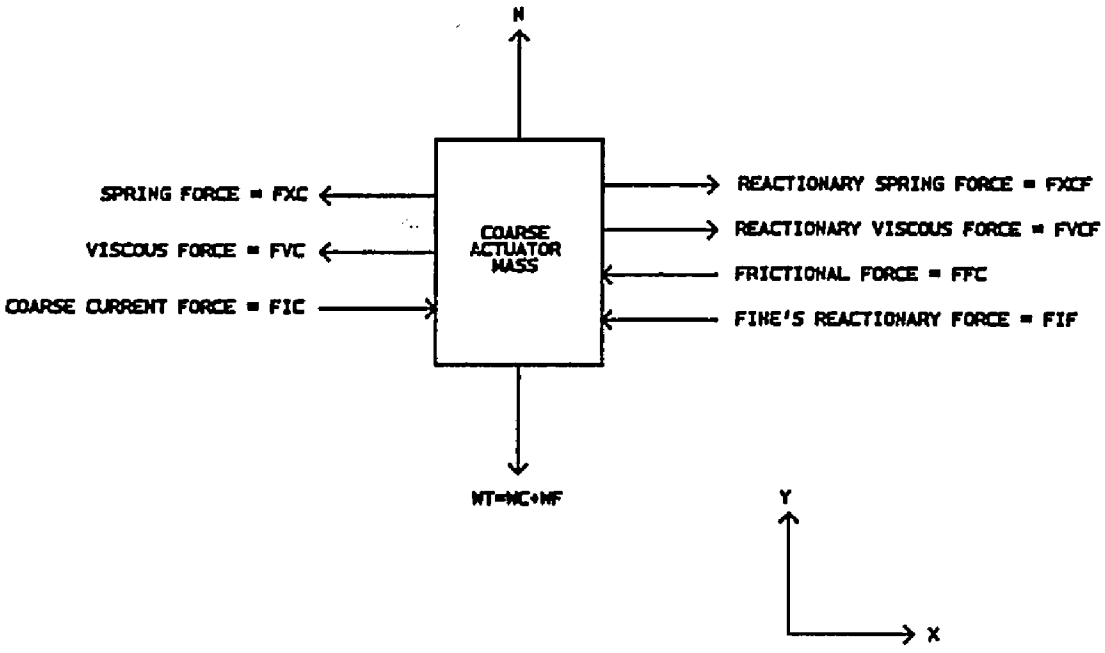

Figure 6. Coarse Actuator Free Body Diagram

$$f_{fc}=\mu\ m_t g \tag{12}$$

where

f_{fc}: is the force due to friction (Newtons),

μ : is the coefficient of friction (unitless),

m_t: is the total mass of the fine and coarse actuators (Kilograms),

and g: is the acceleration due to gravity (Meters/Sec/Sec).

The result of summing the forces in the x-direction provides:

$$f_{ic}-f_{vc}-f_{xc}+f_{xcf}+f_{vcf}-f_{fc}-f_{if}=m_t\ddot{a}_c \tag{13}$$

where

a_c: is the coarse actuator's acceleration (Meter/Sec/Sec).

$$a_c=(f_{ic}-f_{vc}-f_{xc}+f_{xcf}+f_{vcf}-f_{fc}-f_{if})/m_t \tag{14}$$

$$=(k_{fc}i_c-k_{vc}v_c-k_{xc}x_c+k_{xcf}(x_f-x_c)+k_{vcf}(v_f-v_c)-\mu\ m_t g-k_{ff}i_f/m_t) \tag{15}$$

As before, the velocity v_c and position x_c of the coarse actuator can be derived from the acceleration by integrations.

$$v_c=\int a_c dt \tag{16}$$

$$x_c=\int v_c dt \tag{17}$$

Fine Actuator Transfer Function. The transfer function for the fine actuator can be derived from equation 6. The derived transfer function will be the relationship of output displacement relative to the disk's surface to the input current. Note that:

$$A_f(s)=X_f(s)s^2 \tag{18}$$

$$V_f(s)=X_f(s)s. \tag{19}$$

Substitution of equations (18) and (19) into equation (6) yields the following equation assuming the coarse actuator is fixed relative to the casting:

$$m_f X_f(s)s^2=k_{ff}I_f(s)-k_{xcf}X_f(s)-k_{vcf}X_f(s)s \tag{20}$$

Hence, $$G_1(s)=X_f(s)/I_f(s)=k_{ff}/(m_f s^2+k_{vcf}s+k_{xcf}). \tag{21}$$

An additional constant must be introduced that accounts for the gain of the tracking error sensor. The units of this constant provides the needed conversion from meters to volts.

k_q: gain of the tracking error sensor (volts/meters).

The resultant transfer function of the plant (fine actuator and tracking error sensor) is:

$$G_2(s)=k_q G_1(s). \tag{22}$$

The transfer function derived portrays the frequency domain characteristics of the actuator as a rigid body. In mechanical implementations of the actuators, the actuator assembly consists of several components. Structural vibration (commonly called mode shapes) may result from the mechanical components not being perfectly rigid and/or rigidly connected. Structural vibrations are resonant behavior that can cause instabilities in the servomechanism if excited. A transfer function for a secondary resonance phenomenon most commonly shows up as a pair of complex poles and a pair of complex zeros at frequencies above the fundamental resonance derived in assuming the structure to be a rigid body.

A representative transfer function for the resonance that could occur in the fine actuator is:

$$G_3(s)=(s^2+a_0s+a_1)/(s^2+b_0s+b_1). \tag{23}$$

The resultant transfer function for the fine actuator system is:

$$G_f(s)=G_2(s)G_3(s). \tag{24}$$

Coarse Actuator Transfer Function. The transfer function for the coarse actuator is derived using the same approach as was used in deriving the transfer function for the fine actuator. Starting with,

$$A_c(s)=X_c(s)s^2 \tag{25}$$

$$V_c(s)=X_c(s)s \tag{26}$$

substitution of equations (25) and (26) into equation (15) yields the following equation assuming the fine actuator is fixed to the coarse actuator and friction is negligible:

$$m_tX_c(s)s^2=k_{fc}I_c(s)-k_{vc}X_c(s)s-k_{xc}X_c(s) \tag{27}$$

$$G_4(s)=X_c(s)/I_c(s)=k_{fc}/(m_ts^2+k_{vc}s+k_{xc}). \tag{28}$$

An additional constant must be introduced that accounts for the gain of the relative position sensor. The units of this constant provides the needed conversion from meters to volts.

k_{rps}: relative position sensor gain (volts/meter)

The resultant transfer function of the coarse actuator and relative position sensor is:

$$G_5(s)=k_{rps}G_4(s). \tag{29}$$

Unlike the fine actuator, the mechanical construction of the coarse actuator has no spring. Typically, the coarse actuator is supported on

guide rails by roller bearings. The mechanical design attempts to minimize all forces that oppose the force due to the current through the coil f_{ic}. Therefore:

$$G_6(s)=k_{rps}k_{fc}/(s(m_t s+k_{vc})). \tag{30}$$

The transfer function of the resonance phenomenon in the coarse actuator has the same form as that found for the fine actuator,

$$G_7(s)=(s^2+c_0 s+c_1)/(s^2+d_0 s+d_1) \tag{31}$$

The resultant transfer function for the coarse actuator is:

$$G_c(s)=G_6(s)G_7(s) \tag{32}$$

Power Amplifier

A sufficient amount of current is required to cause the desired mechanical motion of the actuator. A transconductance power amplifier will be used to accomplish this in an effective way from the control voltage of the electronic compensation. This type of an amplifier provides a unique amount of current output for a specific voltage level at the input. The way this is accomplished is shown in Figure 7 by the use of a block diagram.

The k_{amp} block represents the open loop gain of the power device. Typically a power operational amplifier is used with an open loop gain of approximately 100 db. This amplifier amplifies the error between the desired current represented by the control voltage v_i and the coil current i_s. The coil current i_s is measured by a voltage drop across the resistor r_s. The k_{bemf} block represents the back emf generated by the velocity

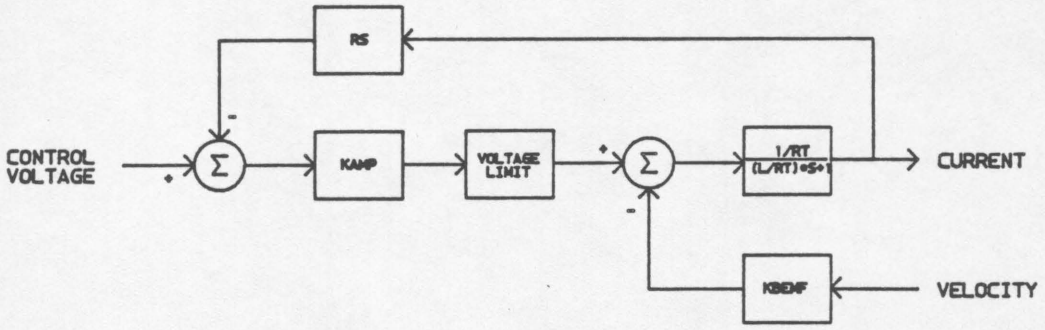

Figure 7. Power Amplifier Block Diagram

of the actuator's coil. This voltage typically opposes the output voltage of the power amplifier. A schematic representation is illustrated in Figure 8.

The output current of the amplifier is passed through a resistor, r_s. The voltage drop v_s across this resistor is proportional to the amount of current i_s flowing through it,

$$v_s=i_s r_s. \tag{33}$$

This voltage v_s is then compared to the input voltage v_i and a error voltage v_e results,

$$v_e=v_i-v_s=v_i-i_s r_s. \tag{34}$$

The error voltage is fed into a high gain power operational amplifier. The output of the power op-amp is equal to the input error voltage times the open loop gain of the device,

$$v_a=k_{amp} v_e \tag{35}$$

where

k_{amp}: is the open loop gain of power amp.
(Volts/Volts).

The power amplifier output voltage is applied directly across the coil of the actuator to produce a current,

$$i_s=v_e k_{amp}/(r_a+r_s+l_a s) \tag{36}$$

where

r_a: is the coil resistance (Ohms),

and l_a: is the coil inductance (Henries).

The actuator's back emf can influence the total amount of potential across the windings.

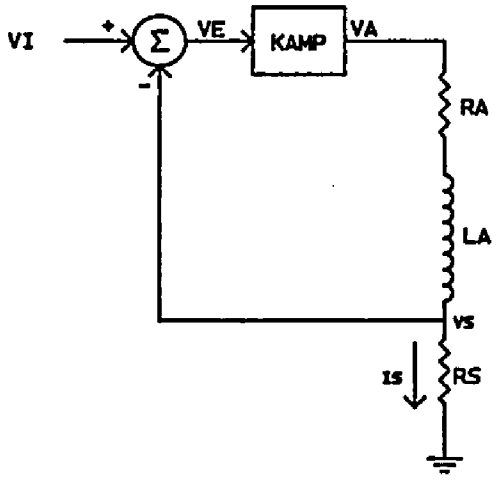

Figure 8. Power Amplifier Schematic

$$v_{bemf}=k_{bemf}v_a \tag{37}$$

where

k_{bemf}: is the back emf constant of the actuator (Volt/Meter/Sec),

and v_a: is the velocity of the actuator (Meter/Sec).

The transfer function of the power amplifier stage can now be derived (Figure 8). This transfer function relates the current output to control voltage input. Assuming that the v_{bemf} is negligible, substitution of equation (34) into (36) and some algebraic manipulation leads to:

$$G_8(s)=\frac{I_s(s)}{V_i(s)}=\frac{1.0}{(r_s+(r_a+r_s+l_as)/k_{amp})} \tag{38}$$

As was previously mentioned, k_{amp} is typically 100 db. This large gain k_{amp} has the desirable effect of placing the pole in the denominator of $G_8(s)$ at a frequency well above the servo open loop bandwidth if the resistances r_a and r_s and the inductive impedance due to l_a are small relative to k_{amp}. Assuming that the above statement is true will reduce $G_8(s)$ to :

$$G_8(s)\simeq 1.0/r_s. \tag{39}$$

Electronic Compensation

The frequency domain characteristics of the servo are to be specified in terms of the bandwidth, phase margin, and gain margin. As a rule of thumb, for satisfactory performance, the phase margin should be between 30 degrees and 60 degrees, and the gain margin should be

greater than 6 db [7] . In order to obtain an indication on how the phase margin influences the requirements of the digital controller, two servo compensators one with 45 degree phase margin and the other with a 10 degree phase margin will be studied. The gain margin will be made greater than 10 db. Typically, the open loop bandwidth of the fine actuator's servomechanism is nearly an order of magnitude greater than that of the coarse actuator's servomechanism. This study will select a 2500 hertz and a 300 hertz open loop bandwidth for the fine actuator and the coarse actuator servomechanism, respectively. Table 1 contains the frequency domain requirements of the two servo systems to be studied.

Table 1

Frequency Domain Specifications to be Used in Present Designs

System #	Actuator	Bandwidth degrees	Phase Margin degrees	Min. Gain Margin dB
1	fine	2500	45	10
1	coarse	300	45	10
2	fine	2500	10	10
2	coarse	300	10	10

Low Frequency Integrator. The objective of the tracking servomechanism is to follow the data track on the disk as the disk rotates. A perfect data track would appear stationary to the tracking servomechanism as the disk rotates. However, the data tracks on the disk are not perfectly circular as a result of imperfections in the disk fabrication. Also, the mounting of the disk to the drive motor is not perfectly concentric about

the axis of rotation. This results in track displacement in the radial direction, commonly called radial runout, as the disk rotates. The radial runout is composed of harmonics of the disk rotational frequency. A typical disk rotational frequency is 50 hertz. The magnitude of the first harmonic radial runout is commonly the largest due to the mounting of the disk to the drive motor.

The use of a proportional plus integral controller (low frequency integrator) in the electronic compensation can provide a significant improvement in the error reduction capability of the servo in following these low frequency radial runout harmonics. Let ω_i denote the location of the zero in the low frequency integrator. The transfer function of the low frequency integrator is,

$$G_9(s)=(s+\omega_i)/s \tag{40}$$

$$=\omega_i/s \quad \text{for} \quad s<<\omega_i \tag{41}$$

$$=s/s=1.0 \quad \text{for} \quad s>>\omega_i \tag{42}$$

Thus the transfer function is that of an integrator for frequencies well below ω_i. This provides high open loop gain and good error reduction performance for these frequencies. Frequencies well above ω_i are not changed in amplitude. The phase of $G_9(s)$ is -90 degrees for frequencies well below ω_i and 0 degrees for frequencies well above ω_i. Therefore it is critical to have ω_i well below the servo open loop bandwidth to avoid $G_9(s)$ from influencing the phase margin of the servo system. The amount of phase lag introduced by $G_9(s)$ can be determined by substituting $j\omega$ for s and solving for the angle in the complex plane.

$$G_9(j\omega)=(j\omega+\omega_i)/(j\omega) \tag{43}$$

$$=1-\omega_i j/\omega \tag{44}$$

and hence,

$$\theta=\tan^{-1}(-\omega_i/\omega). \tag{45}$$

The amount of phase lag due to the low frequency integrator can now be calculated for any ω by equation (45). This equation could also be used in a design application when the maximum amount of phase lag due to the low frequency integrator at the servomechanism's open loop bandwidth is specified and the location of the zero ω_i is unknown.

Phase Lead Compensator. A phase lead compensator will be used to obtain the desired amount of phase margin at the required open loop bandwidth. The transfer function of a phase lead compensator is:

$$G_{10}(s)=\omega_p(s+\omega_z)/(\omega_z(s+\omega_p)). \tag{46}$$

The pole-zero locations are selected to provide the desired amount of phase lead at the servo open loop bandwidth. $G_{10}(s)$ has zero db of gain at frequencies well below the bandwidth. The gain at frequencies well above the bandwidth is related to the amount of phase lead (pole-zero spacing). The larger the phase lead, the larger the high frequency gain. This high frequency gain directly reduces the gain margin of the servo by amplifying the high frequencies. The phase of $G_{10}(s)$ can be calculated using the same approach used in deriving the phase of the low frequency integrator $G_9(s)$. The end product of analyzing $G_{10}(s)$ leads to a means of determining the pole-zero locations. Let PL be the desired amount of phase lead. Then a constant γ can be defined by [7] :

$$\gamma=(1-\sin(PL))/(1+\sin(PL)). \tag{47}$$

Let ω_{bw} denote the open loop bandwidth in radians/sec. The pole location can be calculated by :

$$\omega_p=\omega_{bw}/(\gamma^{0.5}). \tag{48}$$

The zero location is given by :

$$\omega_z=\gamma\omega_p. \tag{49}$$

The pole and zero are related to the bandwidth ω_{bw} by:

$$\omega_{bw}=(\omega_z\omega_p)^{0.5}. \tag{50}$$

Mapping to the Z Domain

A pole-zero mapping technique will be used to derive the z-domain compensator transfer function from the s-domain compensator transfer function [8] . The complete forms of the s-domain compensator for both the fine and the coarse servomechanisms are identical. Only the values of the gain and the pole and the zero are different. The following is the form of the compensator transfer function in the s-domain:

$$G_{11}(s)=\frac{K_1\omega_p(s+\omega_i)(s+\omega_z)}{\omega_z s(s+\omega_p)}. \tag{51}$$

All poles and zeros of $G_{11}(s)$ are mapped according to the mapping relation $z=e^{sT}$ where T denotes the sampling period. The resultant form of the equivalent z-domain transfer function is:

$$G_1(z)=\frac{K_2(z-z_i)(z-z_z)}{(z-z_0)(z-z_p)} \tag{52}$$

where

$$z_i=e^{-\omega_i T} \tag{52a}$$

$$z_z=e^{-\omega_z T} \tag{52b}$$

$$z_p=e^{-\omega_p T} \tag{52c}$$

and $$z_0=e^{-0T}=1.0\ . \tag{52d}$$

The gain K_2 of the z-domain transfer function is calculated by selecting a critical frequency ω_c and equating the magnitudes of the continuous and discrete-time transfer functions at that critical frequency. An appropriate critical frequency for this study is the fundamental rotational frequency of the optical disk. The frequency spectrum of the radial runout will have a large component at this frequency due to the lack of concentricity in the mounting of the optical disk to the drive hub. The time domain difference equation can now be derived from the z domain transfer function. Notice that

$$Y(z)(z-z_0)(z-z_p)=X(z)K_2(z-z_i)(z-z_z) \tag{53}$$

$$Y(z)[z^2-(1+z_p)z+z_p]=X(z)K_2[z^2-(z_i+z_z)z+z_i z_z], \tag{54}$$

inverse z-transformation leads to the recursion equation

$$y(k)=a_0y(k-1)-a_1y(k-2)+b_0x(k)-b_1x(k-1)+b_2x(k-2) \tag{55}$$

where

$$a_0=1+z_p \tag{55a}$$

$$a_1=-z_p \tag{55b}$$

$$b_0=K_2 \tag{55c}$$

$$b_1=-K_2(z_i+z_z) \tag{55d}$$

$$b_2=K_2z_iz_z. \tag{55e}$$

DSL Frequency Domain Program

The detailed listings of the DSL programs that simulate the fine and coarse servomechanisms in the frequency domain are given in Appendix A and Appendix B respectively. The programs are designed to determine the analog and digital compensators of the form of $G_{11}(s)$ and $G_1(z)$ by using the equations previously derived.

It is now necessary to define the parameters of the plant. The following is a typical parameter set of a tracking actuator system found in optical disk drives.

Fine Actuator:

force constant=k_{ff}=0.3 newtons/amp

spring constant=k_{xcf}=193 newtons/meter

viscous constant=k_{vcf}=0.3 newtons/meter/second

mass=m_f=3 grams

resistance=r_f=10 ohms

inductance=l_f=200 microhenries

power amp. open loop gain=k_{amp}=100,000 volts/volts

power amp. resistor=r_s=1 ohm

transfer function for the secondary resonance=

$$\frac{0.892(s^2+4523s+(113097)^2)}{s^2+4272s+(106814)^2}.$$

Coarse Actuator:

force constant=k_{fc}=7.5 newtons/amp

spring constant=k_{xc}=0 newtons/meter

viscous constant=k_{vc}=1.8 newtons/meter/second

mass=m_c=200 grams

resistance=r_c=6 ohms

inductance=l_c=3 millihenries

power amp. open loop gain=k_{amp}=100,000 volts/volts

power amp. resistor=r_s=1 ohm

coeff. of friction=μ =0.0

transfer function for the secondary resonance=

$$\frac{0.826(s^2+553s+(13823)^2)}{s^2+503s+(12566)^2} .$$

Sensor's sensitivity:

tracking error sensor=$1.5(10^6)$ volts/meter

relative position sensor=$2.5(10^3)$ volts/meter .

Disk characteristics:

track density=$2(10^{-6})$ meters/track

radial runout=$r_1+r_2+r_3+r_4+r_5$,

where r_1-r_5 represent the repeatable radial runout components of the disk. r_1 is the first harmonic component of the runout. The shape is sinusoidal with a frequency equal to the rotational frequency of the disk. The remaining components r_2-r_5 have frequencies 2, 3, 4, and 5 times respectively that of r_1. The zero to peak magnitude of the components are:

$r_1=50(10^{-6})$ meters

$r_2=7(10^{-6})$ meters

$r_3=5(10^{-7})$ meters

$r_4=3(10^{-7})$ meters

$r_5=9(10^{-8})$ meters.

DSL Program Input

The following information about the servo system must be provided by the user.

1. Plant transfer function $G_p(s)$.
2. Open loop bandwidth BW (degrees).
3. Phase margin PM (degrees).
4. Amount of phase lag θ_i (degrees) allowed by the low frequency integrator at the open loop bandwidth.
5. Sampling frequency f_s (Hertz).
6. Critical frequency (Rad/Sec).

DSL Program Algorithm

The following is a chronological procedure that the DSL program performs in order to determine the required compensation.

1. Measure the phase Θ_p of the plant transfer function at the specified open loop bandwidth.
2. Calculate the zero location ω_i of the low frequency integrator (eqn.45) such that the input specification Θ_i is satisfied.
3. Calculate the total amount of phase lead Θ_c degrees required from the phase lead compensator at the open loop bandwidth such that the phase margin (PM) input specification is satisfied.
4. Calculate the pole ω_p and zero ω_z locations (eqns. 47, 48, 49) of the phase lead compensator that provide Θ_c degrees of phase lead.
5. The gain K_1 (eqn. 51) is calculated to meet the bandwidth input specification. This completes the design of $G_{11}(s)$.
6. Map the s plane poles and zeros into the z plane (eqns 52a-d).
7. Calculate the gain of the digital compensator K_2 (eqn. 52).
8. Calculate the coefficients (a_0,a_1,b_0,b_1,b_2) of the difference equation (eqn. 55a-e).
9. Generate Bode plots of the actuator and sensor, analog compensator, open loop and closed loop transfer functions.

Program Output

The required gain and location of the pole and the zero for the analog compensators that satisfy the design specifications found in Table 1 for the actuator parameters noted in section 2.3 are given in Table 2. Notice the larger spacing between the pole and the zero for the 45 degree phase margin system.

Table 2

Analog Compensation - Gain, Pole, and Zero Values.

System #1: (PM=45 degrees, Fine GM=17.1 dB, Coarse GM=14.9 dB)

Compensator (actuator)	Bandwidth (hertz)	Gain K_1 (volt/volt)	ω_i (rad/sec)	ω_z (rad/sec)	ω_p (rad/sec)
fine	2.5 Khz	0.61	1374.3	5770.6	42758
coarse	300 hz	1.4	164.91	690.46	5145.9

System #2: (PM=10 degrees, Fine GM=26 dB, Coarse GM=24.5 dB)

Compensator (actuator)	Bandwidth (hertz)	Gain K_1 (volt/volt)	ω_i (rad/sec)	ω_z (rad/sec)	ω_p (rad/sec)
fine	2.5 Khz	1.27	1374.3	12128	20345
coarse	300 hz	2.93	164.91	1452.5	2446.1

DSL Bode Plots. The following several pages contain the Bode plots for the servo systems. The Bode plots of the plant (actuator and sensor), analog compensation, open loop transfer function, and the closed loop transfer function are given to clarify the contribution the compensator makes to the overall servomechanism response. Figures 9 through 12 are of the fine actuator's servomechanism with a 45 degree phase margin. Figures 13 through 15 are of the fine actuator's servomechanism with a 10 degree phase margin. Figures 16 through 19 are of the coarse actuator's servomechanism with a 45 degree phase margin. Figures 20 through 22 are of the coarse actuator's servomechanism with a 10 degree

phase margin. The solid line in the figures represents the magnitude of the transfer function. The dotted line represents the phase of the transfer function.

From Figure 9 it may be noted that the amplitude response of the fine actuator and sensor $G_f(s)$ has two resonant peaks. The peak located at 40 hertz results from the poles of $G_2(s)$. The secondary resonant peak resulting from $G_3(s)$ is located at 20 Khz. Figure 10 is a Bode plot of the analog compensator $G_c(s)$ that will provide an overall phase margin of 45 degrees for the fine actuator servomechanism. Notice the low frequency gain for improved error reduction at the lower frequency harmonics of the radial runout. The maximum phase occurs at the servomechanism open loop bandwidth (2.5 Khz.) to meet the phase margin specification. The result of generating the open loop transfer function of this analog compensator with the fine actuator and sensor is illustrated in Figure 11. The open loop bandwidth is 2.5 Khz with a phase margin of 45 degrees and a gain margin of 17.1 dB. Figure 12 is the Bode plot of the closed loop system.

Figure 13 is a Bode plot of the analog compensator that will provide an overall phase margin of 10 degrees for the fine actuator servomechanism. Notice the small amount of phase lead at the open loop bandwidth as compared to the compensator whose frequency response is presented in Figure 10. The result of using this analog compensator with the fine actuator is pictured in Figure 14. The open loop bandwidth is

2.5 Khz with a phase margin of 10 degrees and a gain margin of 26 dB. Figure 15 is the Bode plot of the closed loop system. Notice the increased magnitude peaking near the closed loop bandwidth as a result of the low phase margin.

From Figure 16 it may be noted that the coarse actuator has one resonant peak at 200 Hertz that is a result of $G_7(s)$. Figure 17 is a Bode plot of the analog compensator that will provide an overall phase margin of 45 degrees for the coarse actuator servomechanism. The maximum phase occurs at the servomechanism open loop bandwidth (300 Hz.) to meet the phase margin specification. The result of generating the open loop transfer function of this analog compensator with the coarse actuator and sensor is illustrated in Figure 18. The open loop bandwidth is 300 Hz with a phase margin of 45 degrees and a gain margin of 14.9 dB. Figure 19 is the Bode plot of the closed loop system.

Figure 20 is the Bode plot of the analog compensator that will provide an overall phase margin of 10 degrees for the coarse actuator servomechanism. Notice the small amount of phase lead at the open loop bandwidth as compared to the compensator whose frequency response was presented in Figure 17. The result of using this analog compensator with the coarse actuator is pictured in Figure 21. The open loop bandwidth is 300 Hz. with a phase margin of 10 degrees and a gain margin of 24.5 dB. Figure 22 is the Bode plot of the closed loop system. Notice the

increased magnitude peaking near the closed loop bandwidth as a result of the low phase margin.

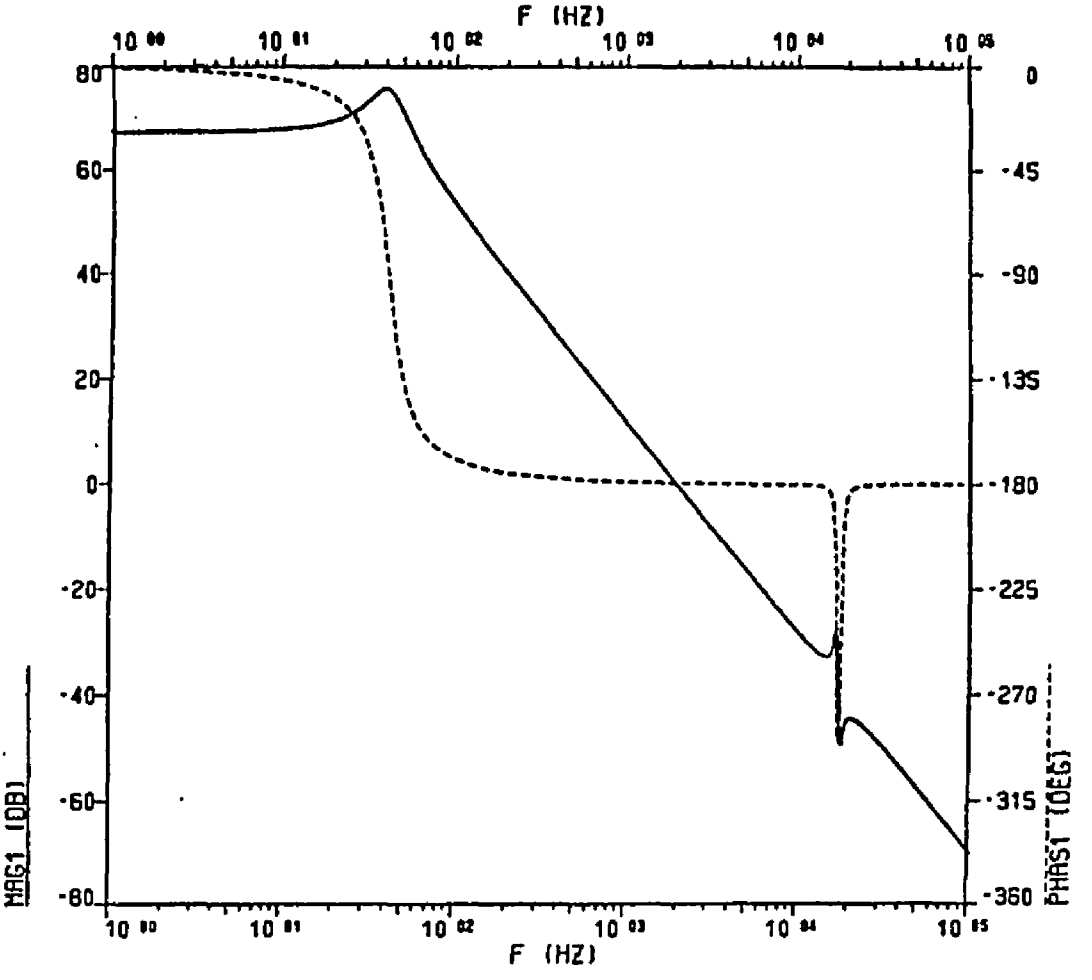

Figure 9. Bode Plot of the Fine Actuator and Sensor

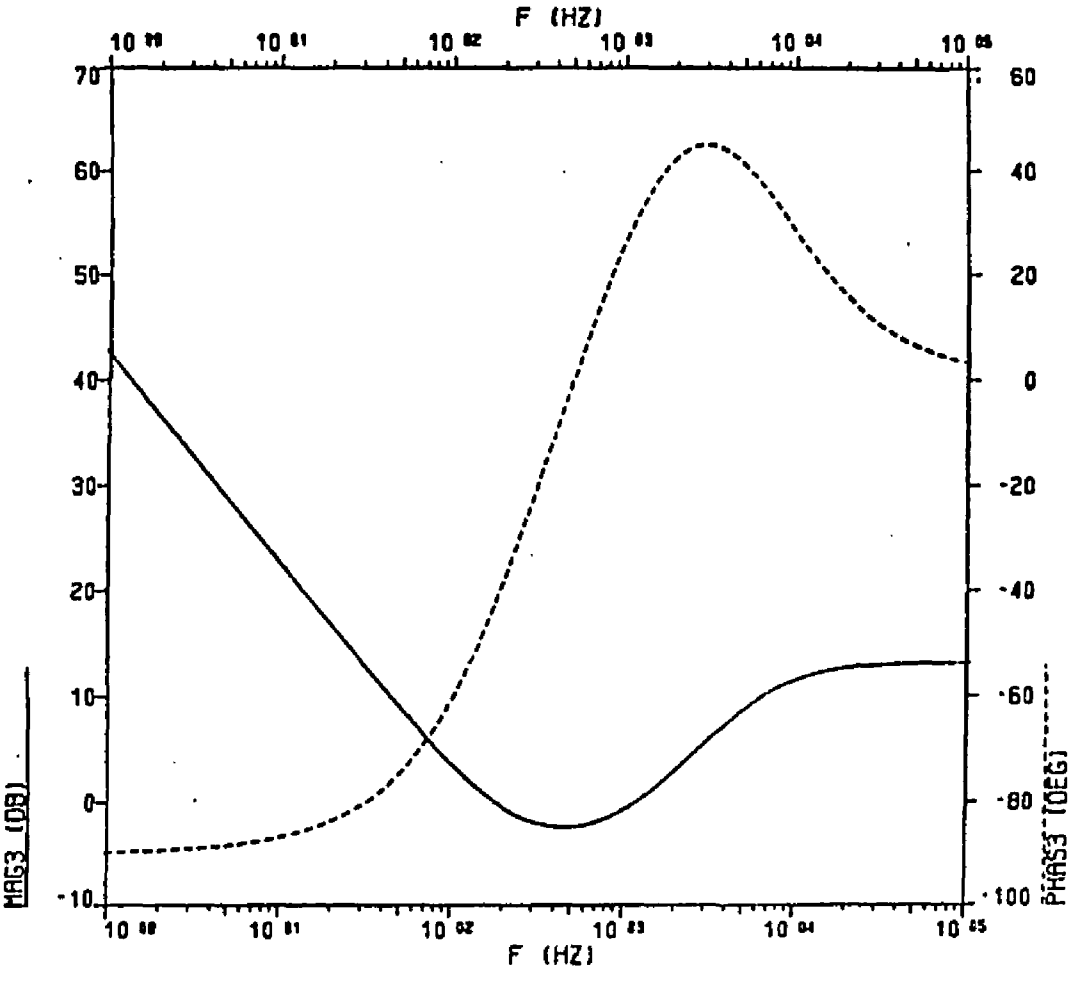

Figure 10. Bode Plot of the Fine Actuator Servo Compensation for 45 Degree Phase Margin

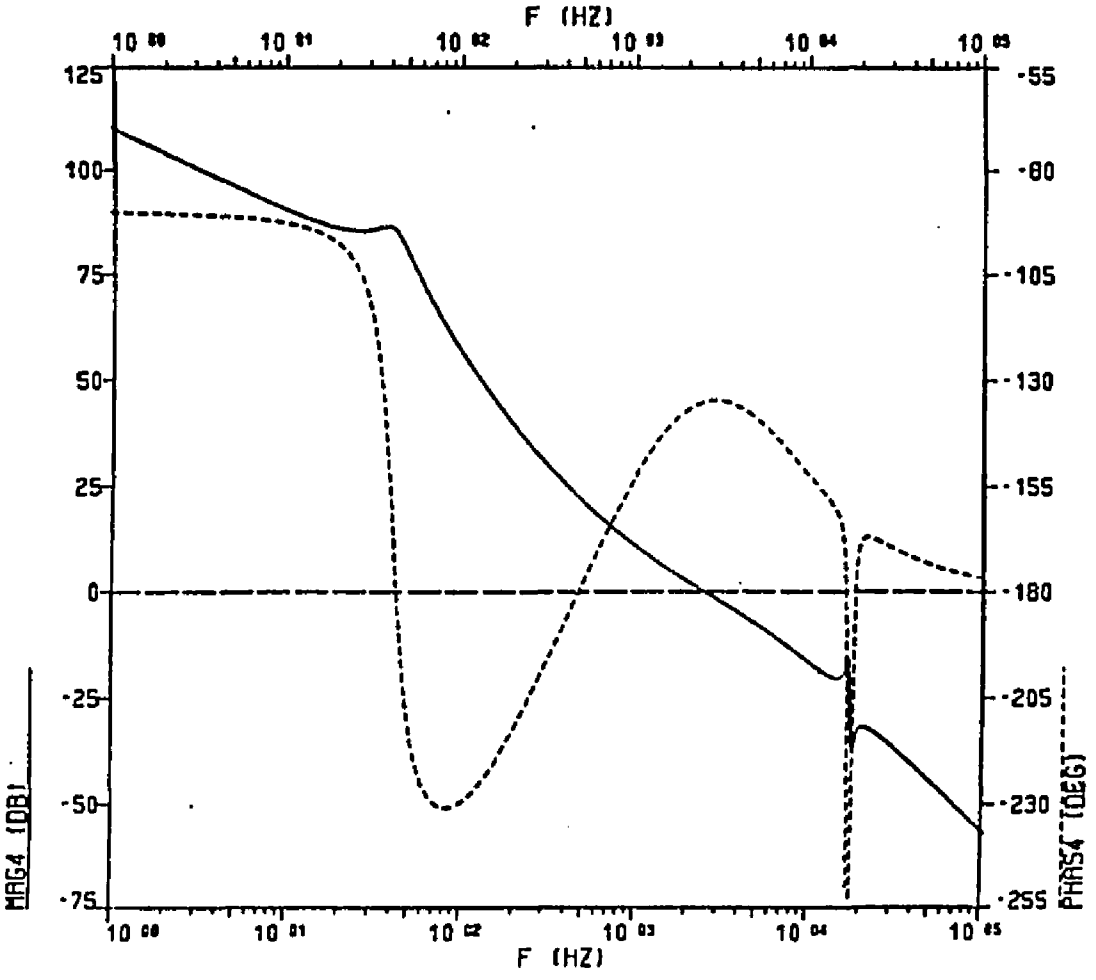

Figure 11. Bode Plot of the Fine Actuator Servo Open Loop Transfer Function (45 Degree Phase Margin)

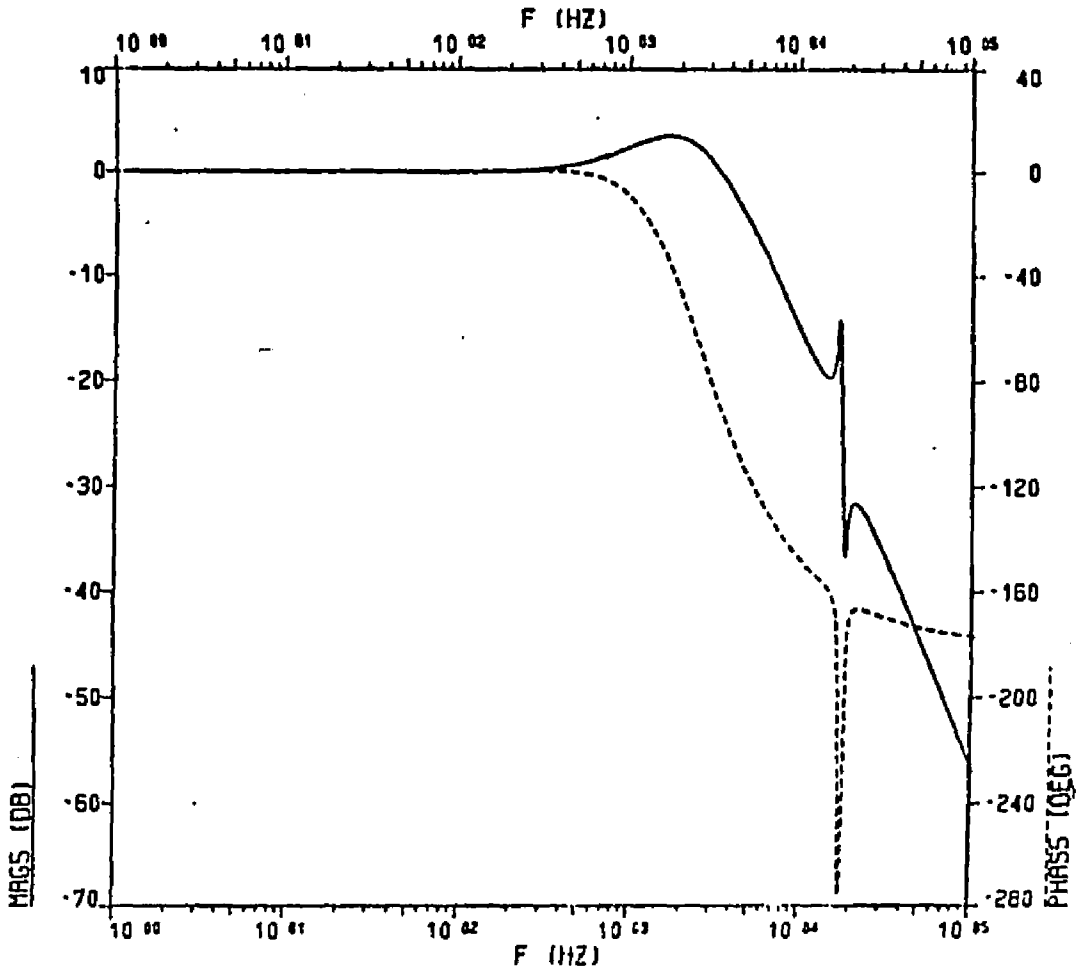

Figure 12. Bode Plot of the Fine Actuator Servo Closed Loop Transfer Function (45 Degree Phase Margin)

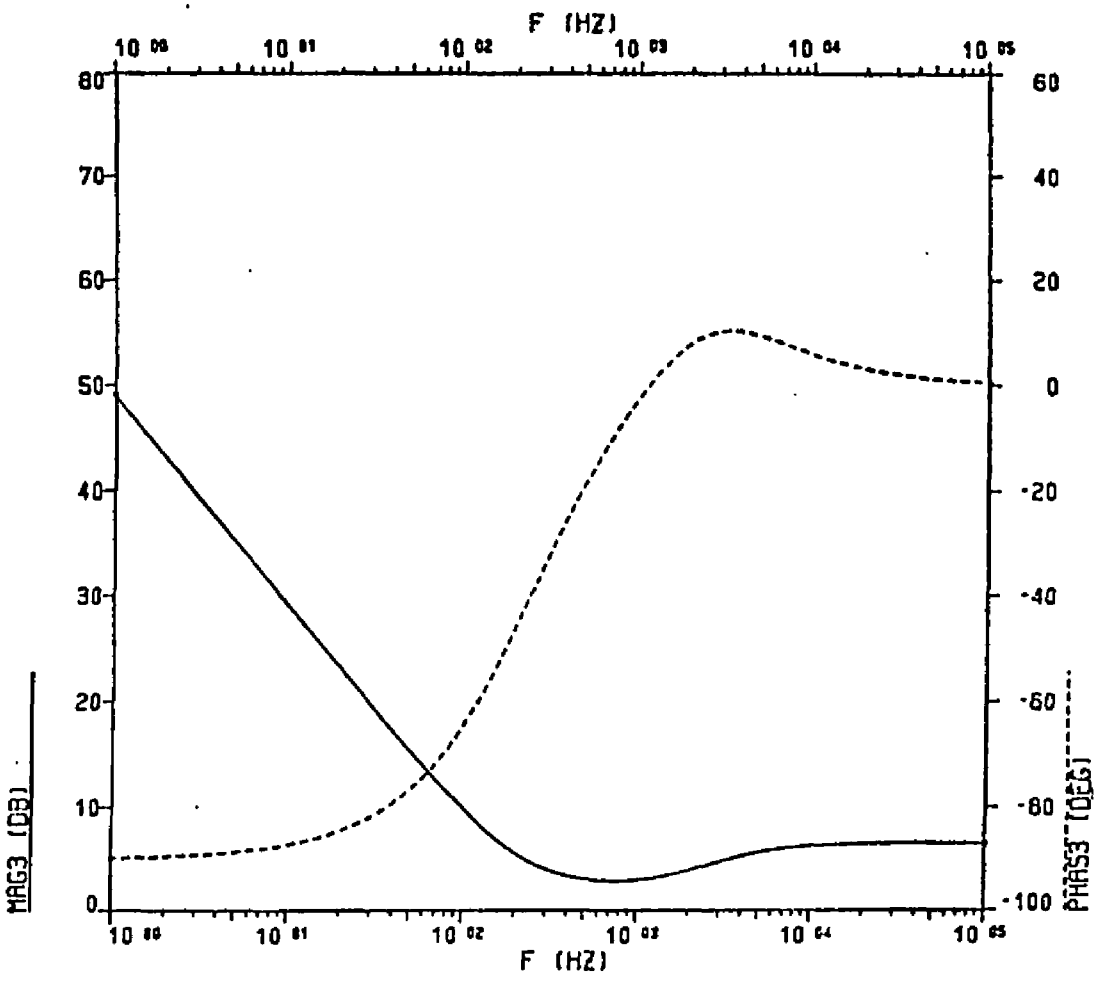

Figure 13. Bode Plot of the Fine Actuator Servo Compensation for 10 Degree Phase Margin

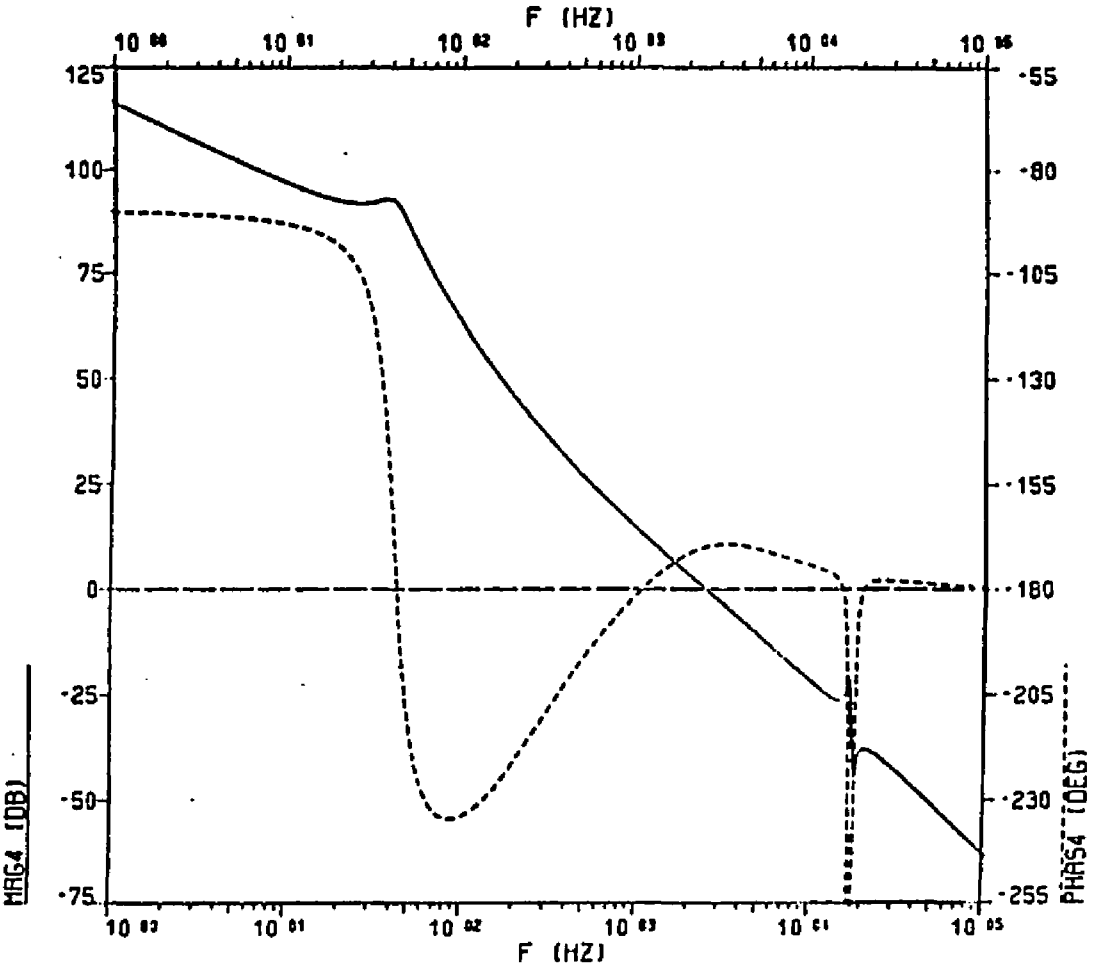

Figure 14. Bode Plot of the Fine Actuator Servo Open Loop Transfer Function (10 Degree Phase Margin)

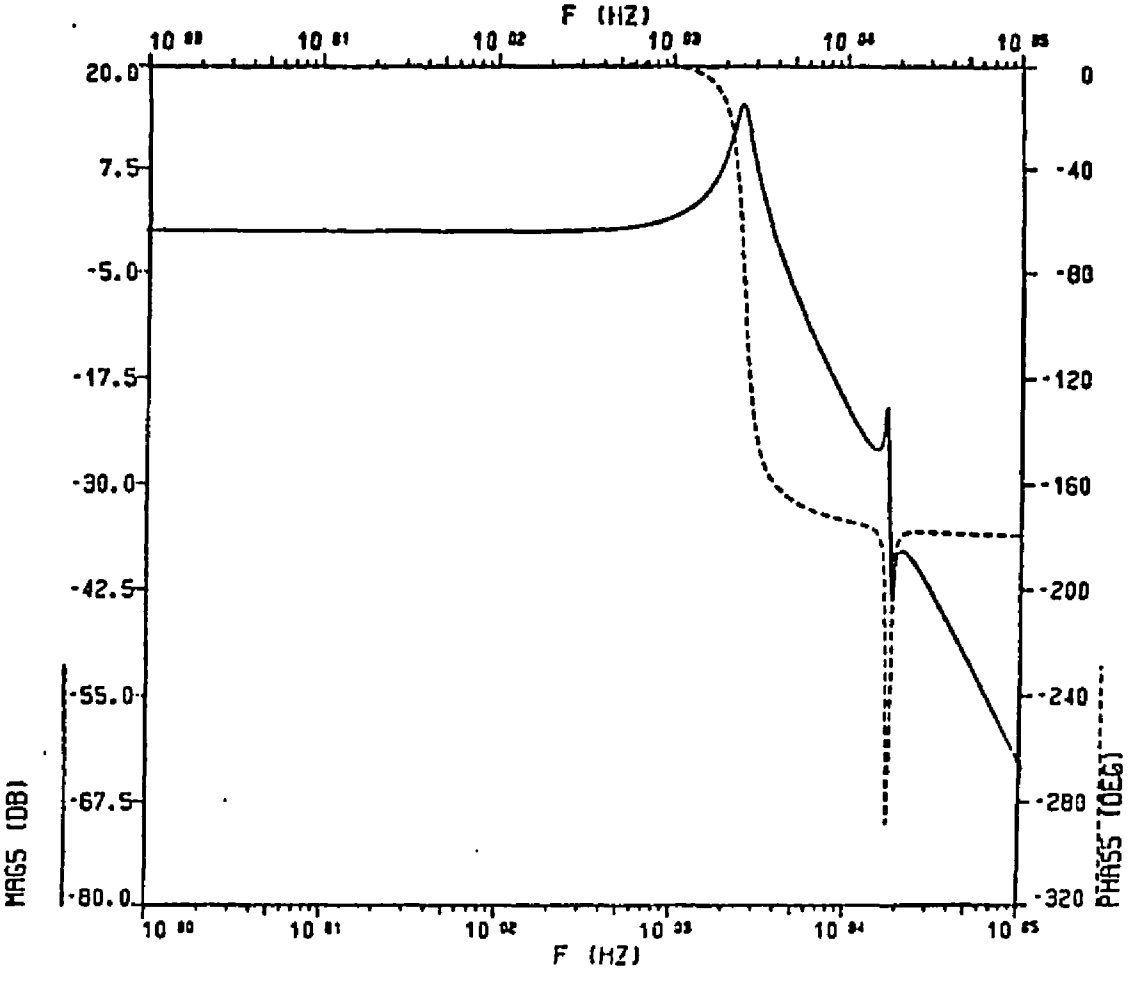

Figure 15. Bode Plot of the Fine Actuator Servo Closed Loop Transfer Function (10 Degree Phase Margin)

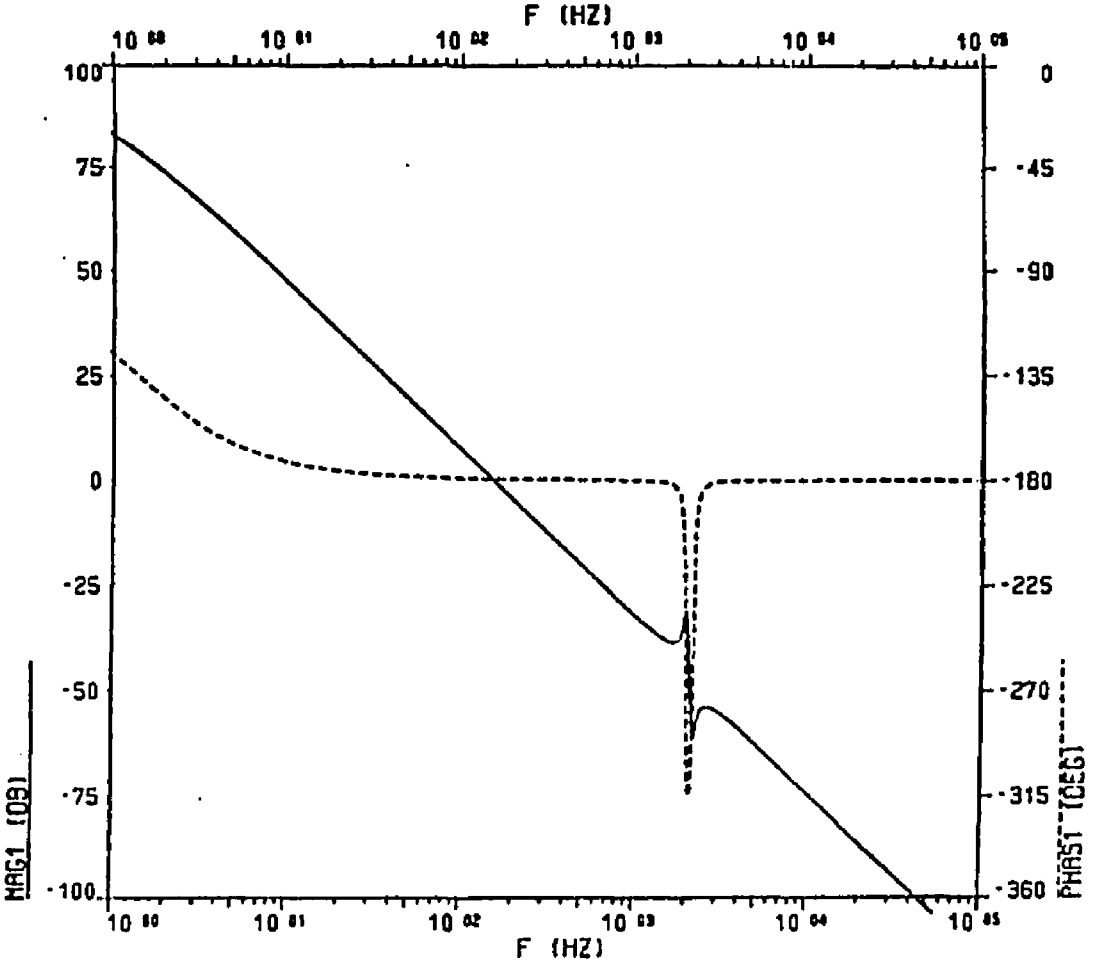

Figure 16. Bode Plot of the Coarse Actuator and Sensor

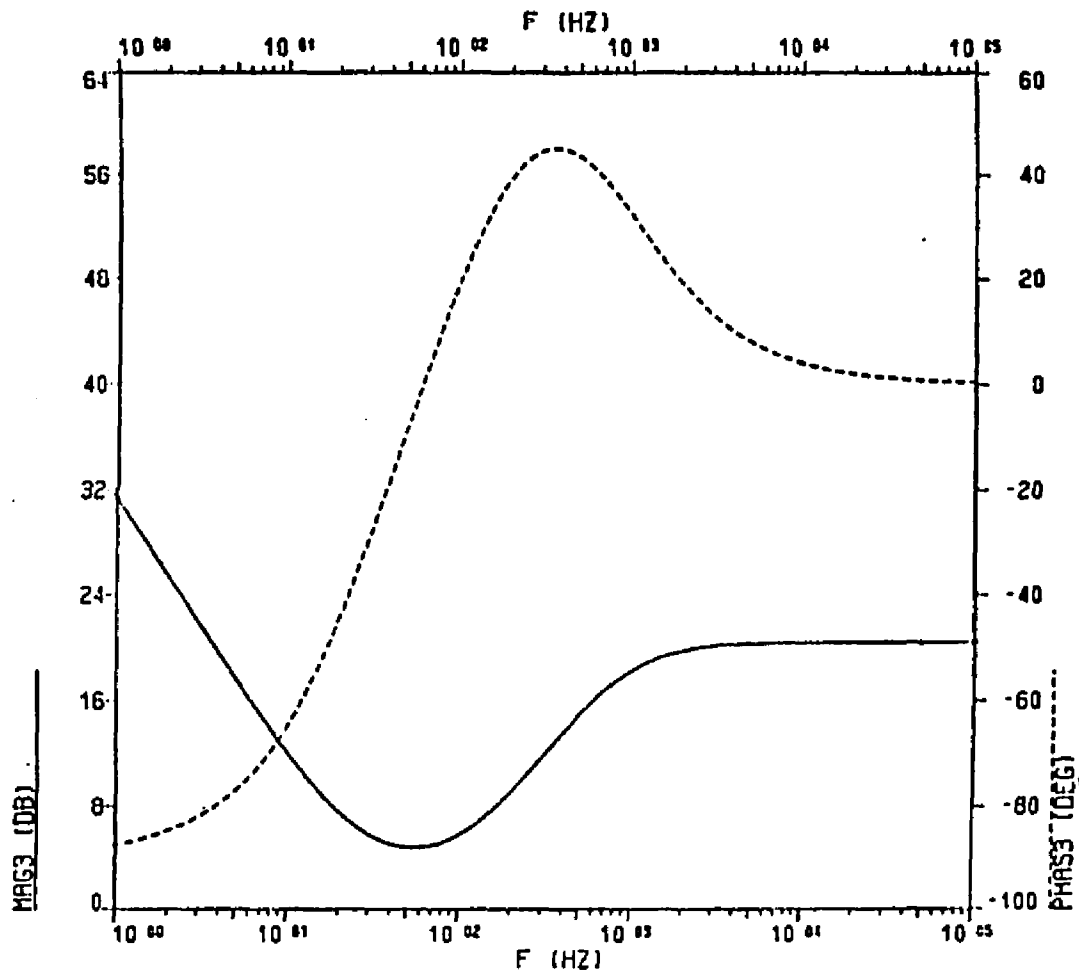

Figure 17. Bode Plot of the Coarse Actuator Servo Compensation for 45 Degree Phase Margin

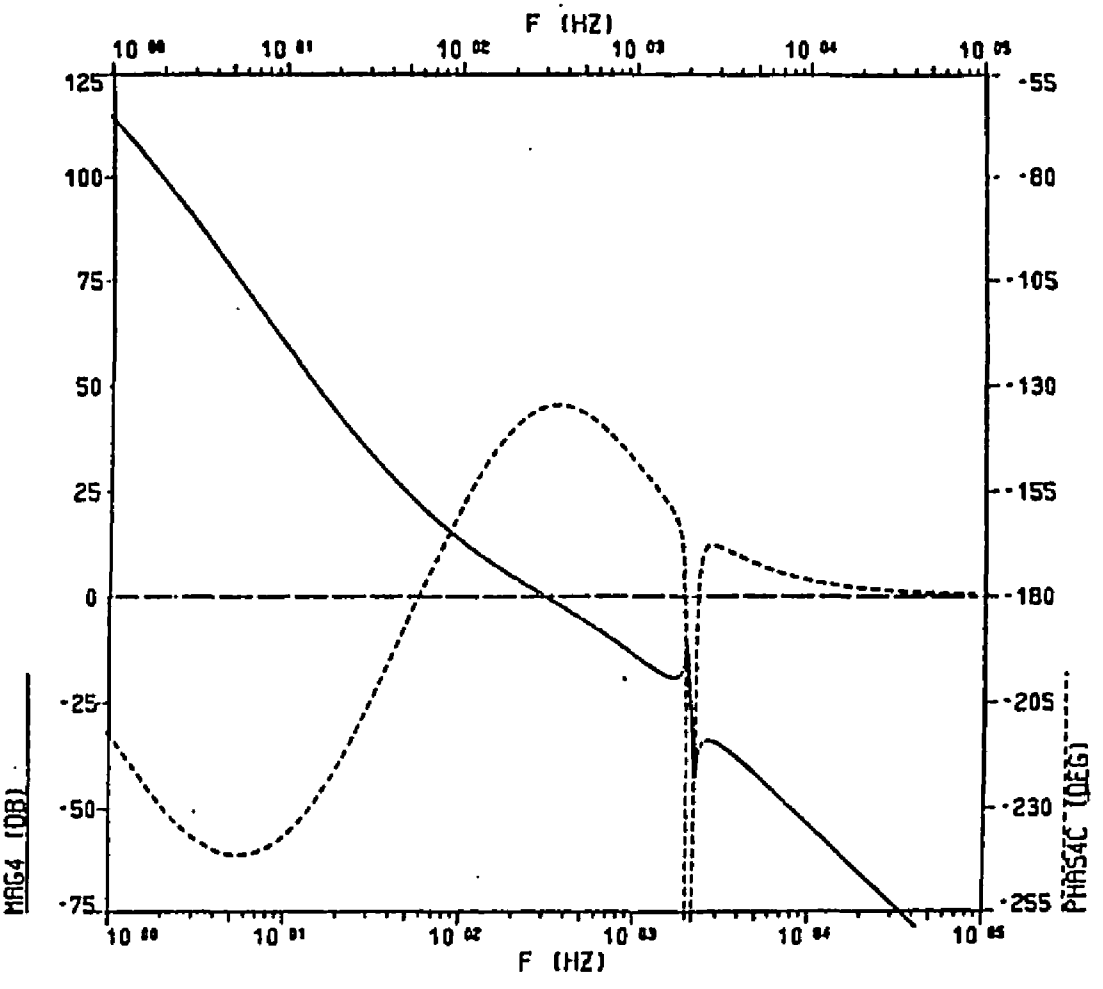

Figure 18. Bode Plot of the Coarse Actuator Servo Open Loop Transfer Function (45 Degree Phase Margin)

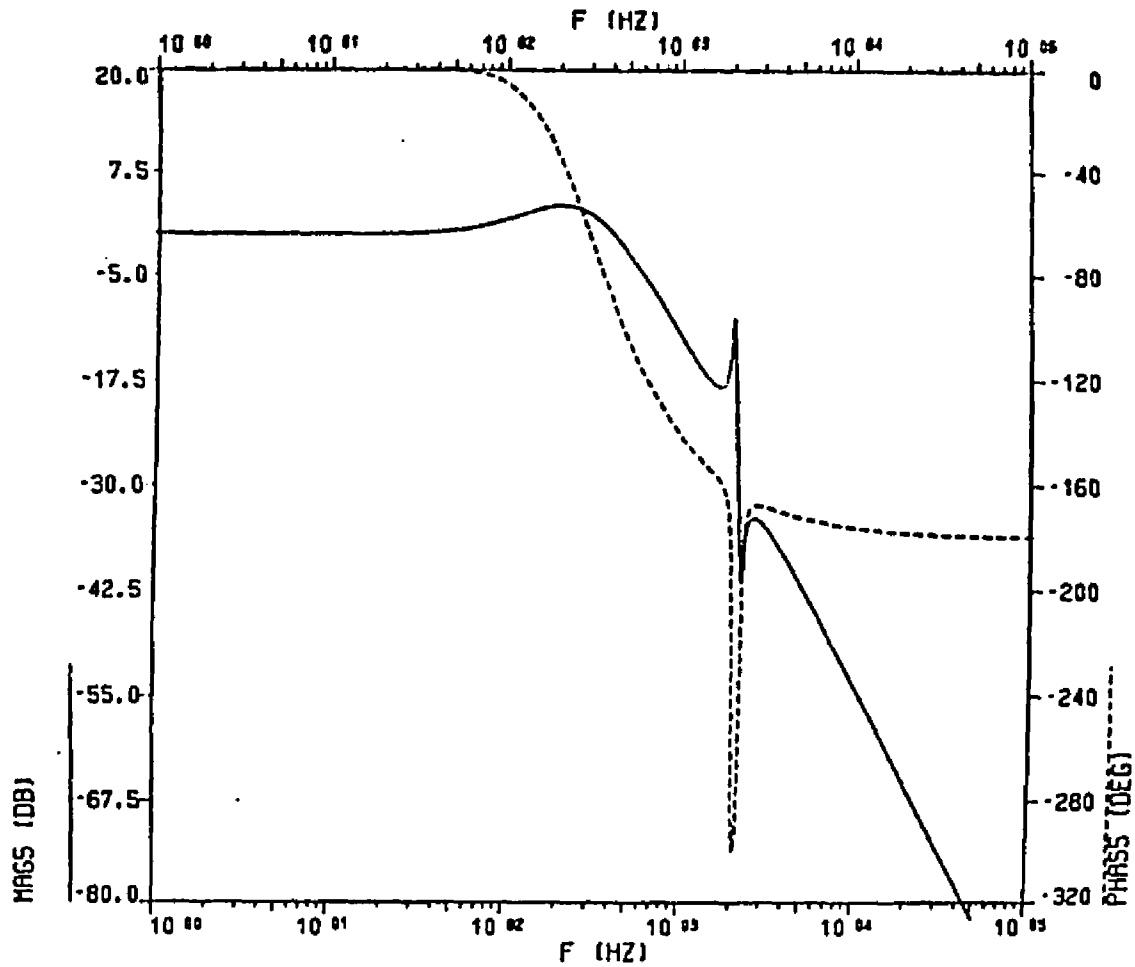

Figure 19. Bode Plot of the Coarse Actuator Servo Closed Loop Transfer Function (45 Degree Phase Margin)

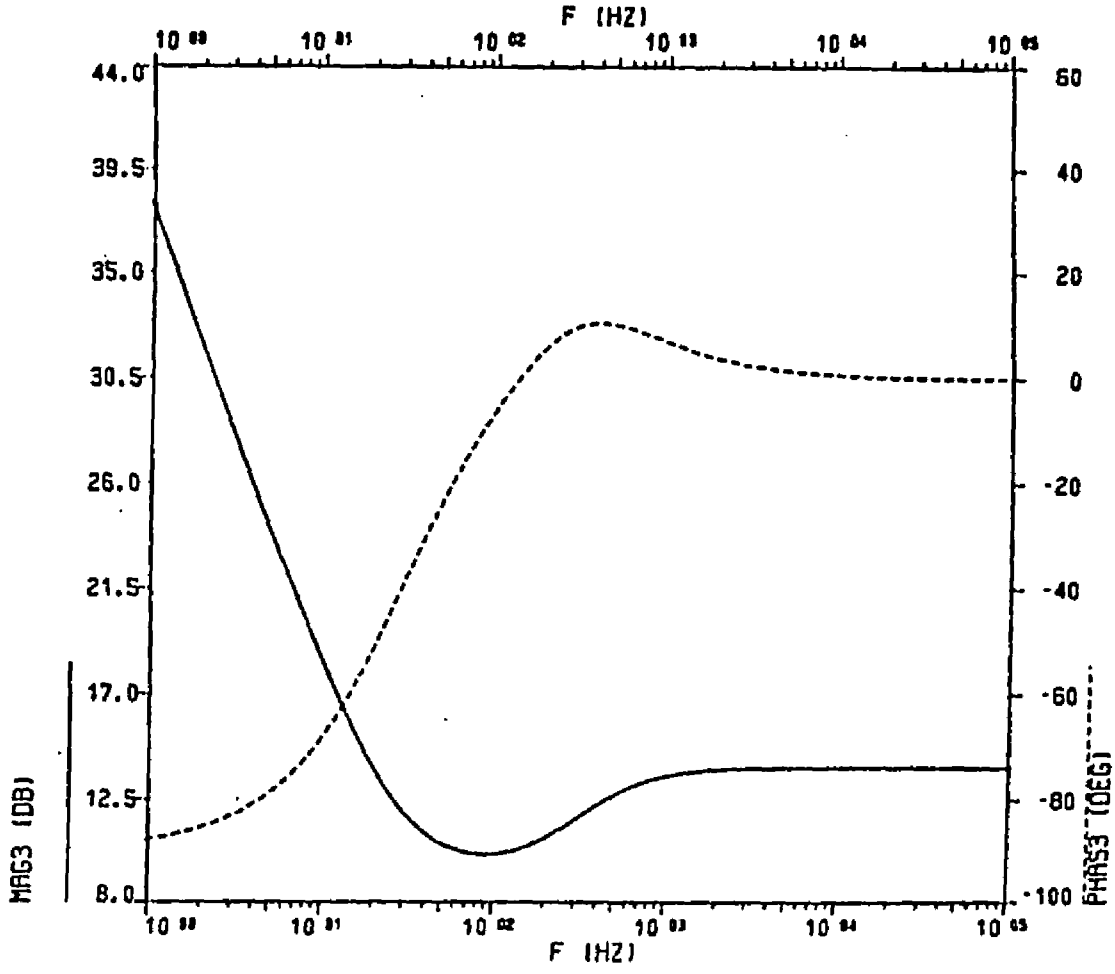

Figure 20. Bode Plot of the Coarse Actuator Servo Compensation for 10 Degree Phase Margin

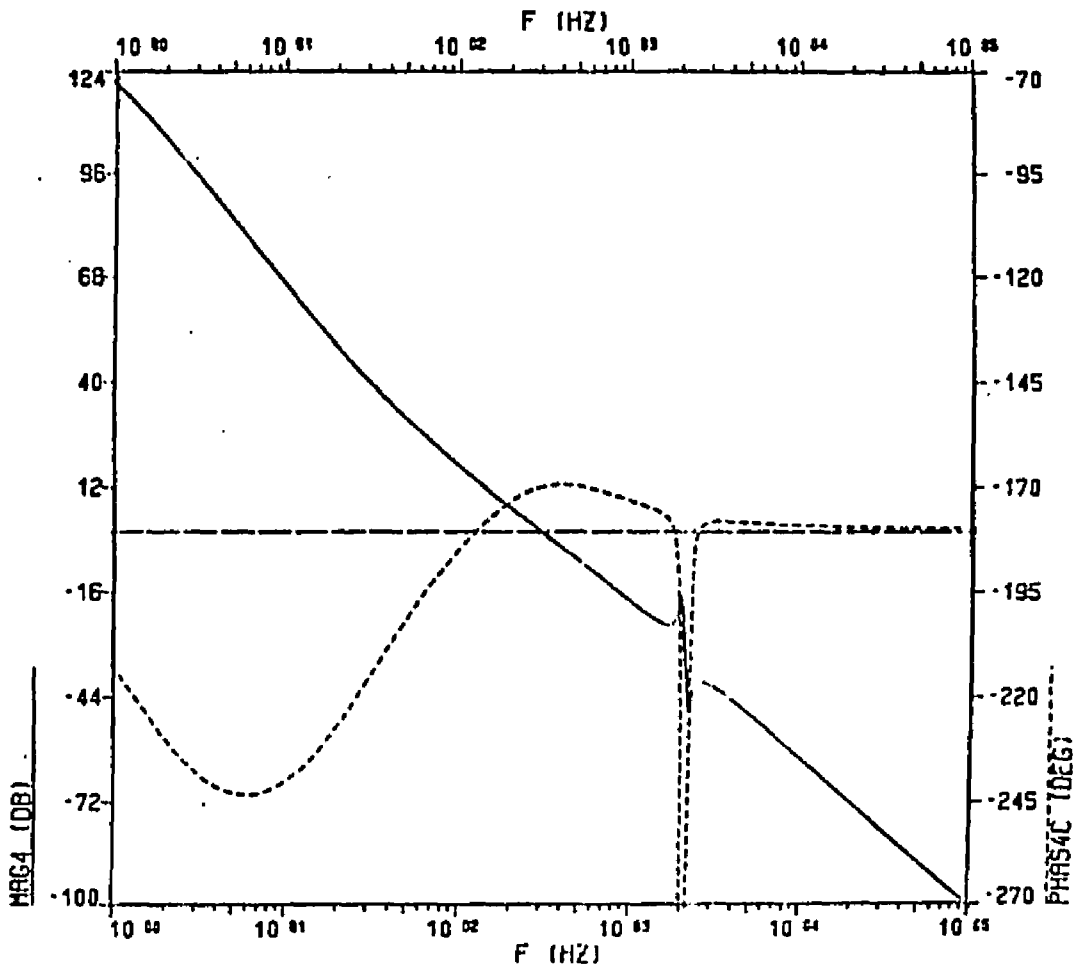

Figure 21. Bode Plot of the Coarse Actuator Servo Open Loop Transfer Function (10 Degree Phase Margin)

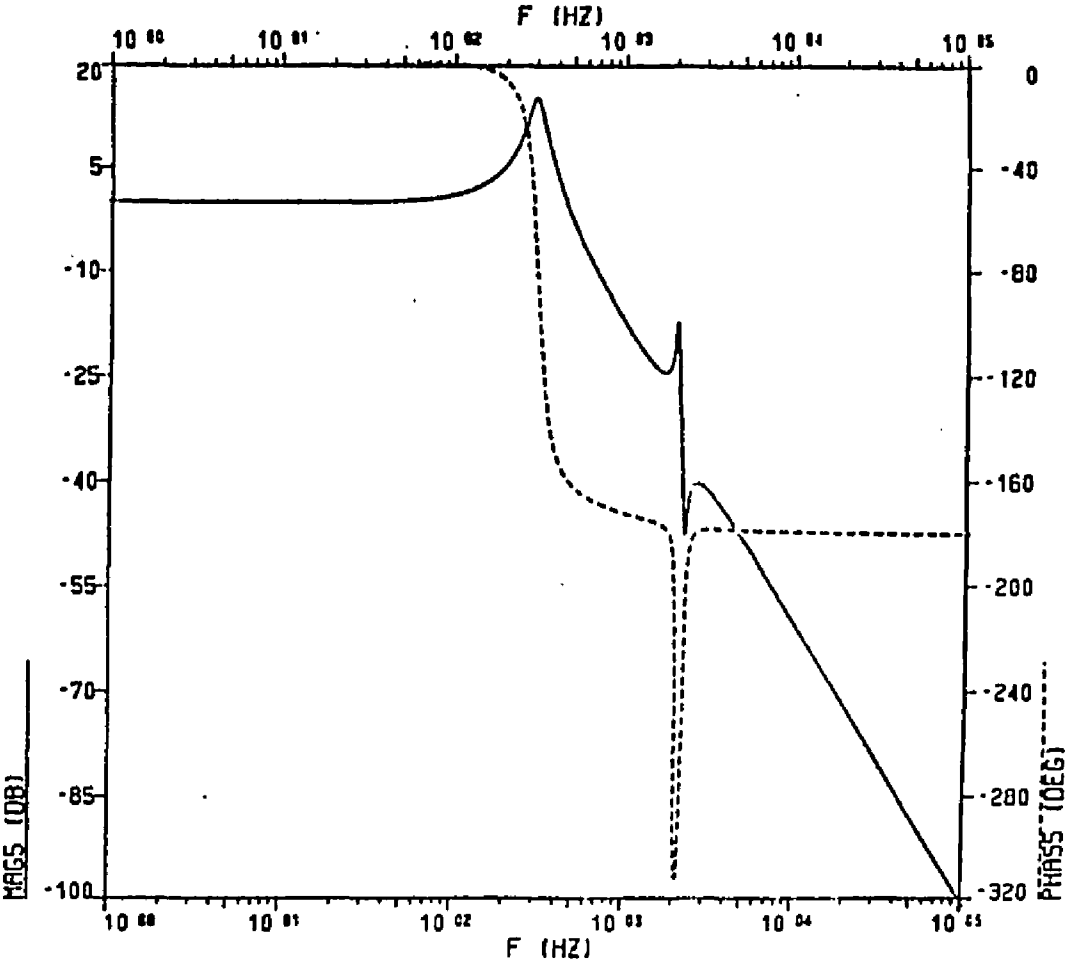

Figure 22. Bode Plot of the Coarse Actuator Servo Closed Loop Transfer Function (10 Degree Phase Margin)

Digital Compensator. Different sampling frequencies were used in the simulation experiments in order to determine their influence on the dynamic performance of the digitally compensated system. The minimum sampling frequencies were selected as a result of preliminary simulations demonstrating instabilities in the servomechanisms for lower sampling frequencies when the computation delay is minimal (1 nsec) and a 16 bit controller is used. An adequate number of significant figures have been included for the coefficients of the difference equation to avoid roundoff errors from influencing the time domain simulation output. The particular sampling frequencies used in this study have been chosen for illustrative purposes only.

The coefficients of the difference equation that describes the compensation used in the fine actuator servomechanism for a 45 degree and a 10 degree phase margin system are given in Table 3.

The coefficients of the difference equation that describes the compensation used in the coarse actuator servomechanism for a 45 degree and a 10 degree phase margin system are given in Table 4.

Table 3

Digital Compensation for the Fine Actuator Servomechanism

System #1 (PM=45):

Coefficient	Sampling Frequencies 10Khz	15Khz	30Khz
a_0	1.0139005	1.0578123	1.2404418
a_1	-1.39004867E-2	-5.78122677E-2	-0.24044182
b_0	1.4683778	1.8834203	2.7089560
b_1	-2.1044002	-3.0004864	-4.8225930
b_2	0.71868922	1.1697224	2.1348616

System #2 (PM=10):

Coefficient	Sampling Frequencies 30Khz	60Khz
a_0	1.5075544	1.7124285
a_1	-0.50755441	-0.71242853
b_0	1.9241248	2.0184915
b_1	-3.1222559	-3.6218616
b_2	1.2267803	1.6117352

Table 4

Digital Compensation for the Coarse Actuator Servomechanism

System #1 (PM=45):

Coefficient	Sampling Frequencies 10Khz	15Khz	30Khz
a_0	1.5977453	1.7095954	1.8423749
a_1	-0.59774534	-0.70959541	-0.84237487
b_0	8.5108295	9.0870851	9.7255805
b_1	-16.314643	-17.666007	-19.176563
b_2	7.8131004	8.5833919	9.4521957

System #2 (PM=10):

Coefficient	Sampling Frequencies 30Khz	60Khz
a_0	1.9216994	1.9600518
a_1	-0.92169939	-0.96005176
b_0	4.8672973	4.9003688
b_1	-9.4778601	-9.6700780
b_2	4.6118240	4.7700309

CHAPTER 3

MODEL VALIDATION

Technique

The frequency domain simulation results from the DSL program will be validated by use of a HP3562A Dynamic System Analyzer. The DSL frequency domain plots will be compared to the resultant plots from equivalent transfer functions synthesized on the HP analyzer. If the plots obtained on the analyzer compare favorably with the DSL program plots, then the assumption that the DSL program is accurately modelling the system can be made.

HP3562A Dynamic System Analyzer

The HP3562A dynamic system analyzer is a microprocessor based test instrument designed to support the development of control systems. It provides a variety of features. The instrument has a built in signal generator. The analysis capabilities provide waveform math, curve fitting, and coherence information. Modelling capabilities allow the synthesis of transfer functions to be made. This is the feature used in this thesis for validating the DSL model.

DSL - HP3562A Comparisons

The following Bode plots were generated on the HP3562A Dynamic System Analyzer. The graph format and axis ranges were purposely made the same as in the DSL Bode plots described in the previous chapter for easy comparison. Figures 23 through 25 are of the fine actuator's servomechanism with a 45 degree phase margin. Figures 26 and 27 are of the fine actuator's servomechanism with a 10 degree phase margin. Figures 28 through 30 are of the coarse actuator's servomechanism with a 45 degree phase margin. Figures 31 and 32 are of the coarse actuator's servomechanism with a 10 degree phase margin. The Bode plots correlate very well with the DSL model. Therefore, the DSL model must be void of programming errors and is an accurate frequency domain representation of the servo systems.

Figure 23 is the Bode plot of the fine actuator and sensor. This Bode plot is to be compared with Figure 9. The photograph located in the upper right hand corner is of the synthesis table of the HP3562A analyzer. The table contains the gain, pole, and zero values of the synthesized transfer function. A photograph of the synthesis table for each of the following Bode plots will be included on the graph. Figure 24 is the Bode plot of the analog compensator that will provide a 45 degree phase margin for the fine actuator servomechanism. This Bode plot is to be compared with Figure 10. The analyzer has cursors that enable the user to obtain an accurate numerical value for a desired location on the curve. The

location of the cursors are denoted by small circles on the curve. The cursors have been placed at the open loop bandwidth of this servo (2.5 Khz.). The value read from the graph at the location of the cursors is printed on the upper left hand corner. The phase is 44.7 degrees and the magnitude is 4.5 dB. The cursor feature is utilized in several of the graphs that follow. Figure 25 is a Bode plot of the fine actuator servomechanism's open loop transfer function. This plot is to be compared with Figure 11. The open loop bandwidth is 2.5 Khz.. The phase margin is 45 degrees and the gain margin is 17 dB.

Figure 26 is the Bode plot of the analog compensator that will provide a 10 degree phase margin for the fine actuator servomechanism. This plot is to be compared with Figure 13. The amount of phase lead at the open loop bandwidth is 9.7 degrees. Figure 27 is the Bode plot of the open loop transfer function. The bandwidth is 2.5 Khz.. The phase margin is 10 degrees and the gain margin is 26 dB.

Figure 28 is the Bode plot of the coarse actuator and sensor. This Bode plot is to be compared with Figure 16. Figure 29 is the Bode plot of the analog compensator that will provide a 45 degree phase margin for the coarse actuator servomechanism. This Bode plot is to be compared with Figure 17. The cursors have been placed at the open loop bandwidth of this servo (300 Hz.). The phase is 44.7 degrees and the magnitude is 11.6 dB. Figure 30 is a Bode plot of the coarse actuator servomechanism's open loop transfer function. This plot is to be compared with Figure 18.

The open loop bandwidth is 300 Hz.. The phase margin is 45 degrees and the gain margin is 14.9 dB.

Figure 31 is the Bode plot of the analog compensator that will provide a 10 degree phase margin for the coarse actuator servomechanism. This plot is to be compared with Figure 20. The amount of phase lead at the open loop bandwidth is 9.7 degrees. Figure 32 is the Bode plot of the open loop transfer function. The bandwidth is 300 Hz.. The phase margin is 10 degrees and the gain margin is 24.5 dB.

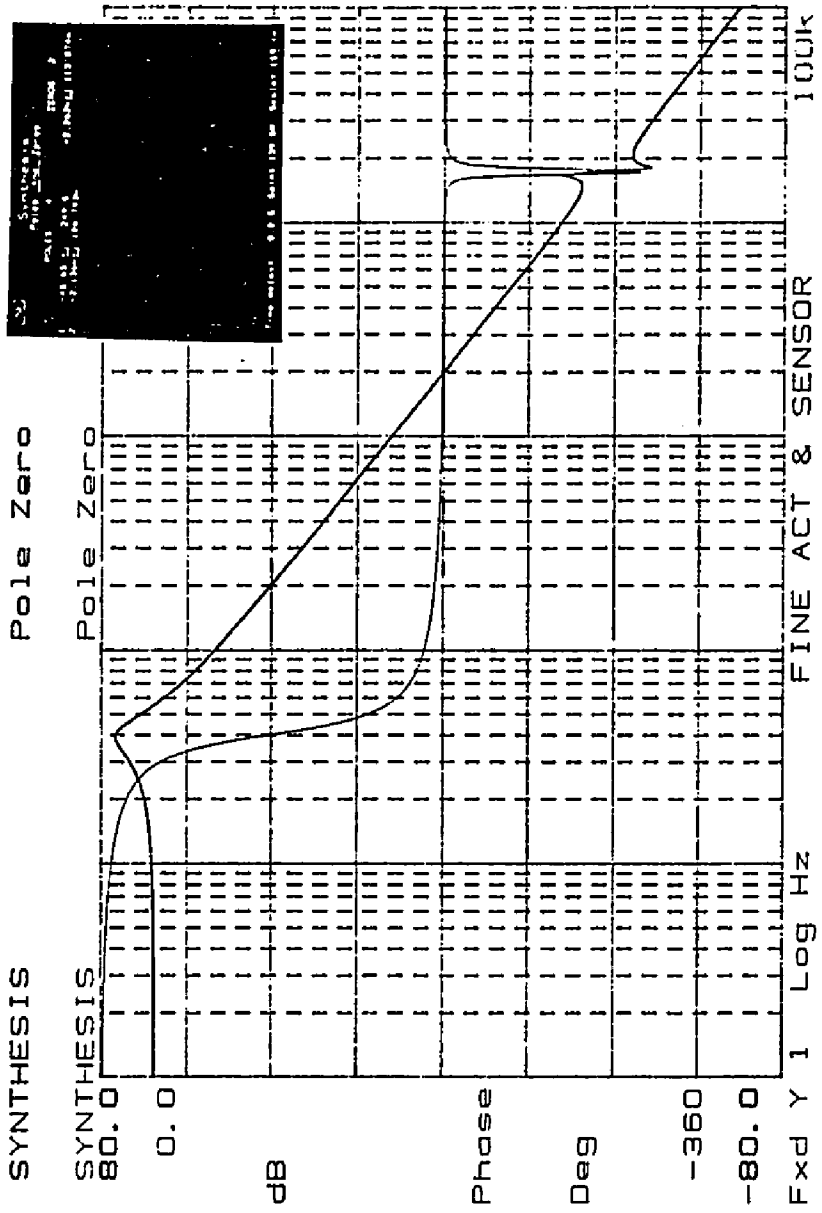

Figure 23. Bode Plot of the Fine Actuator and Sensor

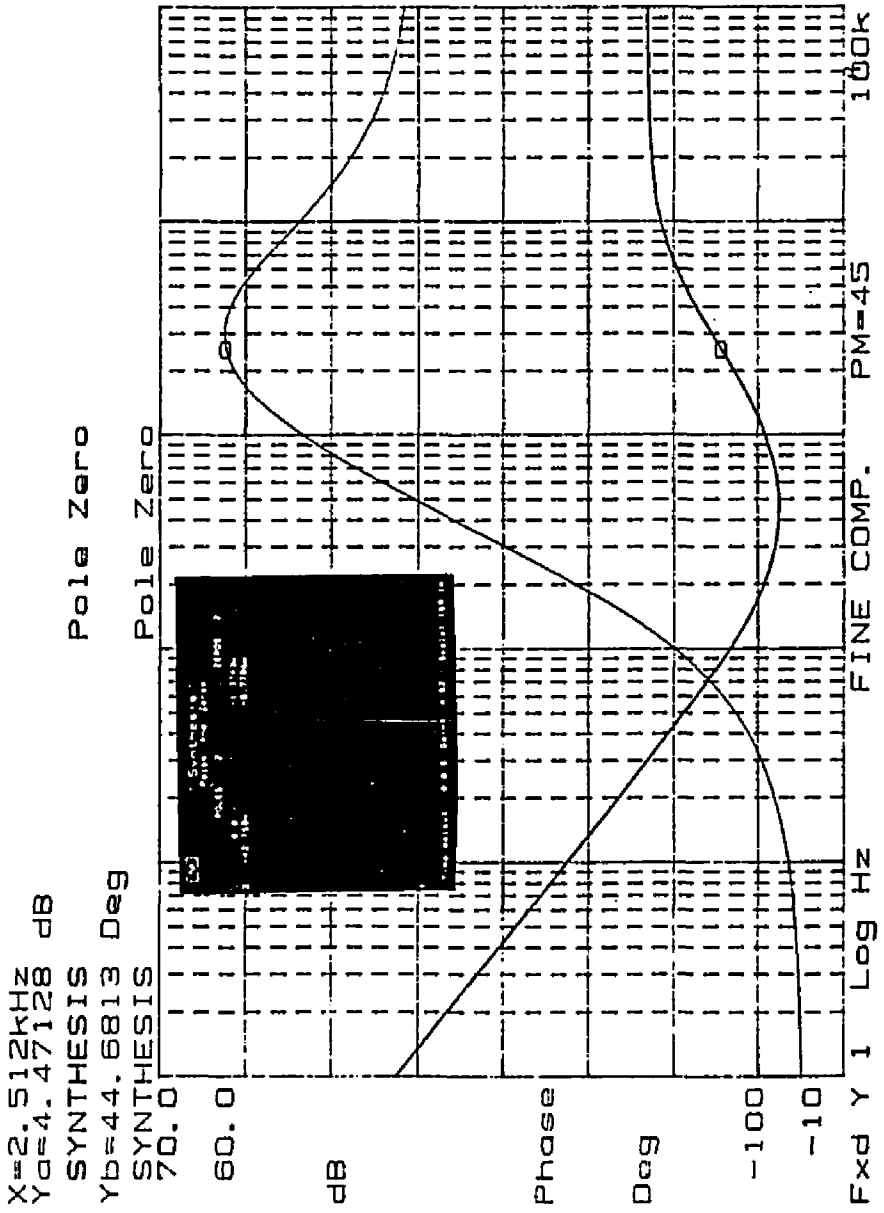

Figure 24. Bode Plot of the Fine Actuator Servo Compensation for 45 Degree Phase Margin

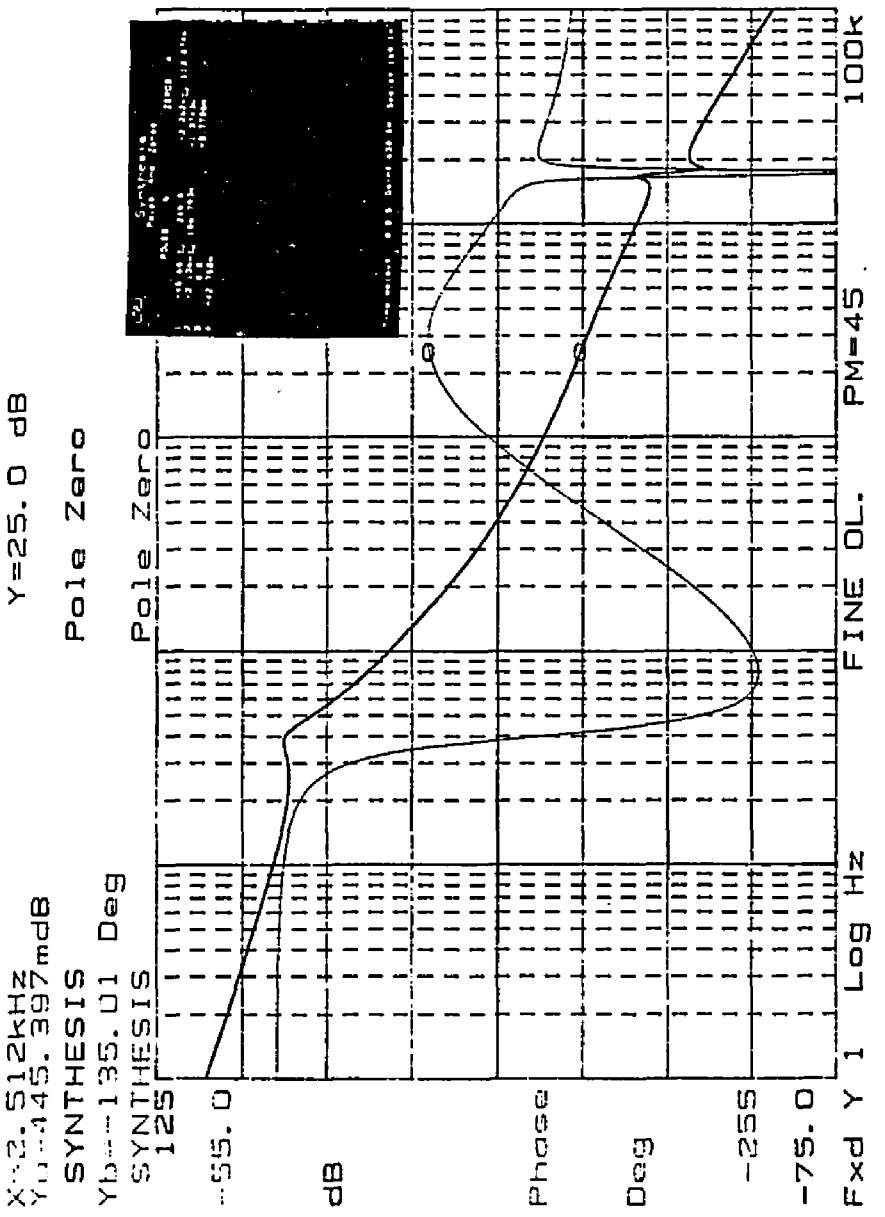

Figure 25. Bode Plot of the Fine Actuator Servo Open Loop Transfer Function (45 Degree Phase Margin)

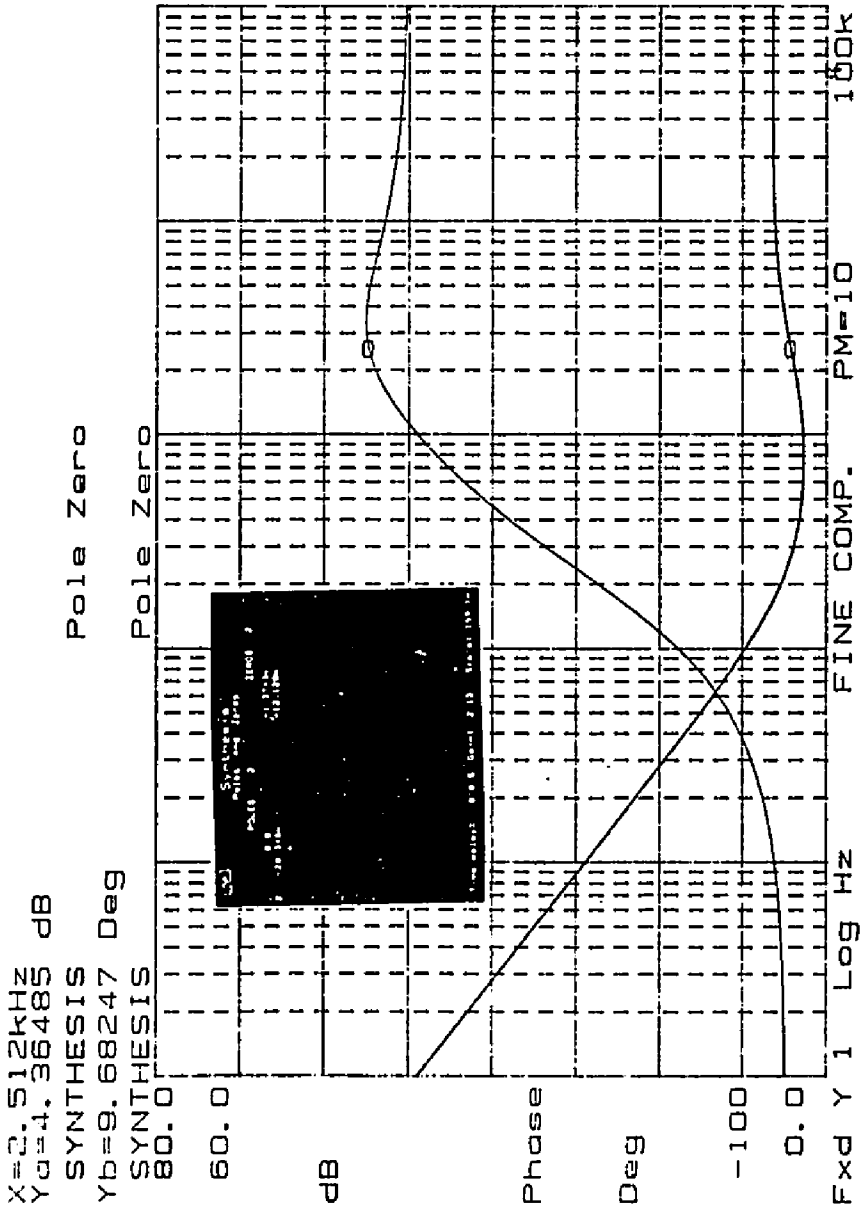

Figure 26. Bode Plot of the Fine Actuator Servo Compensation for 10 Degree Phase Margin

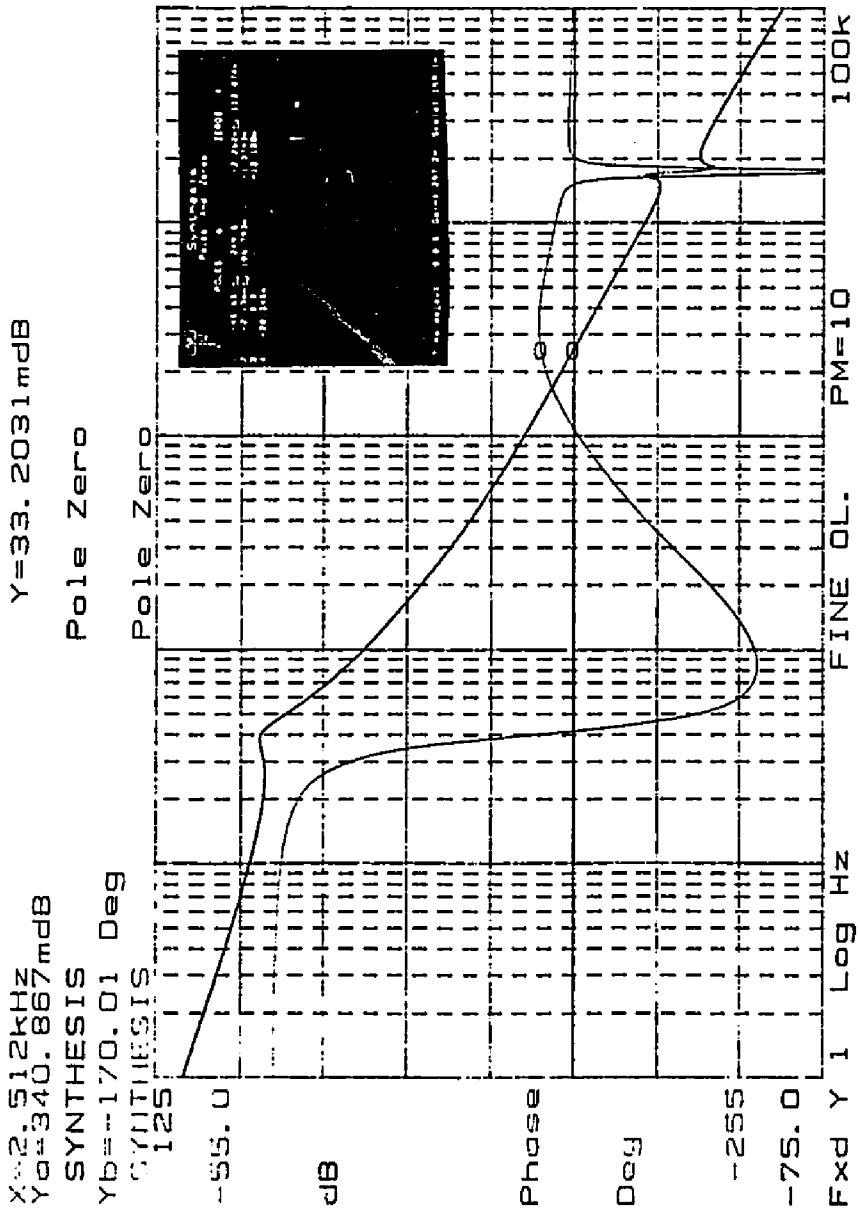

Figure 27. Bode Plot of the Fine Actuator Servo Open Loop Transfer Function (10 Degree Phase Margin)

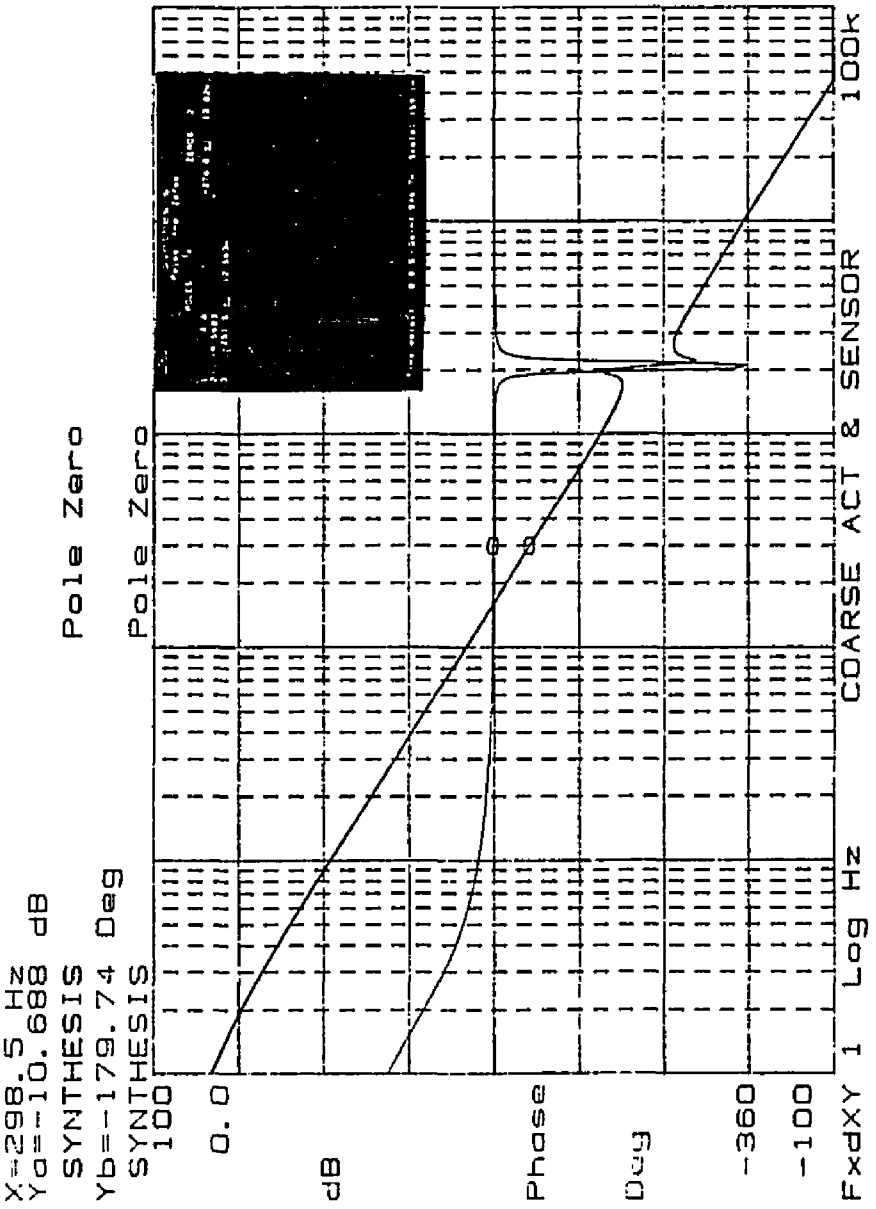

Figure 28. Bode Plot of the Coarse Actuator and Sensor

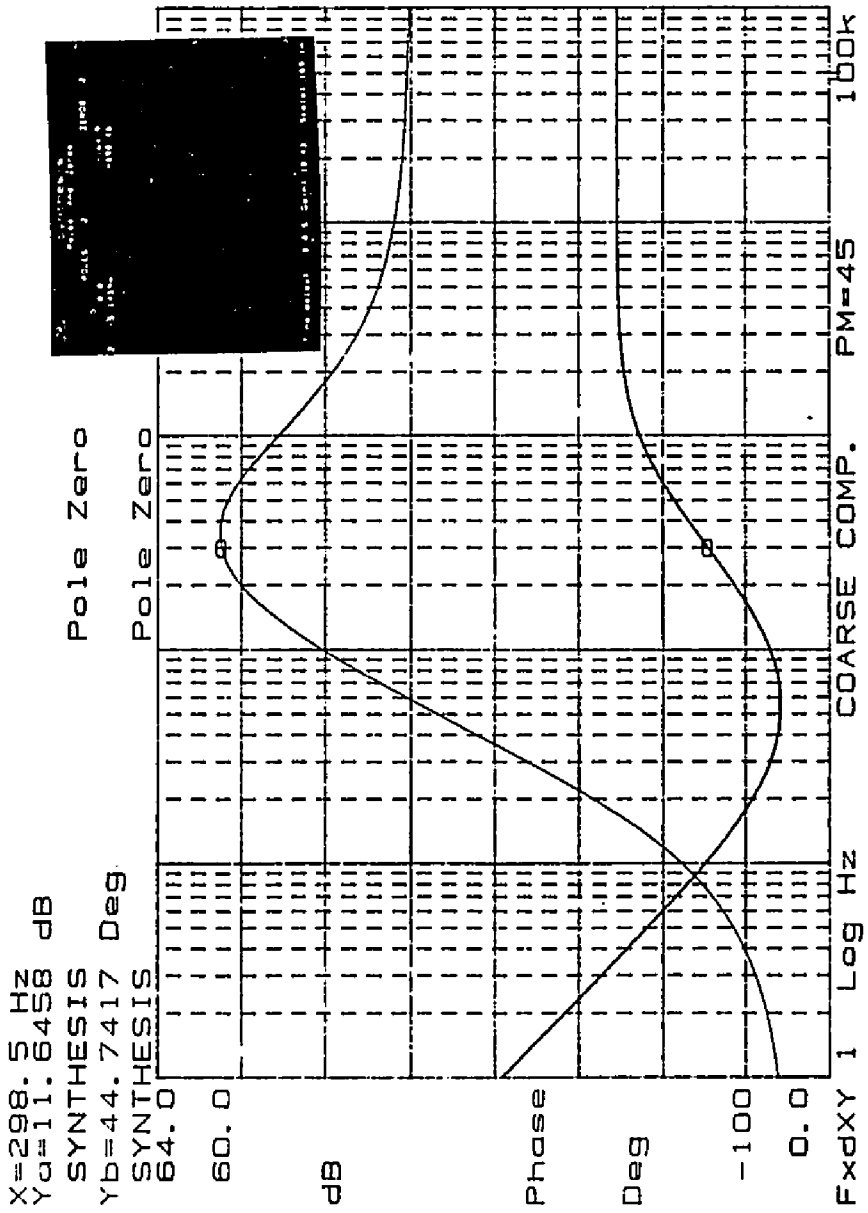

Figure 29. Bode Plot of the Coarse Actuator Servo Compensation for 45 Degree Phase Margin

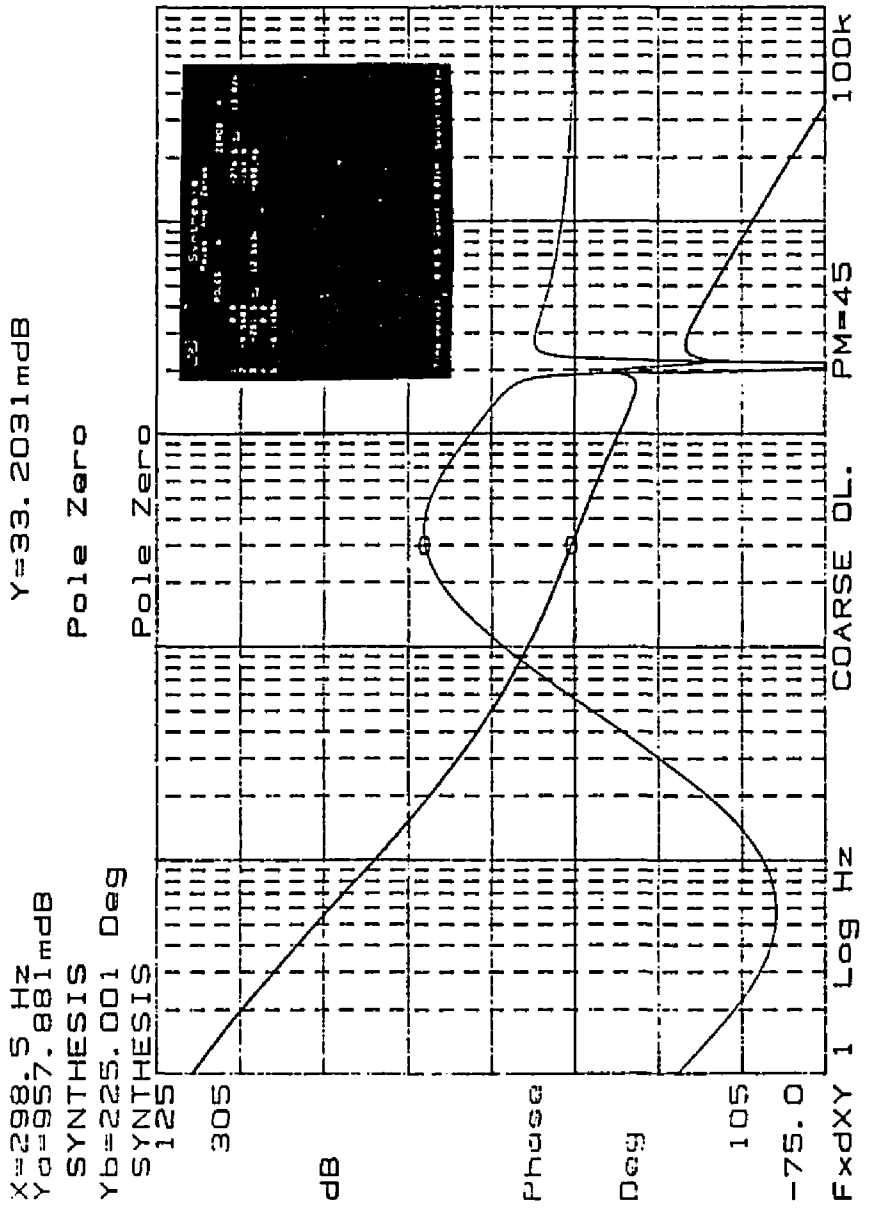

Figure 30. Bode Plot of the Coarse Actuator Servo Open Loop Transfer Function (45 Degree Phase Margin)

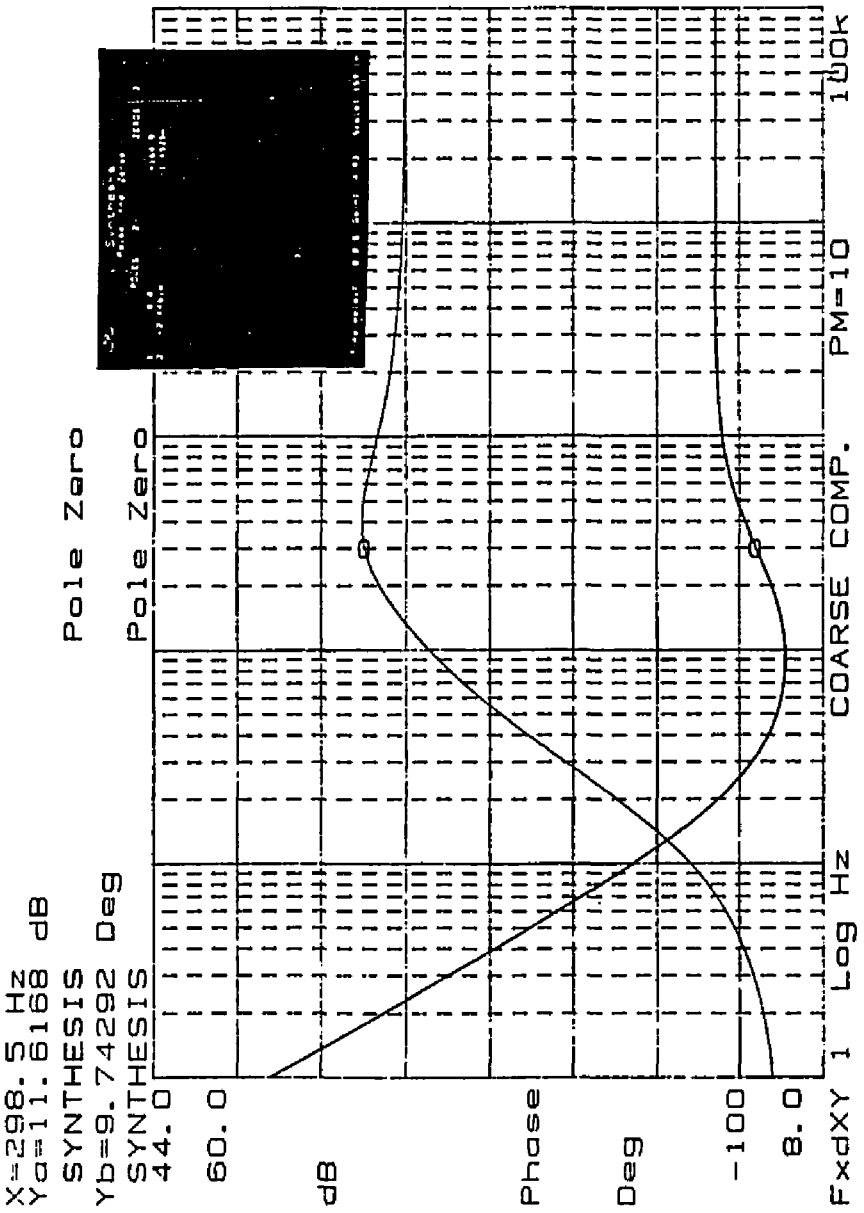

Figure 31. Bode Plot of the Coarse Actuator Servo Compensation for 10 Degree Phase Margin

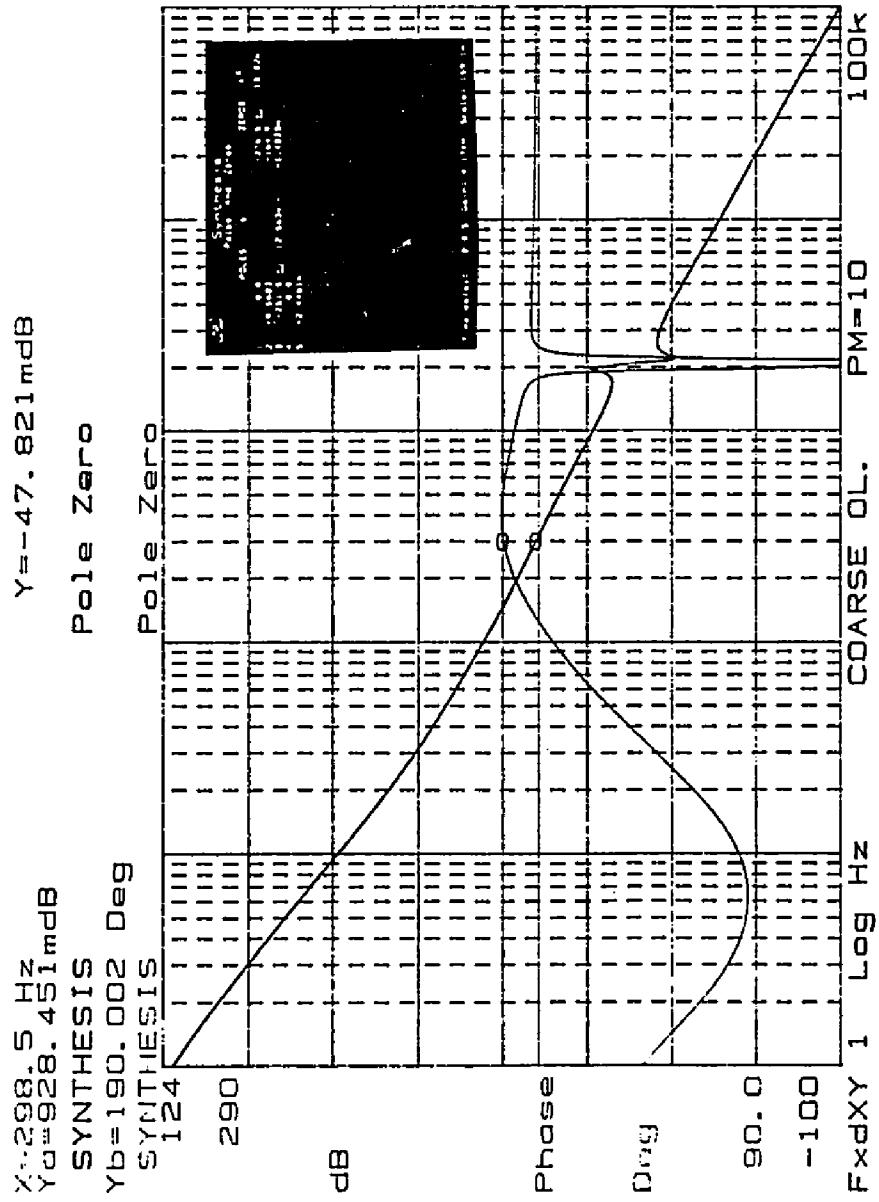

Figure 32. Bode Plot of the Coarse Actuator Servo Open Loop Transfer Function (10 Degree Phase Margin)

CHAPTER 4

CONTROLLER DEVELOPMENT AND PERFORMANCE ANALYSIS

DSL Time Domain Program Structure

The DSL time domain program simulates the dual actuator servomechanism whose parameters have been previously discussed. The listing of the DSL program is given in Appendix C. The program simultaneously simulates an analog and a digitally compensated servo system as they follow the same track on a rotating disk. The net result will be to compare the track following characteristics of the servomechanisms and reach some conclusions on the requirements of the digitally compensated systems.

Initial Segment

All variables are assigned their numerical values in this segment. DSL control parameters such as simulation time and integration technique are initialized here. A fourth order fixed step Runge-Kutta integration technique is used in this program. Some initial simulations were run and it was found that an integration interval of 200 nsec. was adequate. The simulation output was not influenced by smaller integration intervals ; however, the output was influenced by larger intervals. A total CPU time of approximately 54 minutes is required for a complete simulation run.

Derivative Segment

All equations describing the dynamics of the analog portion of the servomechanisms are located in the derivative segment. These include:

1. track dynamics,
2. tracking error sensors,
3. fine actuator analog compensation,
4. fine actuator power amplifiers,
5. fine actuator electromechanics,
6. relative position sensors,
7. coarse actuator analog compensation,
8. coarse actuator power amplifiers,
9. coarse actuator electromechanics.

Sample Segment

The sample segment models the digital compensator. This segment is entered twice per sampling period. At the sampling instant it is entered to measure and quantize the compensator input. It is also entered a prescribed period of time after the sampling instant to output the recently calculated control voltage into the servomechanism's power amplifier. This period of time corresponds to the amount of computation delay specified by the user.

Dynamic Segment

This segment calculates the positional errors of the servomechanisms. The errors are used for graphical output.

Terminal Segment

This segment is entered at the completion of a simulation run. It is here that the program will determine if another simulation is to be performed as a result of the user's input. The user input specifies how many simulations are to be made corresponding to the different number of bits or computation delays to be studied. This allows the overlaying of graphs portraying servo performance as a function of number of bits or computation delay. Graph statements are also included in this segment.

Quantization Model

The voltage range to be quantized by the analog-to-digital (A/D) and the digital-to-analog (D/A) converters were determined by performing a simulation run on the analog servo. The peak-to-peak amplitude of the voltage present at the analog compensator's input and output were measured to determine the total voltage range that will need to be quantized. This measurement was performed on the fine servomechanism and the coarse servomechanism for the 45 degree and the 10 degree phase margin systems. Figures 33 though 36 are the results of the measurements. The solid line

represents the input voltage and the dotted line represents the output voltage of the analog compensator in these figures.

Figure 33 illustrates the voltages present at the input and output of the analog compensator for the fine servomechanism with a 45 degree phase margin. The maximum peak-to-peak voltage that will need to be quantized by the A/D and D/A converters is 0.2 Volts.

Figure 34 illustrates the voltages present at the input and output of the analog compensator for the fine servomechanism with a 10 degree phase margin. The maximum peak-to-peak voltage that will need to be quantized by the A/D and D/A converters is again 0.2 Volts. Notice the transient behavior near the start of the simulation prior to reaching steady state. This is a result of the low phase margin.

Figure 35 illustrates the voltages present at the input and output of the analog compensator for the coarse servomechanism with a 45 degree phase margin. The maximum peak-to-peak voltage that will need to be quantized by the A/D and D/A converters is in this case 0.7 Volts.

Figure 36 illustrates the voltages present at the input and output of the analog compensator for the coarse servomechanism with a 10 degree phase margin. The maximum peak-to-peak voltage that will need to be quantized by the A/D and D/A converters is again 0.7 Volts. The phase

margin had less influence on the magnitude of the voltages present at the input and output of the analog compensator.

The quantization levels can now be defined by dividing the total voltage range by the number of discrete levels.

$$v_{qlf}=0.2/(2^n) \tag{56}$$

$$v_{qlc}=0.7/(2^n) \tag{57}$$

where

n: denotes the number of bits.

The quantizer model approximates the continuous signal to within half a quantum level. Figure 37 illustrates the quantization effects for 16, 14, 12, and 10 bits. A 0.2 Volt range was quantized. The analog voltage is a continuous ramp. The 16 bit quantization is the small stair step voltages while the 14, 12, and 10 bit quantization are the increasingly larger stair step voltages, respectively.

The quantization of the difference equation coefficients was included in the DSL simulation program by an approach similar to the previously discussed method. The quantization range was selected as twice the largest coefficient in the recursion equation.

Computation Delay Model

The algorithm for modelling the computation delay was discussed in Section 4.1. The computation delays studied are 1 nanosecond and 3.3,

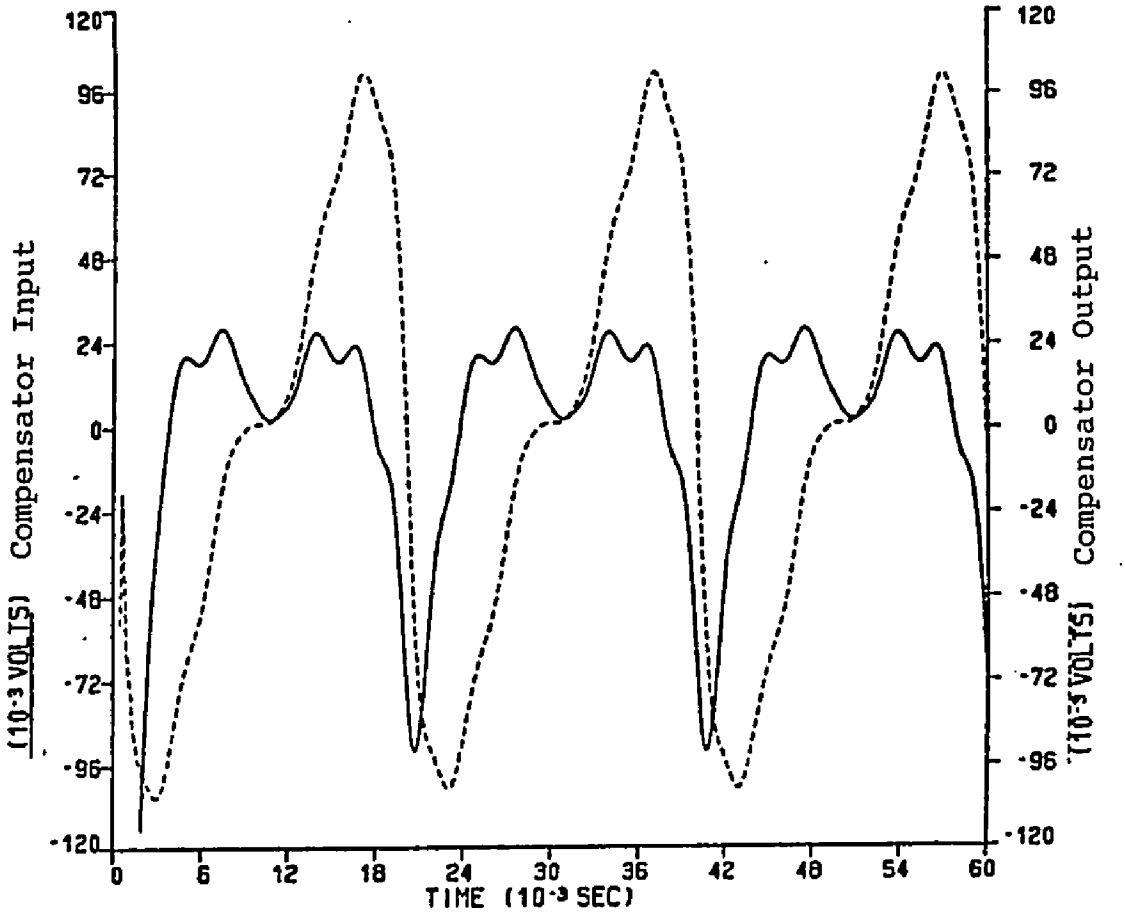

Figure 33. Analog Compensator I/O for the Fine Servo - PM=45

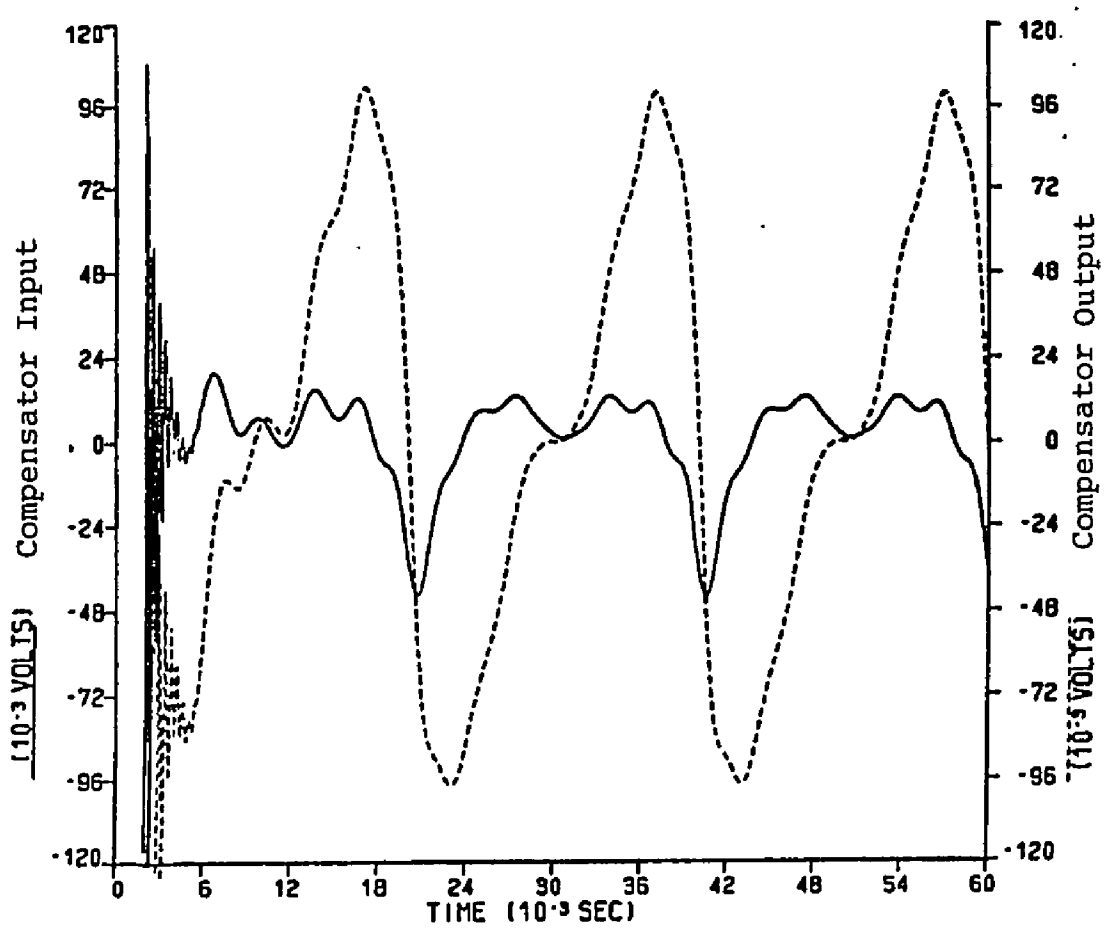

Figure 34. Analog Compensator I/O for the Fine Servo - PM=10

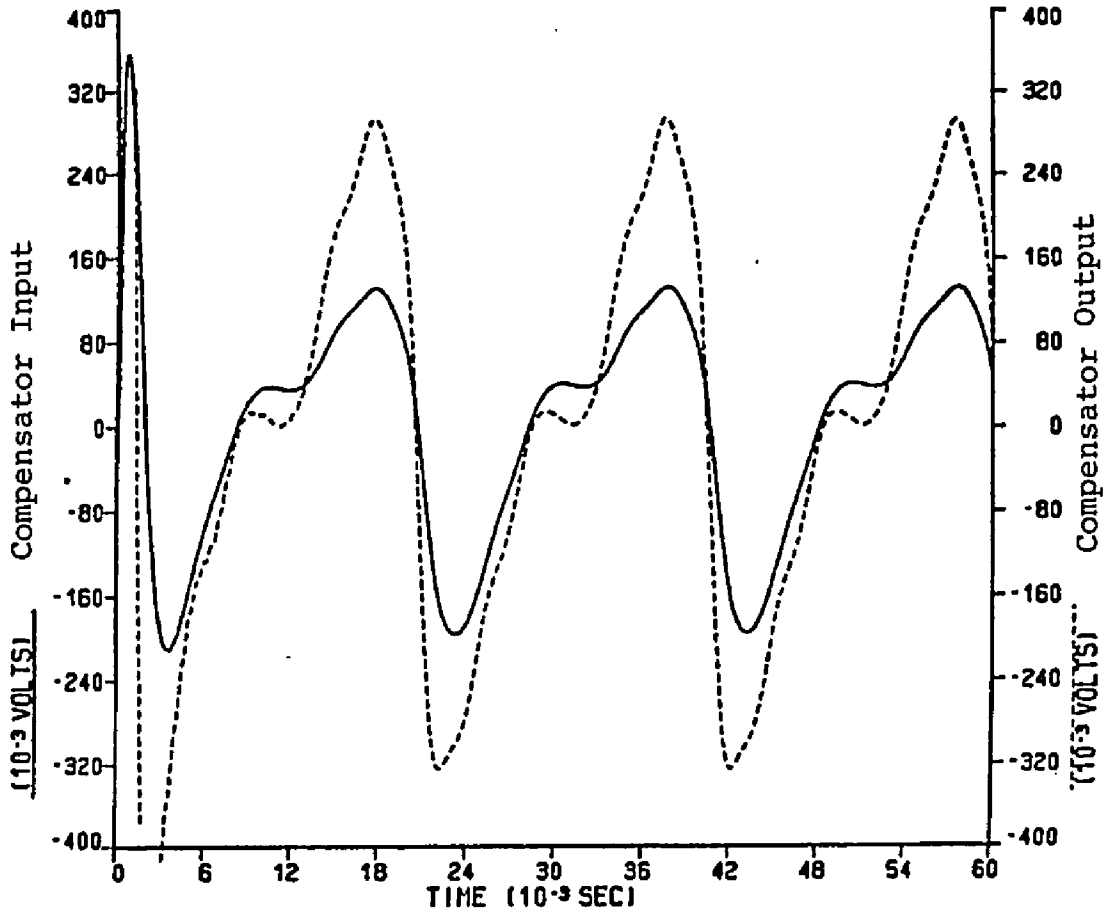

Figure 35. Analog Compensator I/O for the Coarse Servo - PM=45

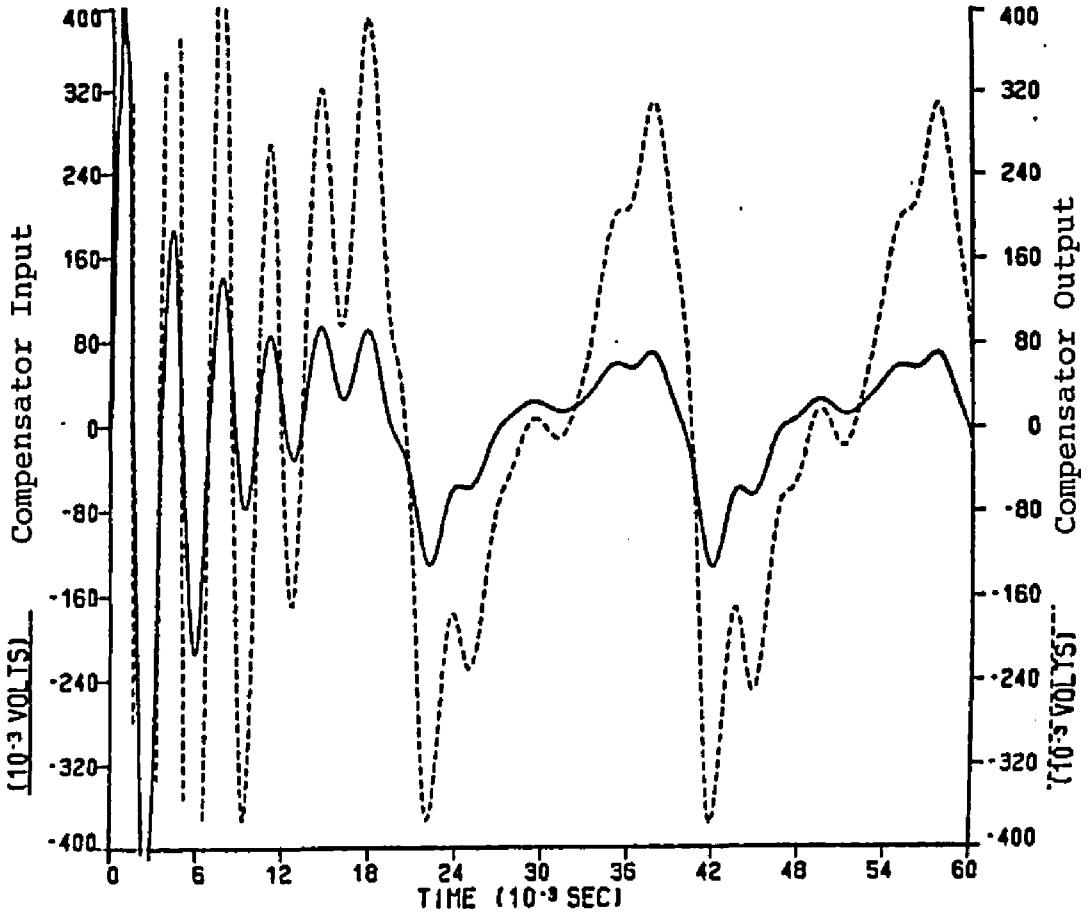

Figure 36. Analog Compensator I/O for the Coarse Servo - PM=10

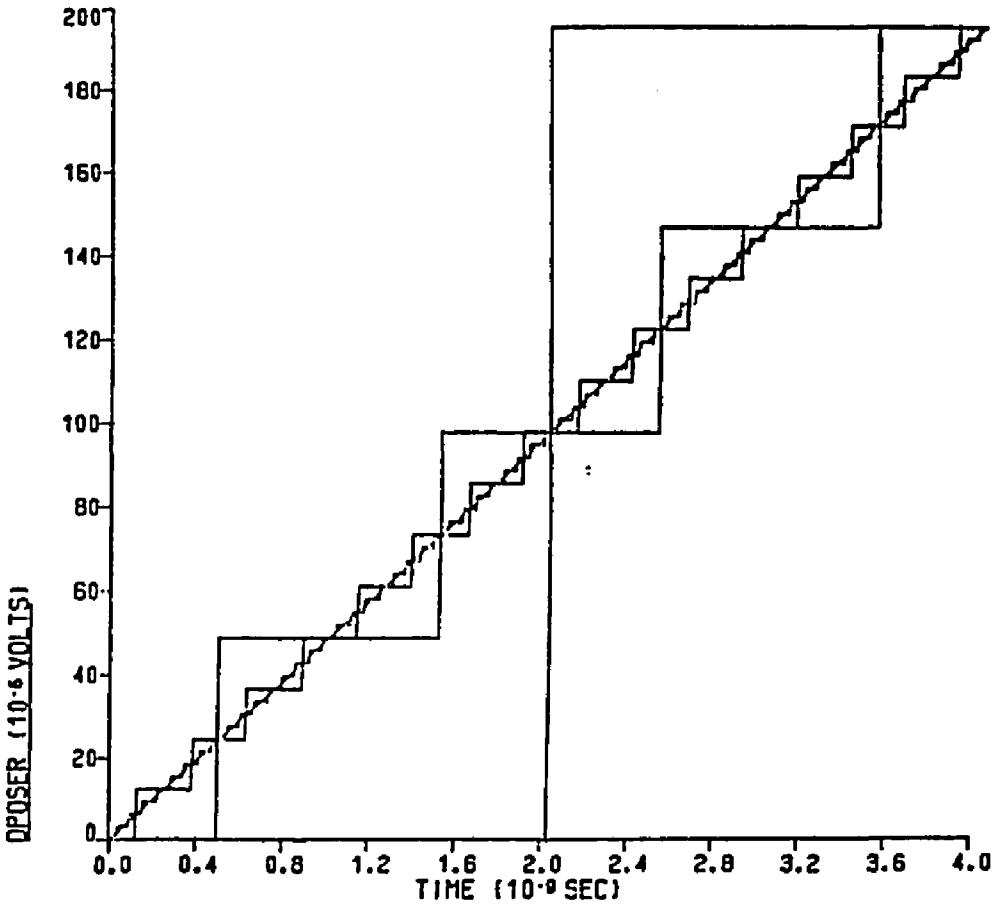

Figure 37. Quantization Effects

16.5, 29.7 microseconds. The 1 nanosecond delay was chosen as a reference value in studying the dynamic performance of the servo. The longer delays are to be compared to the negligible 1 nsec delay. The microsecond delays were chosen because they represented 10, 50, and 90 percent of a sampling period when the sampling rate is 30 Khz. Initial simulations demonstrated stable digital servo performance at 30 Khz when only 8 bits were used. A graphical representation of the 3.3, 16.5, and 29.7 microsecond delays on the digital compensator output are shown in Figure 38. The solid line is for a 1 nanosecond delay.

A pure time delay in the time domain corresponds directly to a phase delay in the frequency domain. The relationship between time delay and phase delay is now described.

$$e^{j\omega T}=\cos(\omega T)+j\sin(\omega T) \tag{58}$$

where T: is a pure time delay.

$$\phi_1=\text{angle}(e^{j\omega_c T})=\omega_c T \tag{59}$$

if $\omega=\omega_c$=servo open loop bandwidth. (60)

The amount of phase delay at the servomechanism's open loop bandwidth for the particular time delays chosen are given in Table 5. The long computation delay will significantly reduce the phase margin in the fine actuator's servo.

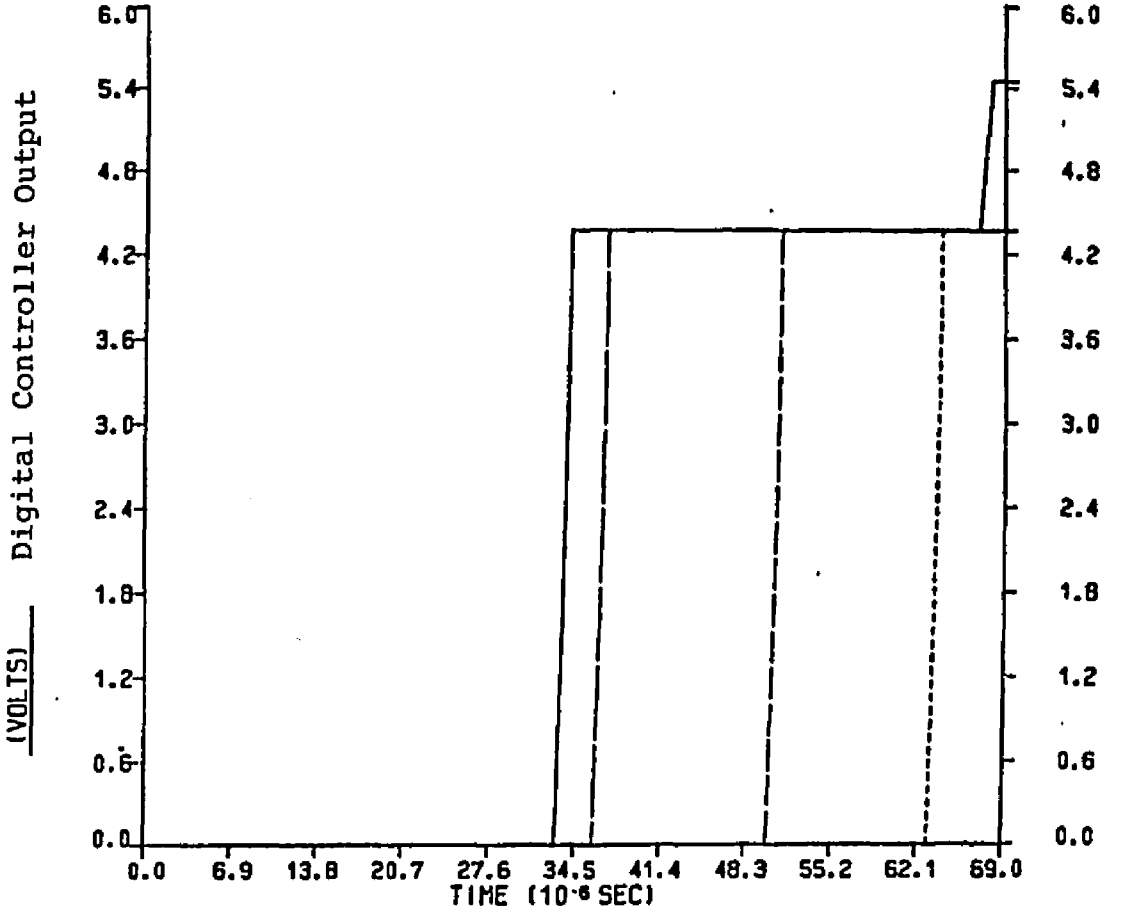

Figure 38. Computation Delay

Table 5
Computation Time Delay Study

Fine Actuator Servomechanism (at 2500 hertz):

Time Delay (sec)	ϕ_1 (degrees)
$1(10^{-9})$	0
$3.3(10^{-6})$	3
$16.5(10^{-6})$	15
$29.7(10^{-6})$	27

Coarse Actuator Servomechanism (at 300 hertz):

Time Delay (sec)	ϕ_1 (degrees)
$1(10^{-9})$	0
$3.3(10^{-6})$	0.4
$16.5(10^{-6})$	1.8
$29.7(10^{-6})$	3.2

Time Domain Simulation Output

The influence of sampling frequency, number of bits, and computation delay will now be studied for the servomechanisms with 45 and 10 degree phase margins. The order in which the study will proceed is:

1. select a sampling frequency F_s,
2. study quantization effects (number of bits) with a 1 nanosecond computation delay,
3. study computation delay effects with 16 bit quantization.

Then a new sampling frequency will be selected and the quantization and computation delay effects reexamined. All simulations were performed for three revolutions of the disk while the disk rotates at 3000 RPM.

45 Degree Phase Margin System - F_s=10 KHZ

Quantization Effects. Figure 39 illustrates the error between the laser beam from the fine actuator and the data track on the optical disk or what is commonly referred to as the tracking error. The unbounded oscillatory curve in this figure is the tracking error of the digitally compensated servomechanism with 16 bits and a 1 nsec. computation delay. The system is clearly unstable, therefore the sampling frequency needs to be increased.

45 Degree Phase Margin System - F_s=15 KHZ

Quantization Effects. The solid line in Figure 40 represents the tracking error for the analog and the 16 bit digital servomechanisms. The dotted line is the tracking error of the 8 bit digital controller. The 8 bit digital controller appears to be adequate in this figure; however, Figure 41 indicates that a stability problem exists in the coarse servomechanism for the 8 bit digital controller. The curves in Figure 41 represent the positional error between the fine actuator and the coarse actuator or what is commonly termed the relative error. The solid curve is the relative error for the analog servomechanism and the 16 bit digital servomechanism.

The large broken curve is the relative error of the 12 bit digital servomechanism. The fine dotted curve is the relative error of the 8 bit digital servomechanism. The 8 bit servo is unstable.

Computation Delay Effects. Figure 42 illustrates the tracking error for the analog servo and the digital servomechanisms that have a 1 nsec. and a 3.3 microsec. computation delay. The three servomechanisms have similar performance during the track following except near zero time. The analog servomechanism's tracking error can be noted by the solid line. The transient characteristics of the digitally compensated servomechanisms are more pronounced near zero time. The large broken curve represents the digital servo with a 1 nsec. delay. The fine dotted line represents the digital servo with a 3.3 microsec. delay. Figure 43 represents corresponding positional error between the fine actuator and the coarse actuator. The coarse servomechanism appears to be less sensitive to the computation delay as is indicated in Table 5.

The large broken line in Figure 44 is the tracking error for the digital tracking servomechanism with a computation delay of 16.5 microsec.. The small broken line in Figure 44 is the tracking error for the digital tracking servomechanism with a computation delay of 29.7 microsec.. These computation delays cause instability.

45 Degree Phase Margin System - F_s=30 KHZ

Quantization Effects. Figure 45 is a plot of the tracking error. The solid line is the analog servo. The large dotted curve is the tracking error of the 16 and 12 bit digital servomechanisms. The fine dotted line is the tracking error of the 8 bit digital servo. The quantization effects appear to be minimal at this sampling rate; however, Figure 46 indicates that the coarse actuator servomechanism experiences an instability when a 8 bit controller is used. Figure 46 is a plot of the relative positional error between the fine actuator and the coarse actuator. The solid line is the error in the analog servo. The large dotted line represents the error for the 16 and 12 bit controllers. The fine dotted line is the error for the 8 bit digital controller.

Computation Delay Effects. The tracking error for the analog servo and digital servomechanisms with different computation time delays are illustrated in Figure 47. No noticeable influence as a result of varying the computation time delays is evident in this figure. Figure 48 is an enlarged view of Figure 47 near zero time. The influence of the computation delay on the dynamic performance is more prevalent at the initial track following. The fine dotted line is the tracking error of the digital controller with a computation time delay of 29.7 microseconds. Figure 49 is the positional error between the fine actuator and the coarse actuator for the different computation delays. A 30 Khz. sample rate with a computation delay below 29.7 microseconds is an adequate performance

criterion to assure that the 45 degree phase margin digital controller has comparable dynamic performance to the 45 degree phase margin analog controller.

10 Degree Phase Margin System - F_s=30 KHZ

Quantization Effects. The two curves in Figure 50 give the tracking error for the analog servo (solid line) and the 16 bit digital servo (dotted line) for the first 1.5 milliseconds of track following. The analog servo exhibits a damped oscillatory response. The digital servo is unstable. The 30 Khz. sample rate is not capable of providing a stable digital servo controller performance.

10 Degree Phase Margin System - F_s=60 KHZ

Quantization Effects. Figure 51 illustrates the tracking error for the analog servo and the 16, 12, and 8 bit digital servo controllers. The solid line represents the analog servo. The two curves with large broken lines represent the 16 and 12 bit digital servomechanisms. The fine dotted line is the tracking error of the 8 bit digital servo. The unbounded oscillatory response of the 8 bit digital servo represents unstable performance. The tracking error for the analog servo and the 16 bit and 12 bit digital servomechanisms are again illustrated in Figure 52. The tracking error axis and time axis have been expanded in order

to illustrate the unstable behavior of the 12 bit digital controller (fine dotted line).

Computation Delay Effects. The fine dotted curve in Figure 53 illustrates the unstable dynamic performance of the digital servo that has a computation time delay of 16.5 microseconds. The solid curve is the tracking error of the analog servo and the large broken lines represent the tracking error of the digital servomechanisms with computation time delays of 1 nanosecond (small amplitude) and 3.3 microseconds (large amplitude). Figure 54 is illustrating the tracking error for the analog servo (solid line), the digital servo with a 1 nanosecond computation time delay (large broken line), and the digital servo with a computation time delay of 3.3 microseconds (fine dotted line). The 3.3 microsecond computation time delay in the digital servomechanism causes instability.

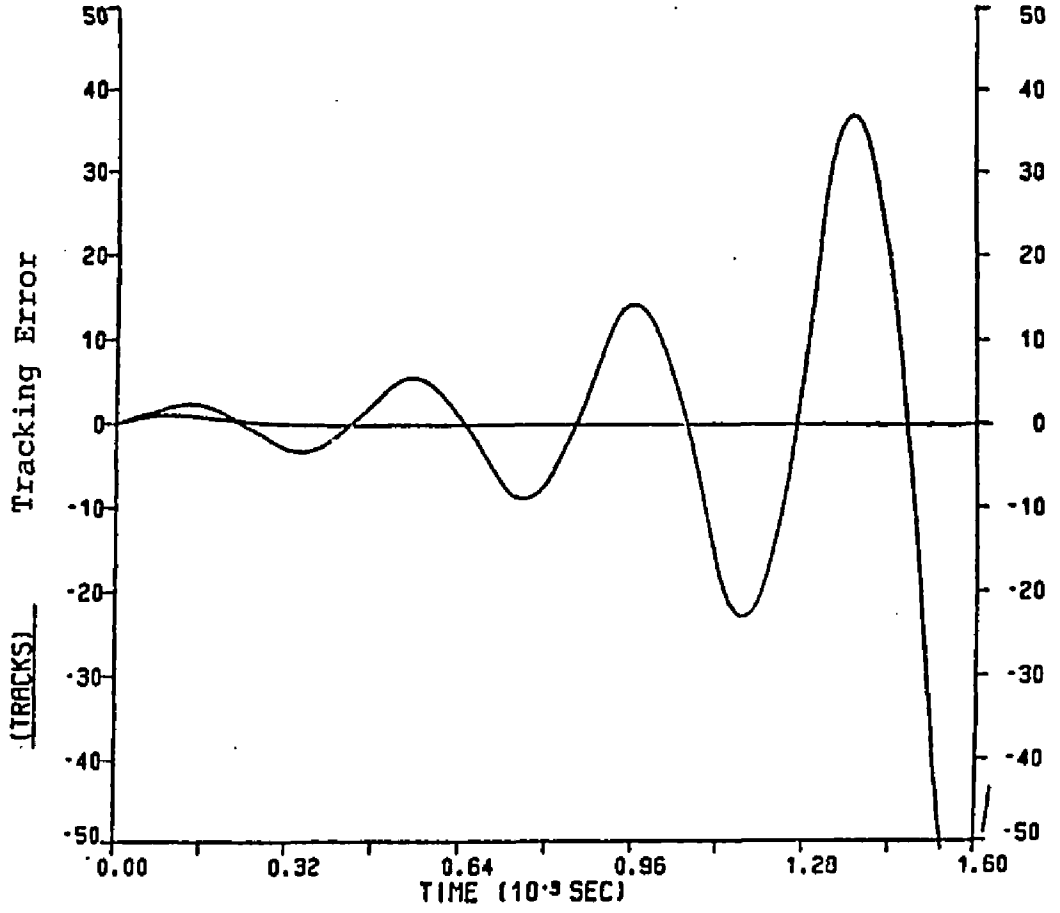

Figure 39. Tracking Error of 45 Degree Phase Margin System With F_s=10KHZ.

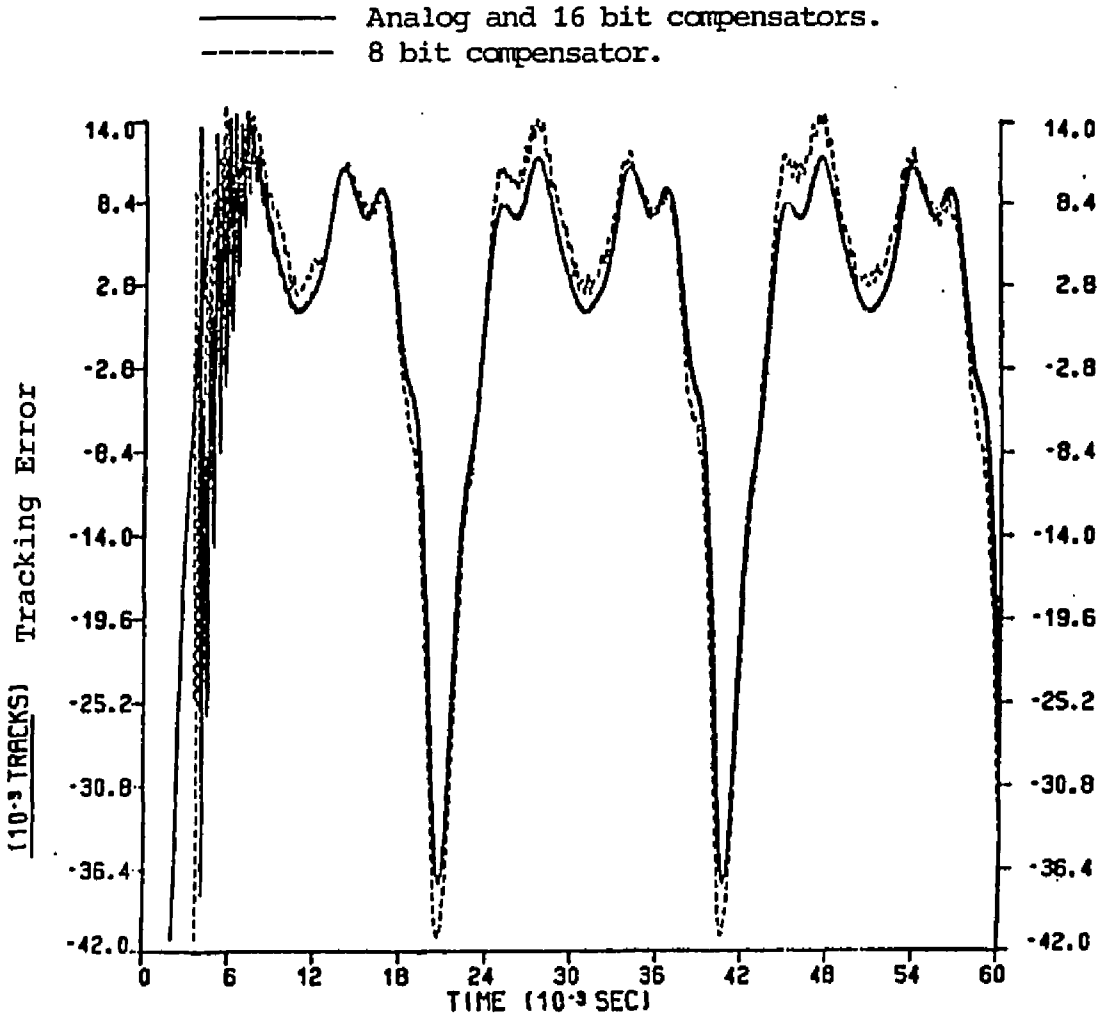

Figure 40. Tracking Error of 45 Degree Phase Margin System With F_s=15KHZ.

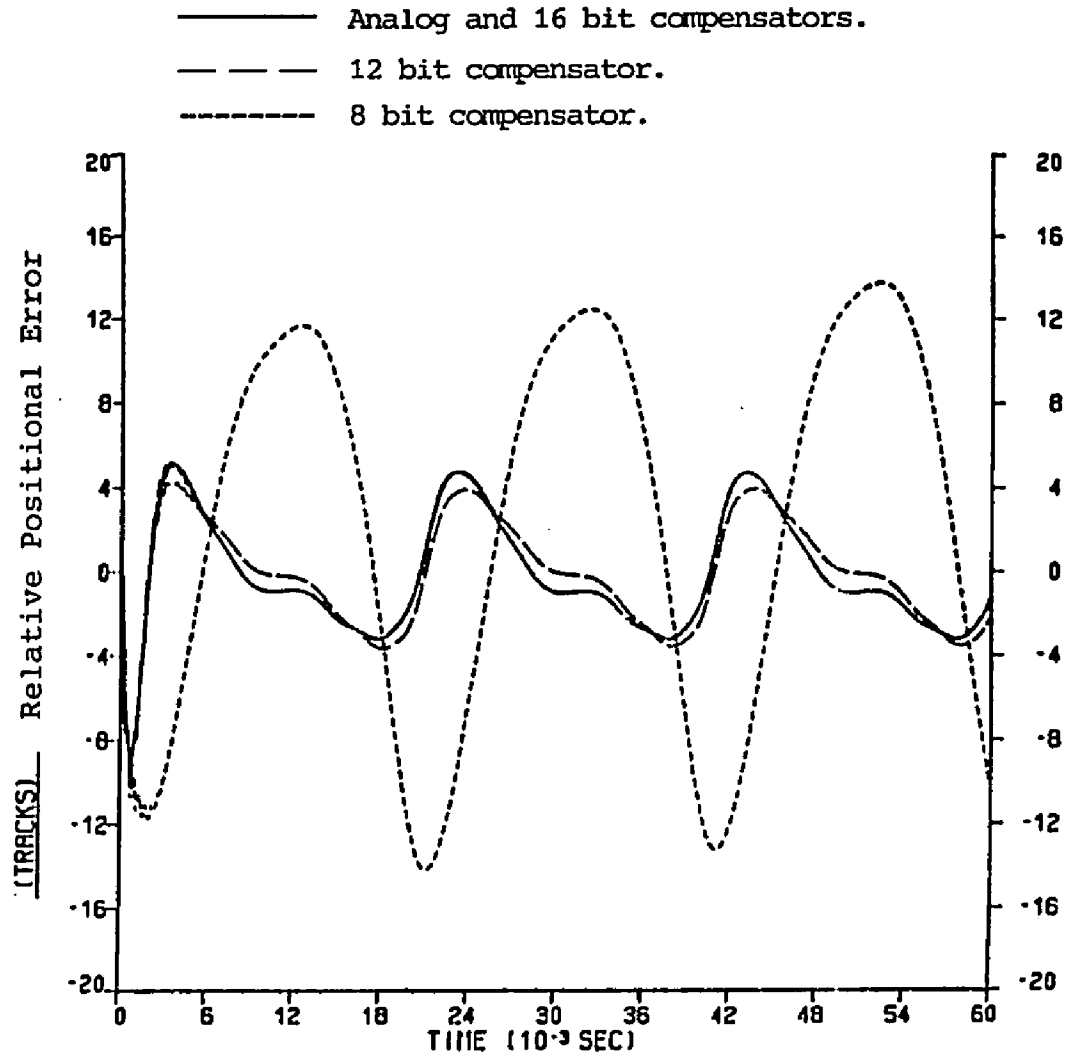

Figure 41. Positional Error Between the Fine and the Coarse Actuator for 8,12, and 16-Bit Digital Servo.

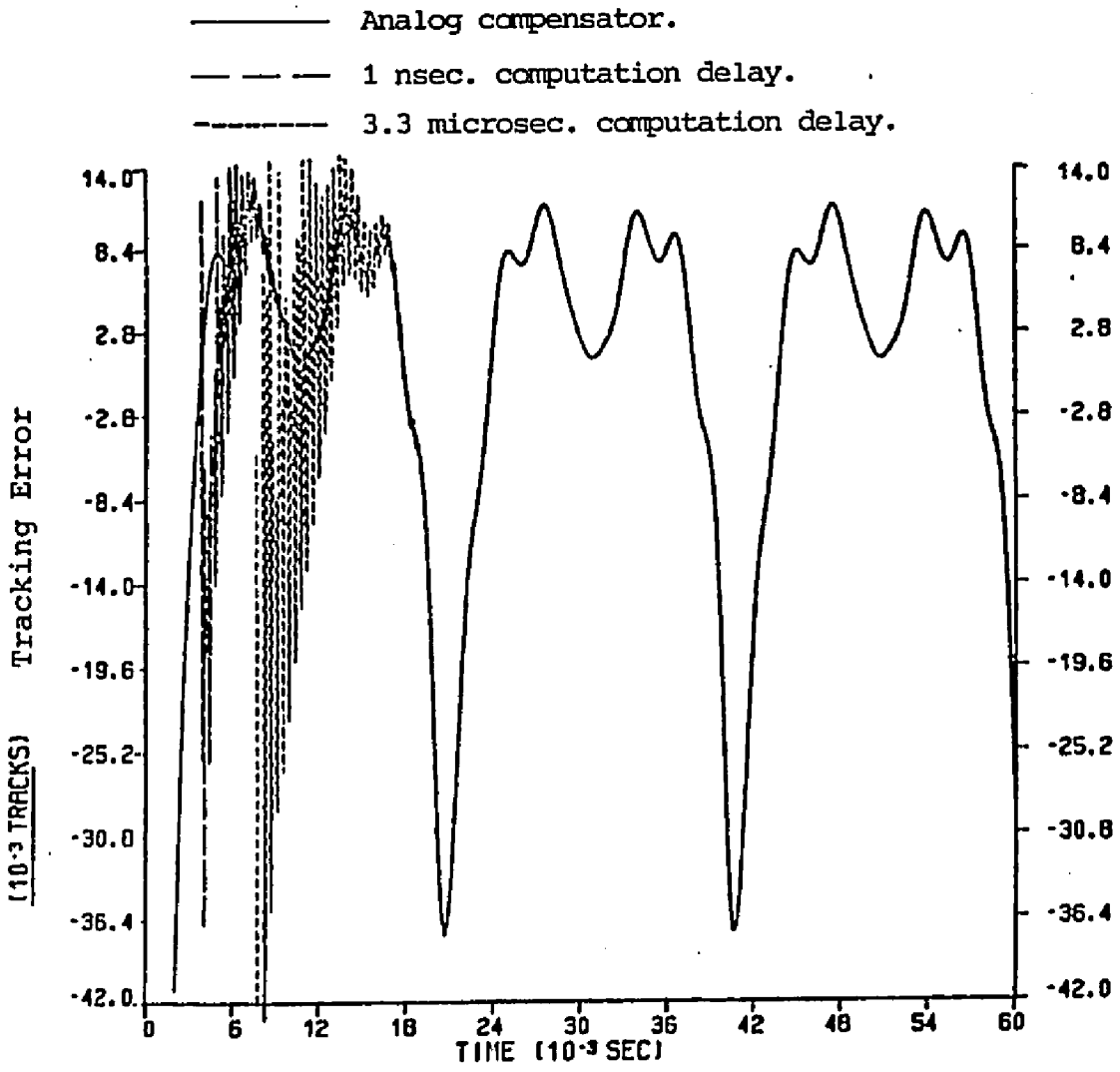

Figure 42. Tracking Error for 1 nsec and 3.3 microsec Computation Delays.

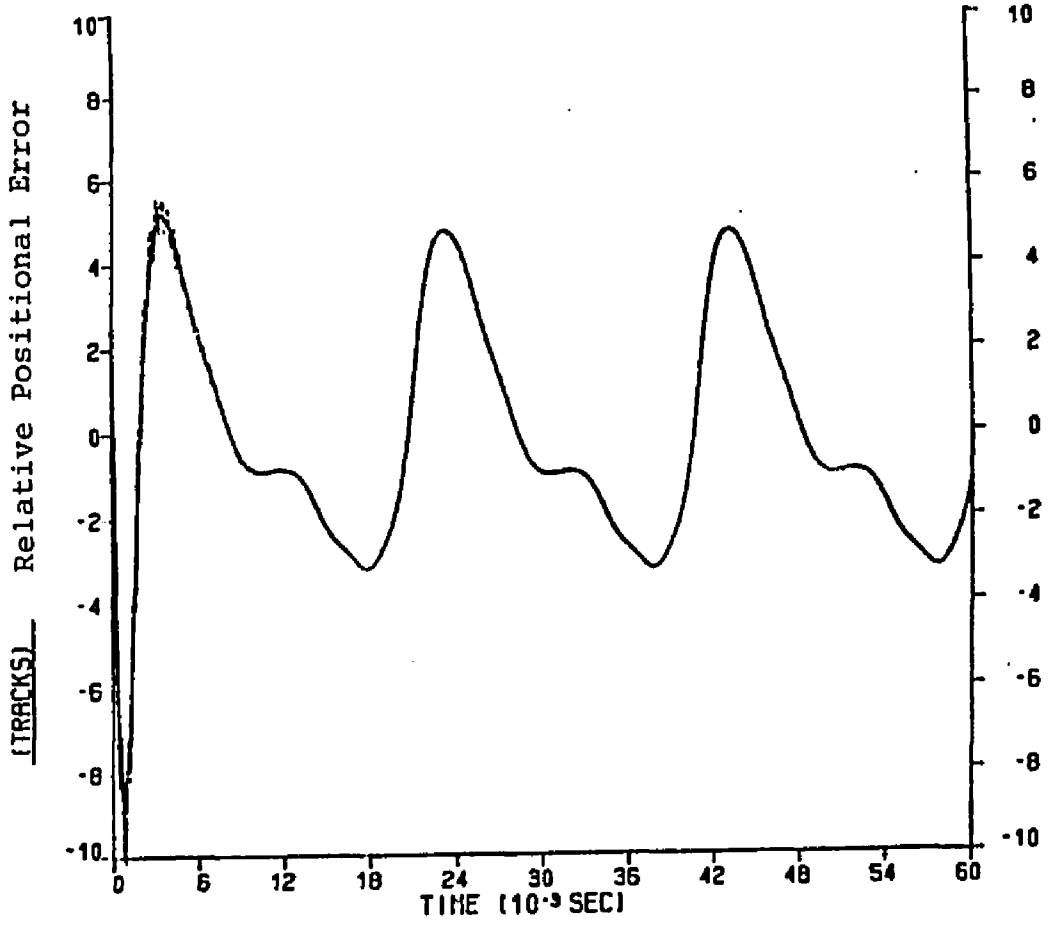

Figure 43. Positional Error Between the Fine and the Coarse Actuator.

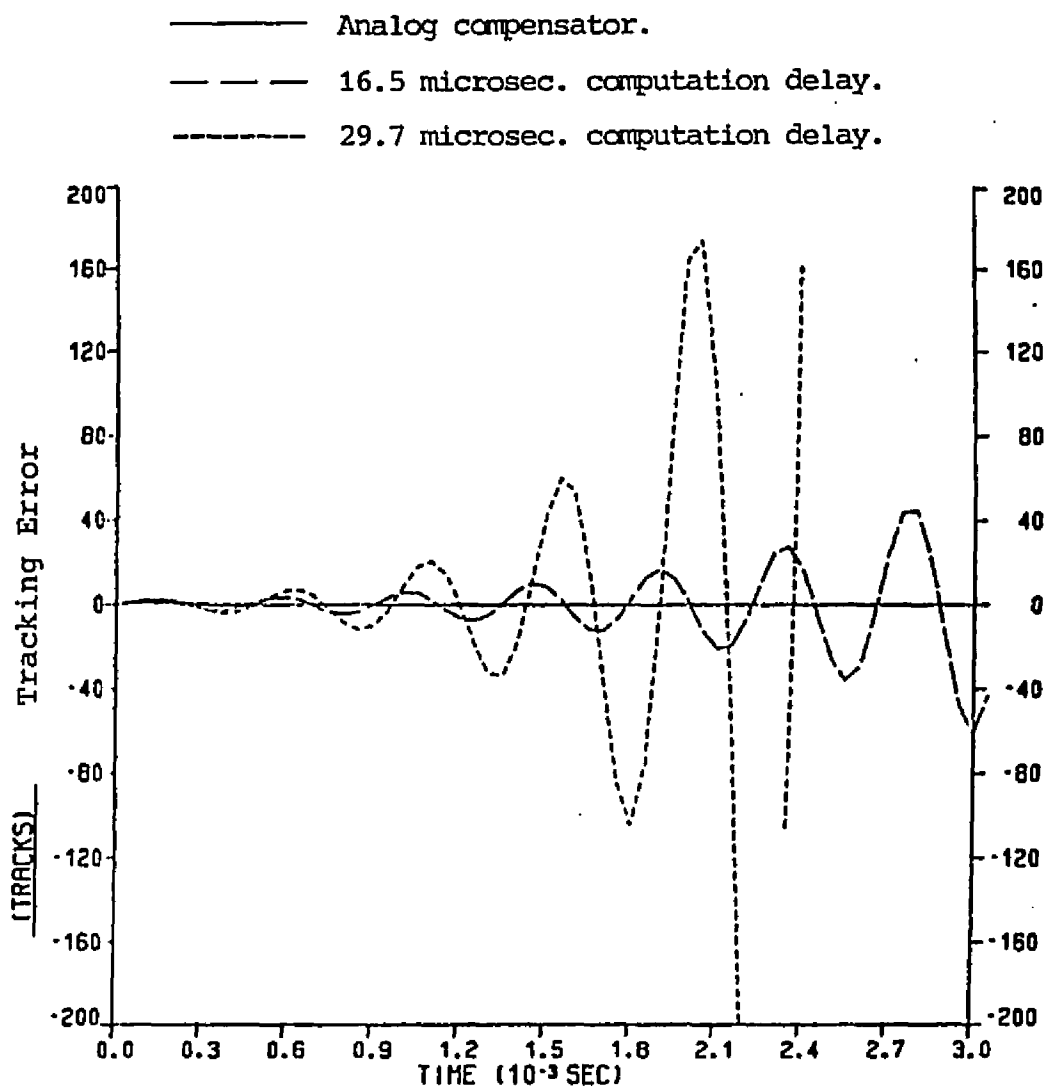

Figure 44. Tracking Error for 16.5 and 29.5 microsec Computation Delays.

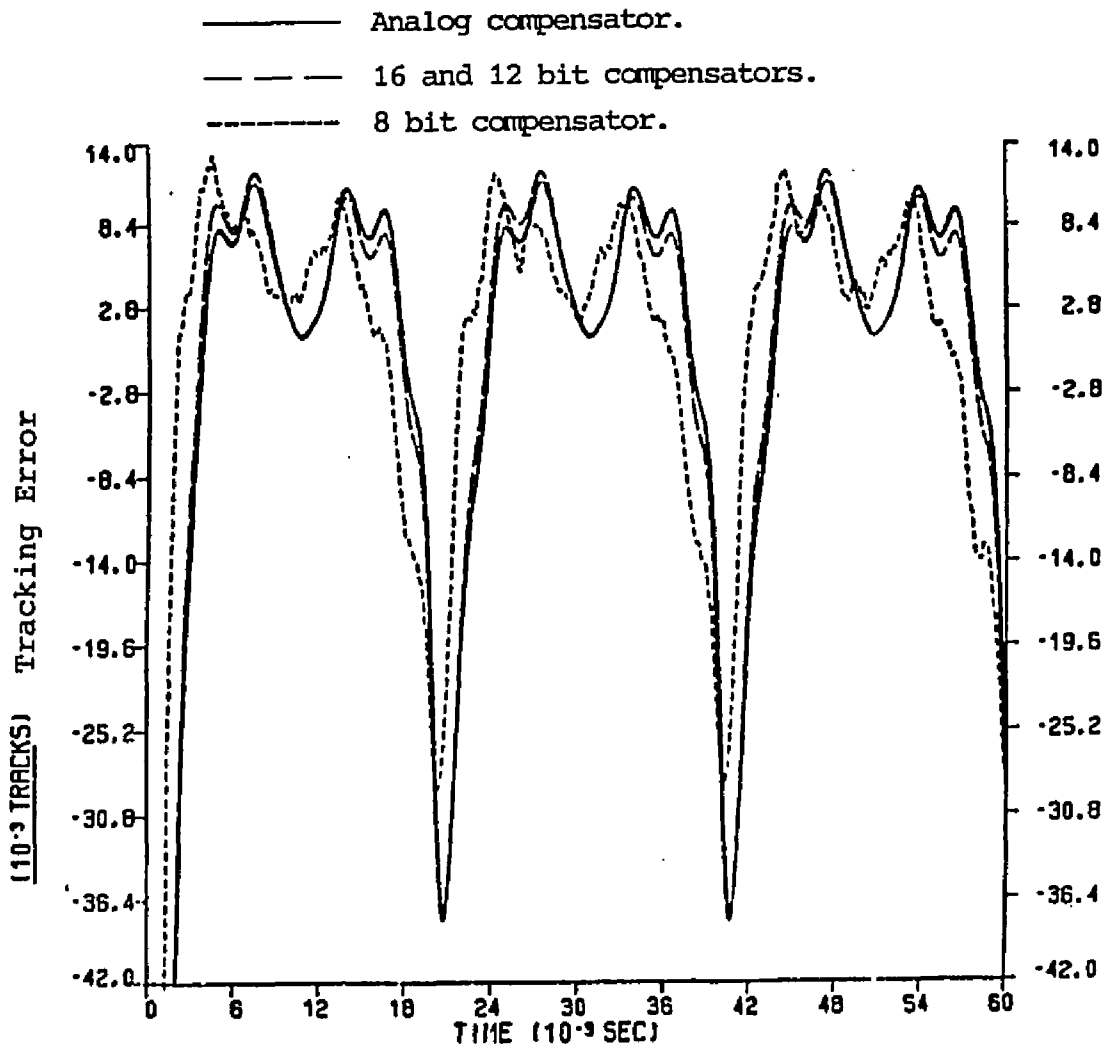

Figure 45. Tracking Error of 45 Degree Phase Margin System With F_s=30KHZ.

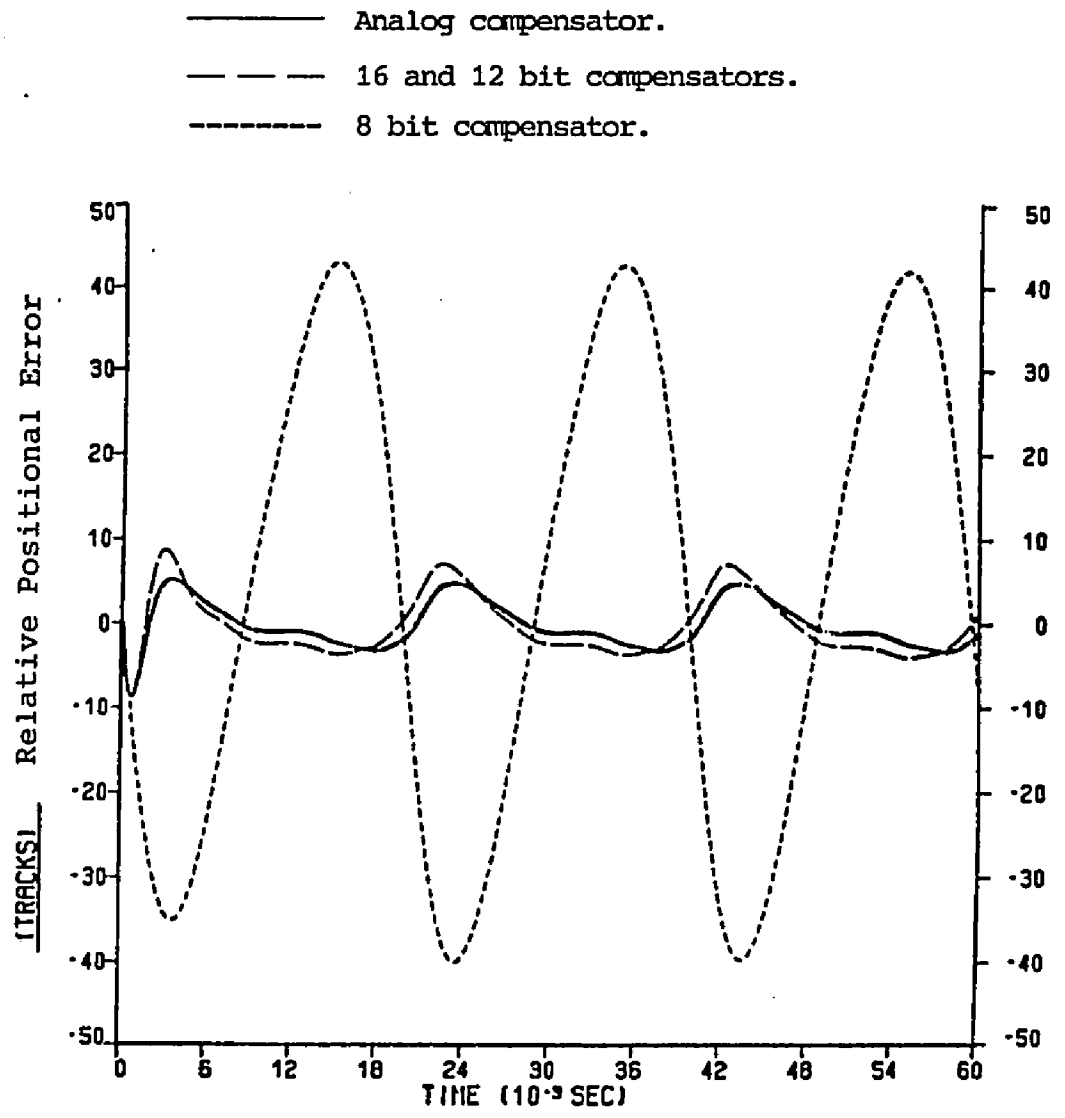

Figure 46. Positional Error Between the Fine and the Coarse Actuator.

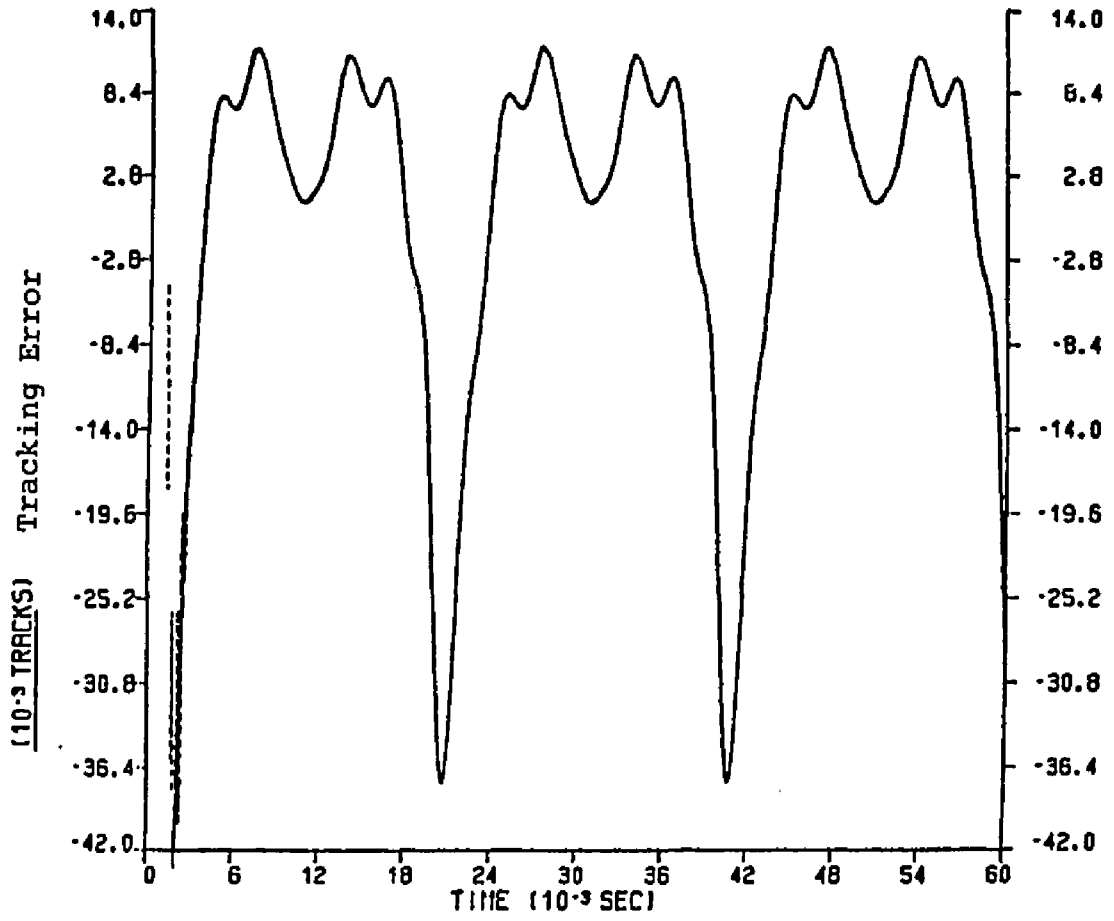

Figure 47. Tracking Error for Different Computation Delays.

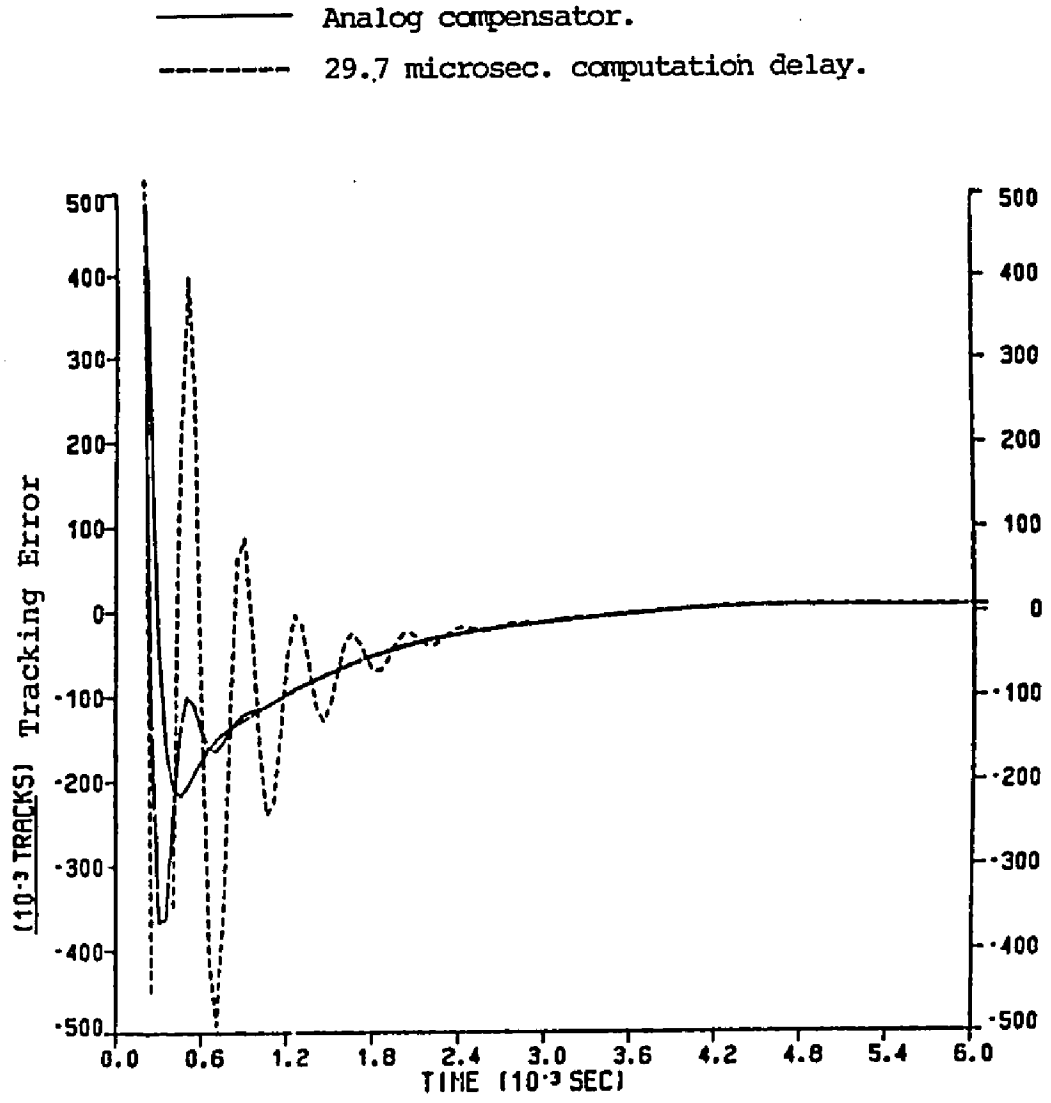

Figure 48. Tracking Error Blowup Near Zero Time.

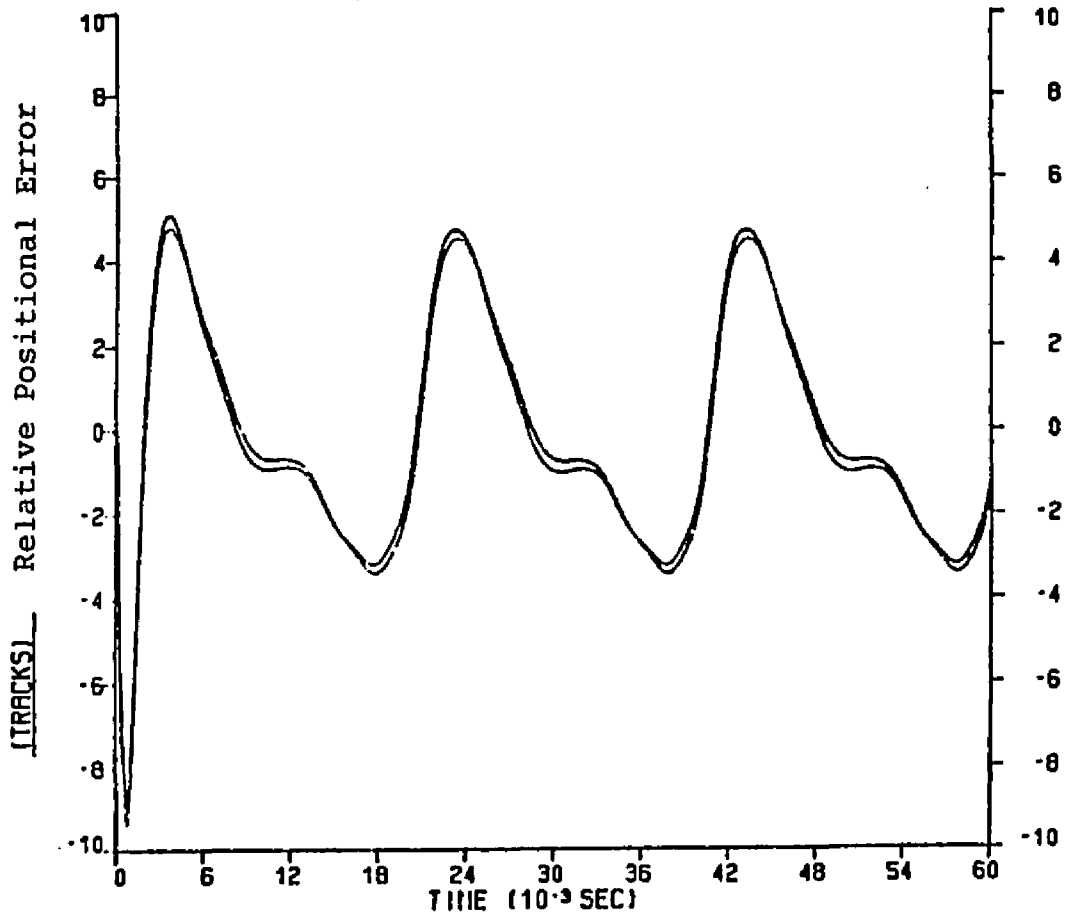

Figure 49. Positional Error Between the Fine and the Coarse Actuator.

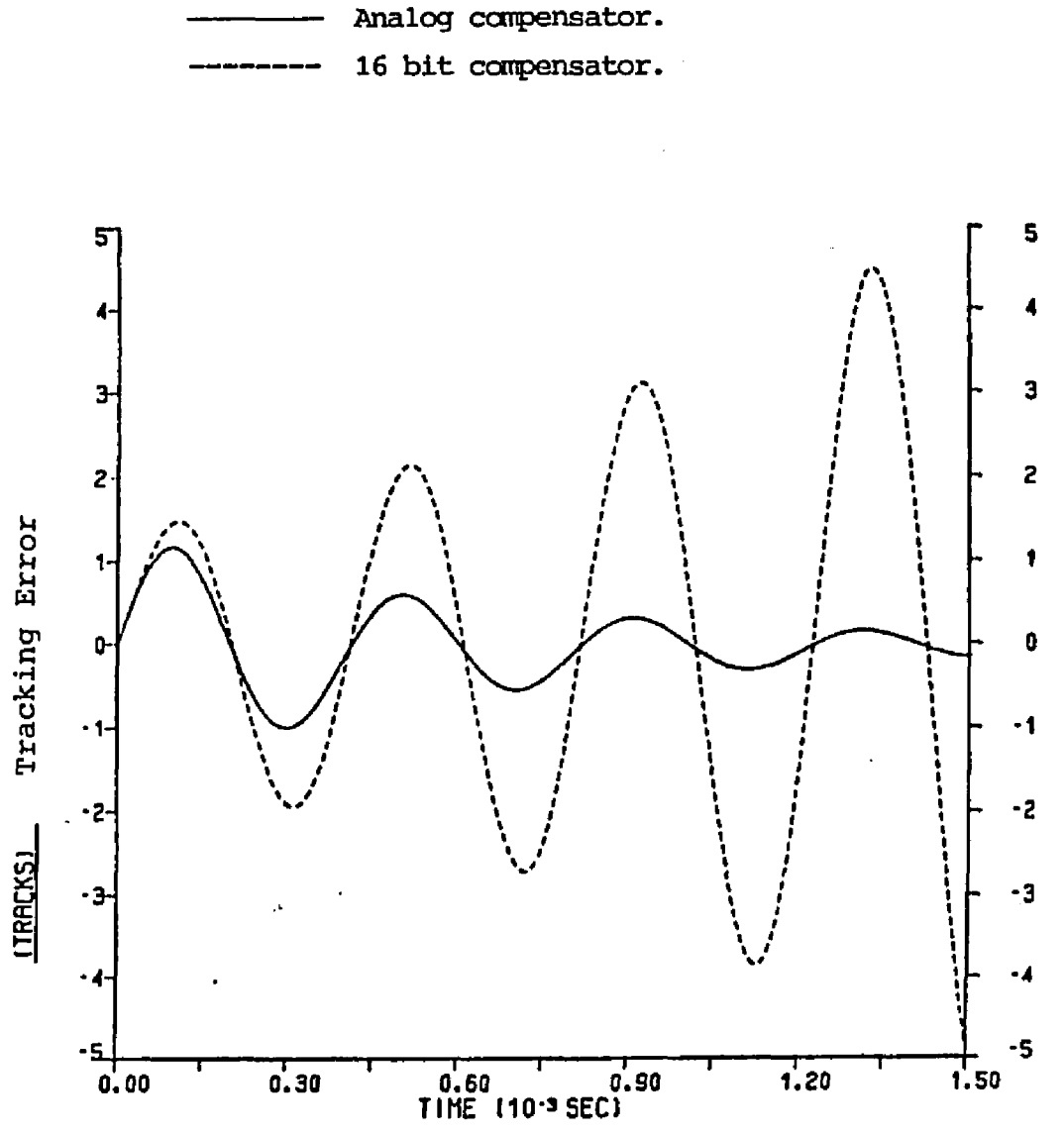

Figure 50. Tracking Error of 10 Degree Phase Margin System With F_s=30KHZ.

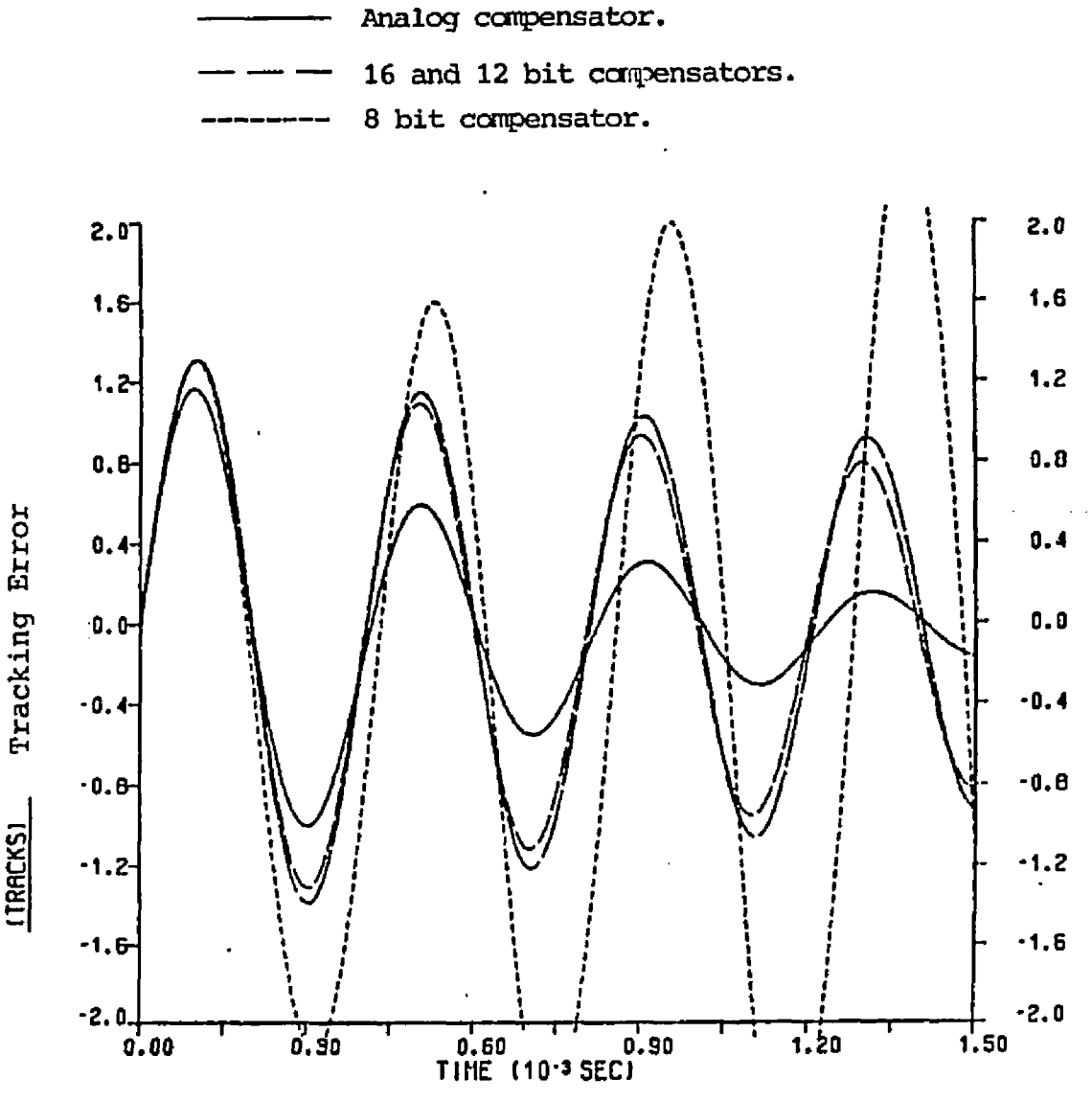

Figure 51. Tracking Error of 10 Degree Phase Margin System With F_s=60KHZ.

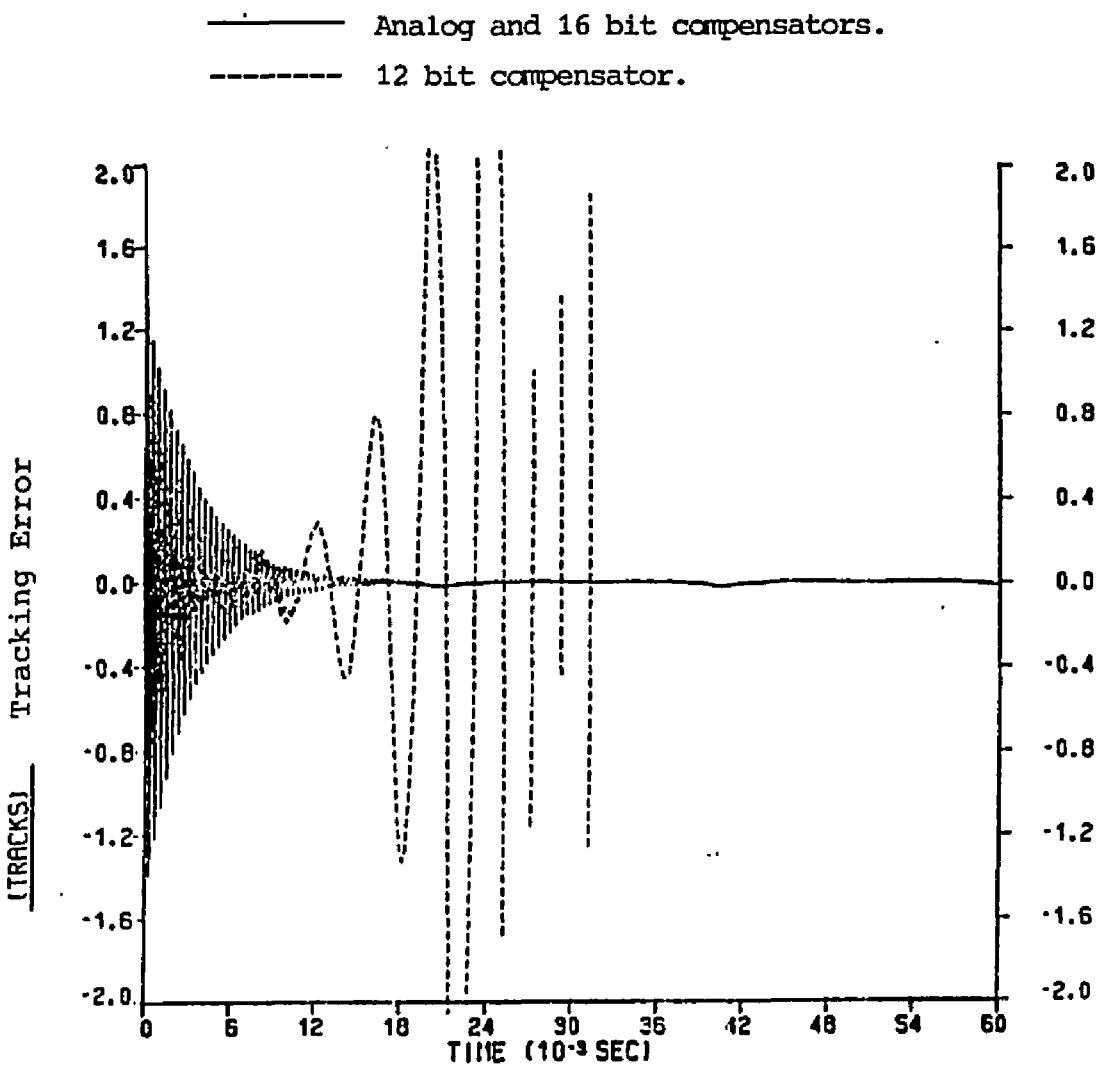

Figure 52. Tracking Error Over an Expanded Time Scale.

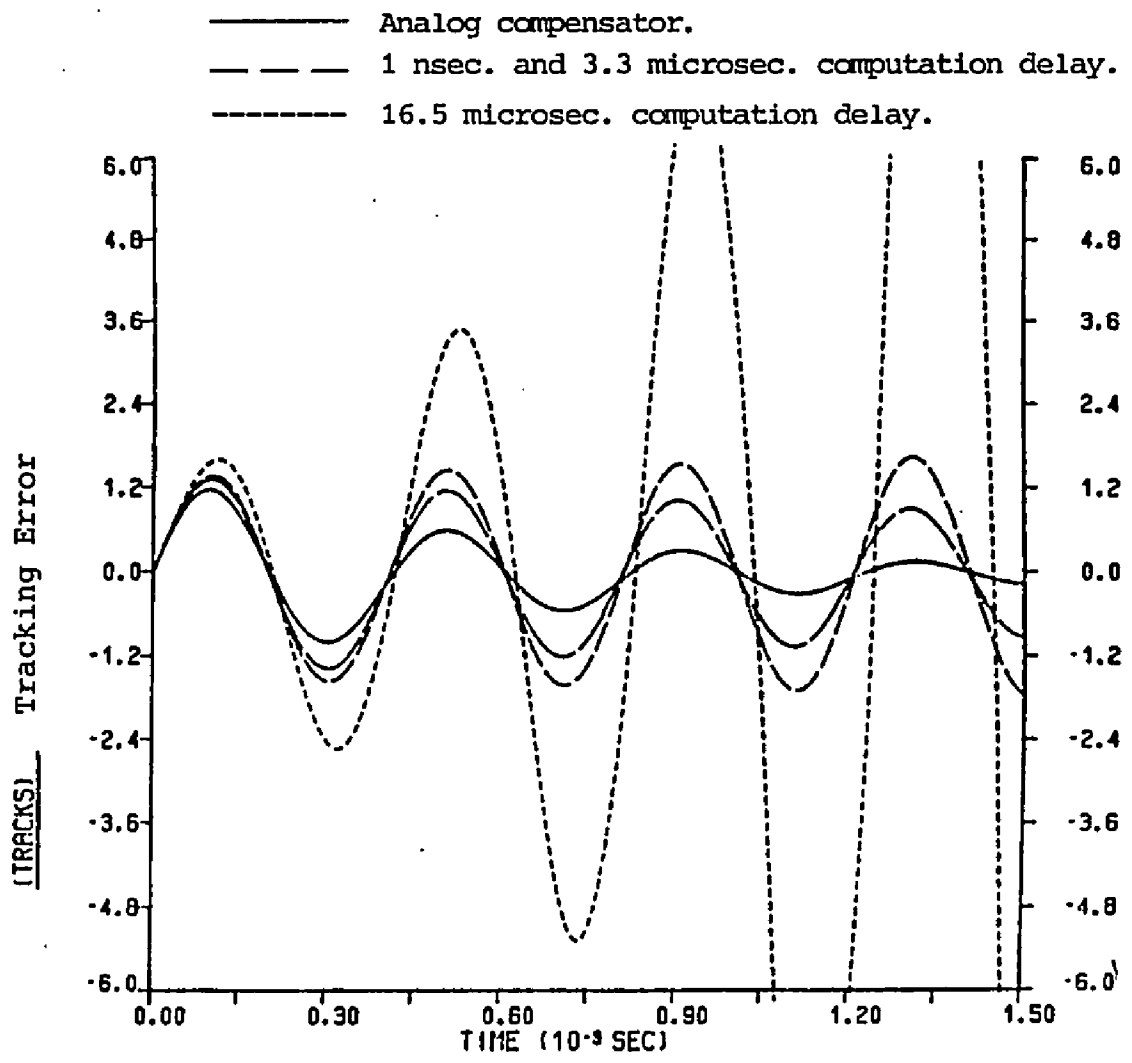

Figure 53. Tracking Error for Different Computation Delays.

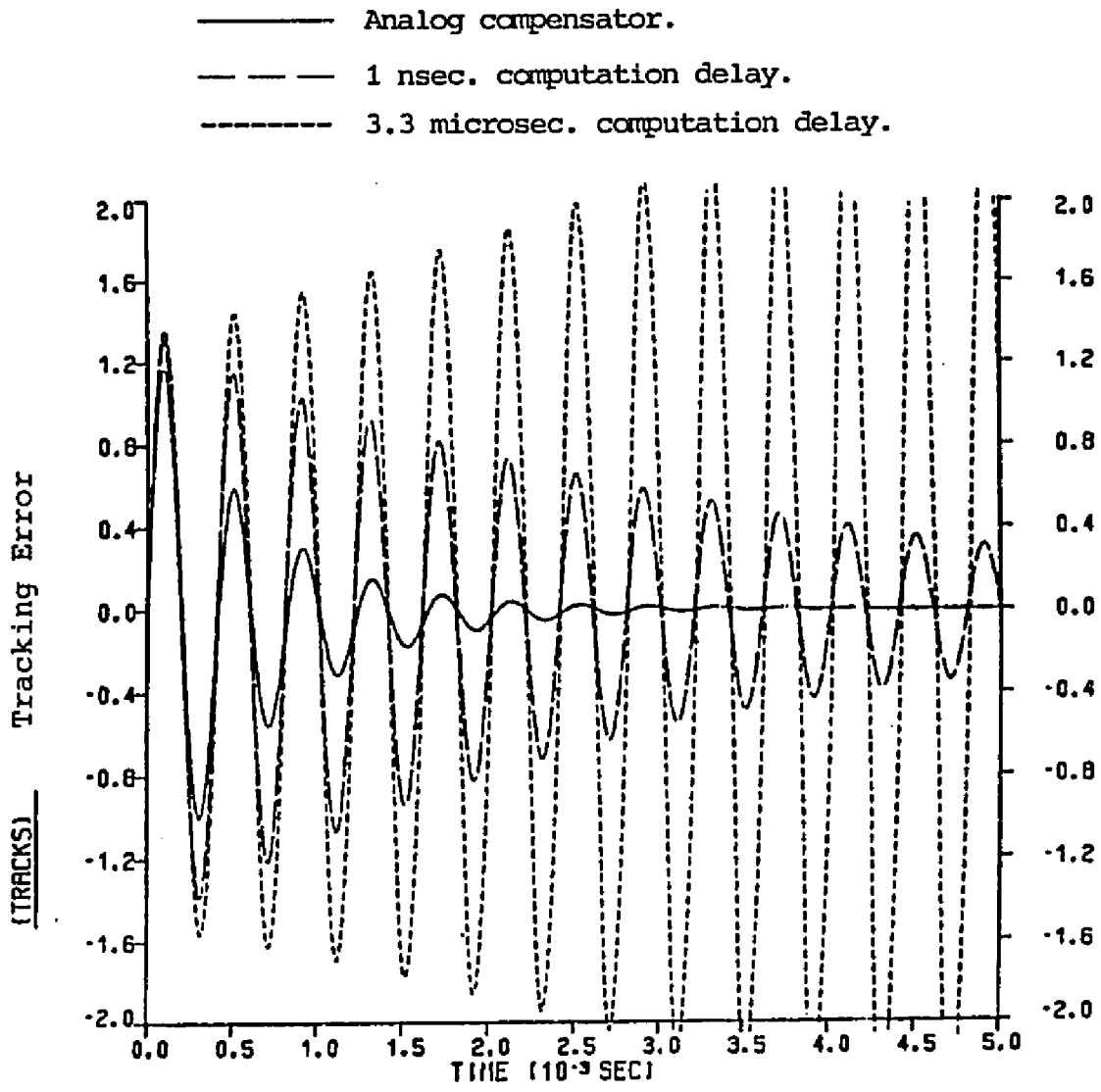

Figure 54. Tracking Error Over an Expanded Time Scale.

CHAPTER 5

CONCLUSIONS

Contributions of this Thesis

A summary of the various developments in this thesis can be given as follows:

1. A general overview on the optical disk drive was given. This included a discussion of the major components which make up an optical disk drive system.
2. Free body diagrams for the fine actuator and the coarse actuator were constructed. The summation of the forces in the tracking direction was used to develop mathematical equations to describe the dynamics. Frequency domain models in the form of transfer functions were derived from these equations.
3. A Transconductance power amplifier architecture was discussed and analyzed.
4. Analog and digital compensators consisting of a phase lead compensator and a low frequency integrator were analyzed. The compensation for a particular tracking servomechanism was designed by a DSL frequency domain program for both a 10 degree and a 45 degree phase margin system. Bode plots of the actuator and sensor, elec-

tronic compensator, open and closed loop transfer functions were generated by the DSL program.

5. The DSL model was validated in the frequency domain by comparing the model's Bode plot output with Bode plots that were generated on an instrument made by Hewlett Packard (HP3562A). The Bode plots compared well, thus reinforcing the fact that the model contained no errors.
6. Time domain simulations on the tracking servomechanism were performed for the 45 degree and the 10 degree phase margin systems. These simulations studied the dynamic performance of the digitally controlled servomechanisms at several sampling frequencies. The influence of quantization and computation delay were examined at each sampling frequency.

The results of this thesis provide useful knowledge on the requirements of a digital controller in terms of sampling rate, number of bits, and computation delay in the context of its application to the design of a tracking servomechanism for an optical disk drive. A servo system with a very small phase margin is difficult to implement in a digital servo with current technologies. The simulations have indicated that the sampling rate would need to be significantly high (>60 Khz) in order to maintain stability. The stability of a servomechanism that has low phase margin (10 degrees) is marginal in accommodating the quantization approximations and the finite time taken for the computation of the difference equations at high sampling frequencies.

The simulations have also indicated that the implementation of the digital servo for this dual actuator system will require a phase margin near 45 degrees and a 16 bit digital controller. The sampling frequency should be at least 30 KHZ. Computation time delay must be less than 29.7 μsec (see Figures 45 and 47).

Suggestions for Further Studies

A more complete study of this system would require additional simulations at different sampling frequencies, quantization levels, and computation delays. The modeling of the quantization effects could be improved by taking a hardware implementation perspective. A suggested approach would be to measure the voltages present at the analog-to-digital and the digital-to-analog converters of the digital servo controller and use this voltage range for quantization. The possibility of using a 8 or 12 bit ADC/DAC with a 16 bit digital controller or other permutations should also be investigated. Other factors that should be included in the model in order to improve the accuracy in the representation of the hardware are: op-amp voltage limits, kinetic friction, static friction, and saturation effects.

APPENDIX A

DSL FREQUENCY DOMAIN PROGRAM FOR THE FINE ACTUATOR

```
TITLE FINE SERVO SIMULATION - FREQUENCY RESPONSE - BODE PLOTS
*
*                 DSL PROG. NAME=THFREQF
*
* 2/10/86   18:20
*
*
*
* THIS PROGRAM IS FOR MSEE THESIS WORK AT THE U.A..  THIS PROGRAM
* WILL GENERATE BODE PLOTS (MAGNITUDE AND PHASE) FOR THE FINE
* ACTUATOR MASTER SERVO.  ONE SET OF PLOTS WILL DISPLAY THE TRANSFER
* FUNCTION OF A CONTINUOUS SERVO.  A SECOND PLOT WILL DISPLAY THE
* TRANSFER FUNCTION OF THE DIGITAL SERVO BY USING THE W-TRANSFORM.
*
*
* THE FOLLOWING ARE THE DEFINITIONS OF THE CONSTANTS
*
* FINE ACTUATOR CONSTANTS:
*   MF:    FINE ACTUATOR'S MASS (KG)
*   KFF:   "               " CURRENT TO TORQUE CONSTANT (N/AMP)
*   KVCF:  "               " MECHANICAL DAMPING CONSTANT (N/M/S)
*   KXCF:  "                            " SPRING CONSTANT (NEWTONS/METER)
*   KQ:    TES,PREAMP,DIVIDER SENSITIVITY (VOLTS/METER)
*   KPF:   SERVO ELECTRONIC GAIN(VOLTS/VOLTS)
*   Z1:    DAMPING COEFFICIENT OF THE ACTUATOR'S RESONANCE
*   W1:    NATURAL RESONANT FREQ. (RADIANS)
*   Z2:    DAMPING COEFFICIENT OF THE ACTUATOR'S RESONANCE
*   W2:    NATURAL RESONANT FREQ. (RADIANS)
*  COMPENSATION PARAMETERS:
*   BW:    SERVO BANDWIDTH
*   PM:    SERVO PHASE MARGIN
*   LFIPL: AMOUNT OF ALLOWABLE PHASE LAG FROM THE LOW FREQ. INTEGRATOR
*   FS:    SAMPLE RATE OF THE DIGITAL COMPENSATOR
*   RPM:   DISK RPM IS USED TO DETERMINE THE CRITICAL FREQ. NEEDED
*          IN CALIBRATING THE DIGITAL CONTROLLER GAIN WITH THE ANALOG
*          CONTROLLERS.
*   A0-A1: COEFFICIENTS OF THE DIFFERNCE EQUATION OF THE DIGITAL CONTROL.
*   B0-B2: COEFFICIENTS OF THE DIFFERNCE EQUATION OF THE DIGITAL CONTROL.
*
**************************************************************************
INITIAL SEGMENT
*
COMPLEX S,Z,WT,G1,G2,G3,G4,G5,G6,GWT
```

```
*
METHOD RKSFX
CONTRL FINTIM=6.0,DELT=2.0D-3
*
FIXED  FGAIN,FPAS,FPI,FPL,FGM
*
INCON  FGAIN=0,FPAS=0,KPF=0.55,FPI=0,FPL=0,FGM=0
*
CONST  KFF=0.3,MF=0.003,KVCF=0.3,KQ=1.5D6,KXCF=193.0, ...
       Z1=0.02,Z2=0.02,W1=113097.0,W2=106814.0, ...
       RPM=3000.0,FS=1.5D4,BW=2500,PM=45,LFIPL=5,ZERO=0.0
*
*
*  CALCULATE THE POLE-ZERO LOCATIONS FOR THE ELECTRONIC COMPENSATION.
*
*
*     ANALOG COMPENSATION:
      IF(FPAS.EQ.1.AND.FGAIN.EQ.0) THEN
        WI=2.0*PI*BW*DTAN(PI*LFIPL/180.0)
        PL=PI*(PM-180-ASP+LFIPL)/180.0
        PLDEG=180.0*PL/PI
        GAMA=(1.0-DSIN(PL))/(1.0+DSIN(PL))
        WP=2.0*PI*BW/DSQRT(GAMA)
        WZ=GAMA*WP
      ENDIF
*
*
*
*
*
*
*     DIGITAL COMPENSATION:
      IF(FGAIN.EQ.1) THEN
*  DEFINE THE SAMPLING PERIOD
        T=1.0/FS
*
*  DEFINE CRITICAL FREQUENCY USED TO CALIBRATE THE GAIN OF THE MAPPED
*  Z TRANSFER FUNCTION
        WC=2.0*PI*RPM/60.0
*
*  MAPPED POLE-ZEROS
        ZI=DEXP(-WI*T)
        ZZ=DEXP(-WZ*T)
        ZP=DEXP(-WP*T)
*
*  DETERMINE THE GAIN OF THE Z-MAPPED TRANSFER FUNCTION
        S=CMPLX(0.0,WC)
        GCL=GAIN(KPF*WP*(S+WI)*(S+WZ)/(WZ*S*(S+WP)))
        GC=10.0**GCL
        Z=CEXP(S*T)
```

```
        GZPL=GAIN((Z-ZI)*(Z-ZZ)/((Z-1.0)*(Z-ZP)))
        GZP=10.0**GZPL
        ALPHA=GC/GZP
*
*  DETERMINE THE COEFFICIENTS IN THE DIFFERENCE EQUATION
        A0=1.0+ZP
        A1=-ZP
        B0=ALPHA
        B1=-ALPHA*(ZI+ZZ)
        B2=ALPHA*ZI*ZZ
*
*       CALL PRINT
      ENDIF
*
*****************************************************************************
*****************************************************************************
*
DYNAMIC SEGMENT
*
      W=10.0**TIME
      F=W/(2.0*PI)
      S=CMPLX(0.0,W)
* FINE ACTUATOR AND SENSOR
      G1=KQ*KFF*(S**2+2*Z1*W1*S+W1**2)/((MF*S**2+KVCF*S+KXCF)* ...
         (S**2+2*Z2*W2*S+W2**2)*1.1211)
      MAG1=20.0*GAIN(G1)
      PHAS1=RADEG*PHASE(0.0,G1)
* SERVO CARD = PHASE LEAD AND PI COMPENSATION
      IF(FPAS.EQ.1) THEN
        G2=WP*(S+WI)*(S+WZ)/(WZ*S*(S+WP))
        MAG2=20.0*GAIN(G2)
        PHAS2=RADEG*PHASE(0.0,G2)
* SERVO CARD PLUS POWER AMP
        G3=KPF*G2
        MAG3=20.0*GAIN(G3)
        PHAS3=RADEG*PHASE(0.0,G3)
* USE THE W-TRANSFORM TO GENERATE THE DIGITAL COMPENSATOR FREQ RESPONSE
* FOR COMPARISON TO THE ANALOG COMPENSATOR.
*       WT=CMPLX(0.0,W)
*       Z=(1.0+WT*T/2.0)/(1.0-WT*T/2.0)
*       GWT=ALPHA*(Z-ZI)*(Z-ZZ)/((Z-1.0)*(Z-ZP))
*       IF(GWT.NE.0.0) THEN
*         MAGWT=20.0*GAIN(GWT)
*         PHASWT=RADEG*PHASE(0.0,GWT)
*       ENDIF
* TOTAL OPEN LOOP TRANSFER FUNCTION
        G4=G1*G3
        MAG4=20.0*GAIN(G4)
        PHAS4=RADEG*PHASE(0.0,G4)
        IF(FGAIN.EQ.1.AND.FPL.EQ.0.AND.F.GE.BW) THEN
```

```
          FPL=1
*         CALL PRINT
        ENDIF
        IF(FGAIN.EQ.1.AND.F.GE.BW.AND.FGM.EQ.0.AND.PHAS4.LE.-180) THEN
          FGM=1
          GM=-MAG4
        ENDIF
* TOTAL CLOSED LOOP TRANSFER FUNCTION
        G5=G4/(1+G4)
        MAG5=20.0*GAIN(G5)
        PHAS5=RADEG*PHASE(0.0,G5)
* LOW FREQ. INTEGRATOR
        G6=(S+WI)/S
        MAG6=20.0*GAIN(G6)
        PHAS6=RADEG*PHASE(0.0,G6)
        IF(FGAIN.EQ.1.AND.FPI.EQ.0.AND.W.GE.WI) THEN
          FPI=1
*         CALL PRINT
        ENDIF
      ENDIF
*
      IF(FPAS.EQ.0.AND.F.GE.BW) CALL ENDRUN
      IF(FPAS.EQ.1.AND.FGAIN.EQ.0.AND.MAG4.LE.0.0) CALL ENDRUN
*****************************************************************
*****************************************************************
*
TERMINAL SEGMENT
*
*
      IF(FGAIN.EQ.1)  CALL PRINT
*
*     DETERMINE THE ACTUATOR AND SENSOR PHASE AT THE DESIRED SERVO BW
      IF(FPAS.EQ.0) THEN
        FPAS=1
        ASP=PHAS1
        CALL RERUN
        GO TO 10
      ENDIF
*
*
      IF(FPAS.EQ.1.AND.FGAIN.EQ.0) THEN
        IF(F.GE.BW) THEN
          FGAIN=1
          DELPLT=2.0D-3
*         DELPRT=3.0D-2
        ELSE
          KPF=KPF+0.01
        ENDIF
        CALL RERUN
```

```
      ENDIF
*
10    CONTINUE
*
PAGE (50)
DIGITS 8
*RINT F,MAG1,PHAS1,MAG3,PHAS3,MAG4,PHAS4,MAG5,PHAS5,MAG6,PHAS6
*RINT BW,PM,GM,LFIPL,PLDEG,FS,RPM,KPF,WI,WZ,WP,A0,A1,B0,B1,B2
PRINT PM,GM,FS,A0,A1,B0,B1,B2,KPF,WI,WZ,WP
*
SAVE  (SUBSAV) F,W,MAG1,PHAS1,MAG3,PHAS3,MAG4,PHAS4,MAG5,PHAS5,ZERO
*
GRAPH (G1MGR/SUBSAV,DE=GA3277,PO=2.5,1.0) ...
      F(LE=7,AX=LOG,NI=5,LO=1.0,PO=0,0,UN=HZ), ...
      MAG1(LE=7,LO=-80,SC=20,NI=8,UN=DB,LI=1)
GRAPH (G1PGR/SUBSAV,DE=GA3277,OV,PO=2.5,1.0) ...
      F(LE=7,AX=LOG,NI=5,LO=1.0,PO=0,7,UN=HZ), ...
      PHAS1(LE=7,LO=-360,SC=45,NI=8,PO=7,UN=DEG,LI=4)
LABEL (G1MGR) FINE ACTUATOR AND SENSOR
GRAPH (G2MGR/SUBSAV,DE=GA3277,PO=2.5,1.0) ...
      F(LE=7,AX=LOG,NI=5,LO=1.0,PO=0,0,UN=HZ), ...
      MAG3(LE=7,NI=8,UN=DB,LI=1)
GRAPH (G2PGR/SUBSAV,DE=GA3277,OV,PO=2.5,1.0) ...
      F(LE=7,AX=LOG,NI=5,LO=1.0,PO=0,7,UN=HZ), ...
      PHAS3(LE=7,PO=7,0,UN=DEG,LI=4,NI=8)
LABEL (G2MGR) ANALOG COMPENSATION
LABEL (G2MGR) PHASE MARGIN = 10 DEGREES
GRAPH (G3MGR/SUBSAV,DE=GA3277,PO=2.5,1.0) ...
      F(LE=7,AX=LOG,NI=5,LO=1.0,PO=0,0,UN=HZ), ...
      MAG4(LO=-75,SC=25,LE=7,NI=8,UN=DB,LI=1)
GRAPH (G3PGR/SUBSAV,DE=GA3277,OV,PO=2.5,1.0) ...
      F(LE=7,AX=LOG,NI=5,LO=1.0,PO=0,7,UN=HZ), ...
      PHAS4(LO=-255,SC=25,LE=7,PO=7,0,UN=DEG,LI=4,NI=8)
GRAPH (G3ZER/SUBSAV,DE=GA3277,PO=2.5,1.0,OV) ...
      F(LE=7,AX=LOG,NI=5,LO=1.0,PO=0,0,UN=HZ), ...
      ZERO(LO=-75,SC=25,LE=7,NI=8,UN=DB,LI=3,AX=OMIT)
LABEL (G3MGR) TOTAL OPEN LOOP TRANSFER FUNCTION - FINE ACTUATOR
LABEL (G3MGR) PHASE MARGIN = 10 DEGREES
GRAPH (G4MGR/SUBSAV,DE=GA3277,PO=2.5,1.0) ...
      F(LE=7,AX=LOG,NI=5,LO=1.0,PO=0,0,UN=HZ), ...
      MAG5(LO=-80,SC=12.5,NI=8,LE=7.0,UN=DB,LI=1)
GRAPH (G4PGR/SUBSAV,DE=GA3277,OV,PO=2.5,1.0) ...
      F(LE=7,AX=LOG,NI=5,LO=1.0,PO=0,7,UN=HZ), ...
      PHAS5(PO=7,0,UN=DEG,LI=4,NI=8,LE=7.0)
LABEL (G4MGR) TOTAL CLOSED LOOP TRANSFER FUNCTION - FINE ACTUATOR
LABEL (G4MGR) PHASE MARGIN = 10 DEGREES
END
STOP
```

APPENDIX B

DSL FREQUENCY DOMAIN PROGRAM FOR THE COARSE ACTUATOR

```
TITLE COARSE SERVO SIMULATION - FREQUENCY RESPONSE - BODE PLOTS
*
*                 DSL PROG. NAME=THFREQC
*
* 2/10/86   18:20
*
*
*
* THIS PROGRAM IS FOR MSEE THESIS WORK AT THE U.A..  THIS PROGRAM
* WILL GENERATE BODE PLOTS (MAGNITUDE AND PHASE) FOR THE COARSE
* ACTUATOR MASTER SERVO.  ONE SET OF PLOTS WILL DISPLAY THE TRANSFER
* FUNCTION OF A CONTINUOUS SERVO.
*
*
* THE FOLLOWING ARE THE DEFINITIONS OF THE CONSTANTS
*
* COARSE ACTUATOR CONSTANTS:
*   MC:    COARSE ACTUATOR'S MASS
*   KFC:   "                " CURRENT TO TORQUE CONSTANT
*   KVC:   "                " MECHANICAL DAMPING CONSTANT
*   KXC:   "                          " SPRING CONSTANT
*   KVCF:  COUPLING MECHANICAL DAMPING CONSTANT (N/M/S)
*   KXCF:  COUPLING SPRING CONSTANT (NEWTONS/METER)
*   KPC:   SERVO ELECTRONIC GAIN(VOLTS/VOLTS)
*   Z1:    DAMPING COEFFICIENT OF THE ACTUATOR'S RESONANCE
*   W1:    NATURAL RESONANT FREQ. (RADIANS)
*   Z2:    DAMPING COEFFICIENT OF THE ACTUATOR'S RESONANCE
*   W2:    NATURAL RESONANT FREQ. (RADIANS)
*  COMPENSATION PARAMETERS:
*   BW:    SERVO BANDWIDTH
*   PM:    SERVO PHASE MARGIN
*   LFIPL: AMOUNT OF ALLOWABLE PHASE LAG FROM THE LOW FREQ. INTEGRATOR
*   FS:    SAMPLE RATE OF THE DIGITAL COMPENSATOR
*   RPM:   DISK RPM IS USED TO DETERMINE THE CRITICAL FREQ. NEEDED
*          IN CALIBRATING THE DIGITAL CONTROLLER GAIN WITH THE ANALOG
*          CONTROLLERS.
*   A0-A1: COEFFICIENTS OF THE DIFFERNCE EQUATION OF THE DIGITAL CONTROL.
*   B0-B2: COEFFICIENTS OF THE DIFFERNCE EQUATION OF THE DIGITAL CONTROL.
*
**********************************************************************
INITIAL SEGMENT
*
COMPLEX S,Z,WT,G1,G2,G3,G4,G5,G6,GWT
```

```
*
METHOD RKSFX
CONTRL FINTIM=6.0,DELT=2.0D-3
*
FIXED  FGAIN,FPAS,FPI,FPL,FGM
*
INCON  FGAIN=0,FPAS=0,KPC=2.9,FPI=0,FPL=0,FGM=0
*
CONST  KFC=7.5,MC=0.2,KVC=1.8,KXC=0.0,MF=0.003, ...
       KAPS=2.5D4,Z1=0.02,Z2=0.02,W1=13823.0,W2=12566.0, ...
       RPM=3000.0,FS=6.0D4,BW=300,PM=10,LFIPL=5,ZERO=0.0
*
      MT=MC+MF
*
*
*  CALCULATE THE POLE-ZERO LOCATIONS FOR THE ELECTRONIC COMPENSATION.
*
*
*     ANALOG COMPENSATION:
      IF(FPAS.EQ.1.AND.FGAIN.EQ.0) THEN
        WI=2.0*PI*BW*DTAN(PI*LFIPL/180.0)
        PL=PI*(PM-180-ASP+LFIPL)/180.0
        PLDEG=180.0*PL/PI
        GAMA=(1.0-DSIN(PL))/(1.0+DSIN(PL))
        WP=2.0*PI*BW/DSQRT(GAMA)
        WZ=GAMA*WP
      ENDIF
*
*
*
*
*
*
*     DIGITAL COMPENSATION:
      IF(FGAIN.EQ.1) THEN
*  DEFINE THE SAMPLING PERIOD
        T=1.0/FS
*
*  DEFINE CRITICAL FREQUENCY USED TO CALIBRATE THE GAIN OF THE MAPPED
*  Z TRANSFER FUNCTION
        WC=2.0*PI*RPM/60.0
*
*  MAPPED POLE-ZEROS
        ZI=DEXP(-WI*T)
        ZZ=DEXP(-WZ*T)
        ZP=DEXP(-WP*T)
*
*  DETERMINE THE GAIN OF THE Z-MAPPED TRANSFER FUNCTION
        S=CMPLX(0.0,WC)
        GCL=GAIN(KPC*WP*(S+WI)*(S+WZ)/(WZ*S*(S+WP)))
```

```
        GC=10.0**GCL
        Z=CEXP(S*T)
        GZPL=GAIN((Z-ZI)*(Z-ZZ)/((Z-1.0)*(Z-ZP)))
        GZP=10.0**GZPL
        ALPHA=GC/GZP
*
*  DETERMINE THE COEFFICIENTS IN THE DIFFERENCE EQUATION
        A0=1.0+ZP
        A1=-ZP
        B0=ALPHA
        B1=-ALPHA*(ZI+ZZ)
        B2=ALPHA*ZI*ZZ
*
*       CALL PRINT
      ENDIF
*
*************************************************************************************
*************************************************************************************
*
DYNAMIC SEGMENT
*
      W=10.0**TIME
      F=W/(2.0*PI)
      S=CMPLX(0.0,W)
* COARSE ACTUATOR AND SENSOR
      G1=KAPS*KFC*(W2**2)*(S**2+2*Z1*W1*S+W1**2)/ ...
         ((MT*S**2+KVC*S+KXC)*(W1**2)*(S**2+2*Z2*W2*S+W2**2))
      MAG1=20.0*GAIN(G1)
      PHAS1=RADEG*PHASE(0.0,G1)
* SERVO CARD = PHASE LEAD AND PI COMPENSATION
      IF(FPAS.EQ.1) THEN
        G2=WP*(S+WI)*(S+WZ)/(WZ*S*(S+WP))
        MAG2=20.0*GAIN(G2)
        PHAS2=RADEG*PHASE(0.0,G2)
* SERVO CARD PLUS POWER AMP
        G3=KPC*G2
        MAG3=20.0*GAIN(G3)
        PHAS3=RADEG*PHASE(0.0,G3)
* USE THE W-TRANSFORM TO GENERATE THE DIGITAL COMPENSATOR FREQ RESPONSE
* FOR COMPARISON TO THE ANALOG COMPENSATOR.
*       WT=CMPLX(0.0,W)
*       Z=(1.0+WT*T/2.0)/(1.0-WT*T/2.0)
*       GWT=ALPHA*(Z-ZI)*(Z-ZZ)/((Z-1.0)*(Z-ZP))
*       IF(GWT.NE.0.0) THEN
*         MAGWT=20.0*GAIN(GWT)
*         PHASWT=RADEG*PHASE(0.0,GWT)
*       ENDIF
* TOTAL OPEN LOOP TRANSFER FUNCTION
        G4=G1*G3
        MAG4=20.0*GAIN(G4)
```

```
          PHAS4=RADEG*PHASE(0.0,G4)
          PHAS4C=PHAS4-360.0
          IF(FGAIN.EQ.1.AND.FPL.EQ.0.AND.F.GE.BW) THEN
            FPL=1
*           CALL PRINT
          ENDIF
          IF(FGAIN.EQ.1.AND.F.GE.BW.AND.FGM.EQ.0.AND.PHAS4C.LE.-180) THEN
            FGM=1
            GM=-MAG4
          ENDIF
* TOTAL CLOSED LOOP TRANSFER FUNCTION
          G5=G4/(1+G4)
          MAG5=20.0*GAIN(G5)
          PHAS5=RADEG*PHASE(0.0,G5)
* LOW FREQ. INTEGRATOR
          G6=(S+WI)/S
          MAG6=20.0*GAIN(G6)
          PHAS6=RADEG*PHASE(0.0,G6)
          IF(FGAIN.EQ.1.AND.FPI.EQ.0.AND.W.GE.WI) THEN
            FPI=1
*           CALL PRINT
          ENDIF
        ENDIF
*
        IF(FPAS.EQ.0.AND.F.GE.BW) CALL ENDRUN
        IF(FPAS.EQ.1.AND.FGAIN.EQ.0.AND.MAG4.LE.0.0) CALL ENDRUN
*************************************************************************
*************************************************************************
*
TERMINAL SEGMENT
*
        IF(FGAIN.EQ.1) CALL PRINT
*
*
*       DETERMINE THE ACTUATOR AND SENSOR PHASE AT THE DESIRED SERVO BW
        IF(FPAS.EQ.0) THEN
          FPAS=1
          ASP=PHAS1
          CALL RERUN
          GO TO 10
        ENDIF
*
*
        IF(FPAS.EQ.1.AND.FGAIN.EQ.0) THEN
          IF(F.GE.BW) THEN
            FGAIN=1
            DELPLT=2.0D-3
*           DELPRT=3.0D-2
          ELSE
            KPC=KPC+0.01
```

```
        ENDIF
        CALL RERUN
      ENDIF
*
10    CONTINUE
*
PAGE (50)
DIGITS 8
*RINT F,MAG1,PHAS1,MAG3,PHAS3,MAG4,PHAS4,PHAS4C,MAG5,PHAS5,MAG6,PHAS6
*RINT BW,PM,GM,LFIPL,PLDEG,FS,RPM,KPC,WI,WZ,WP,A0,A1,B0,B1,B2
PRINT FS,A0,A1,B0,B1,B2,PM,KPC,WI,WZ,WP
*
*
SAVE  (SUBSAV) F,W,MAG1,PHAS1,MAG3,PHAS3,MAG4,PHAS4C,MAG5,PHAS5,ZERO
*
FIXED  FGAIN,FPAS,FPI,FPL,FGM
SAVE (SUBSAV) F,W,MAG1,PHAS1,MAG3,PHAS3,MAG4,PHAS4C,MAG5,PHAS5,ZERO
GRAPH (G1MGR/SUBSAV,DE=GA3277,PO=2.5,1.0) ...
      F(LE=7,AX=LOG,NI=5,LO=1.0,PO=0,0,UN=HZ), ...
      MAG1(LE=7,LO=-100,SC=25,NI=8,UN=DB,LI=1)
GRAPH (G1PGR/SUBSAV,DE=GA3277,OV,PO=2.5,1.0) ...
      F(LE=7,AX=LOG,NI=5,LO=1.0,PO=0,7,UN=HZ), ...
      PHAS1(LE=7,LO=-360,SC=45,NI=8,PO=7,UN=DEG,LI=4)
LABEL (G1MGR) COARSE ACTUATOR AND SENSOR
GRAPH (G2MGR/SUBSAV,DE=GA3277,PO=2.5,1.0) ...
      F(LE=7,AX=LOG,NI=5,LO=1.0,PO=0,0,UN=HZ), ...
      MAG3(LO=8,SC=4.5,LE=7,NI=8,UN=DB,LI=1)
GRAPH (G2PGR/SUBSAV,DE=GA3277,OV,PO=2.5,1.0) ...
      F(LE=7,AX=LOG,NI=5,LO=1.0,PO=0,7,UN=HZ), ...
      PHAS3(LE=7,PO=7,0,UN=DEG,LI=4,NI=8)
LABEL (G2MGR) ANALOG COMPENSATION
LABEL (G2MGR) PHASE MARGIN = 10 DEGREES
GRAPH (G3MGR/SUBSAV,DE=GA3277,PO=2.5,1.0) ...
      F(LE=7,AX=LOG,NI=5,LO=1.0,PO=0,0,UN=HZ), ...
      MAG4(LO=-100,SC=28,LE=7,NI=8,UN=DB,LI=1)
GRAPH (G3PGR/SUBSAV,DE=GA3277,OV,PO=2.5,1.0) ...
      F(LE=7,AX=LOG,NI=5,LO=1.0,PO=0,7,UN=HZ), ...
      PHAS4C(LO=-270,SC=25,LE=7,PO=7,0,UN=DEG,LI=4,NI=8)
GRAPH (G3ZER/SUBSAV,DE=GA3277,PO=2.5,1.0,OV) ...
      F(LE=7,AX=LOG,NI=5,LO=1.0,PO=0,0,UN=HZ), ...
      ZERO(LO=-100,SC=28,LE=7,NI=8,UN=DB,LI=3,AX=OMIT)
LABEL (G3MGR) TOTAL OPEN LOOP TRANSFER FUNCTION - COARSE ACTUATOR
LABEL (G3MGR) PHASE MARGIN = 10 DEGREES
GRAPH (G4MGR/SUBSAV,DE=GA3277,PO=2.5,1.0) ...
      F(LE=7,AX=LOG,NI=5,LO=1.0,PO=0,0,UN=HZ), ...
      MAG5(LO=-100,SC=15,NI=8,LE=7.0,UN=DB,LI=1)
GRAPH (G4PGR/SUBSAV,DE=GA3277,OV,PO=2.5,1.0) ...
      F(LE=7,AX=LOG,NI=5,LO=1.0,PO=0,7,UN=HZ), ...
      PHAS5(PO=7,0,UN=DEG,LI=4,NI=8,LE=7.0)
LABEL (G4MGR) TOTAL CLOSED LOOP TRANSFER FUNCTION - COARSE ACTUATOR
```

```
LABEL (G4MGR) PHASE MARGIN = 10 DEGREES
END
STOP
```

APPENDIX C

DSL TIME DOMAIN PROGRAM

```
TITLE MSEE THESIS DIGITAL SERVO   -  DSL TIME DOMAIN MODEL
*
* 2/15/86   14:51
*
*                  DSL PROGRAM NAME = THTIM1
*
* THIS PROGRAM WILL SIMULATE THE MASTER/SLAVE SERVO USED TO CONTROL THE
* VOICE COIL ACTUATORS.
*
* THE FOLLOWING ARE THE DEFINITIONS OF THE CONSTANTS
*
*
* COARSE ACTUATOR CONSTANTS:
*   MC:    MASS (KG)
*   KFC:   CURRENT TO TORQUE CONSTANT (NT/AMP)
*   KVC:   MECHANICAL DAMPING CONSTANT (NT/M/SEC)
*   KXC:   SPRING CONSTANT (NT)
*   MUC:   COEFFICIENT OF KINETIC FRICTION
*   G:     ACCELLERATION DUE TO GRAVITY
*   ACPOS: POSTION - ANALOG SERVO
*   ACVEL: VELOCITY - ANALOG SERVO
*   ACACC: ACCELLERATION - ANALOG SERVO
*   DCPOS: POSTION - DIGITAL SERVO
*   DCVEL: VELOCITY - DIGITAL SERVO
*   DCACC: ACCELLERATION - DIGITAL SERVO
*   C( ):  NUMERATOR OF THE FINE ACTUATOR'S MECHANICAL RESONANCE
*   D( ):  DENOMINATOR OF THE FINE ACTUATOR'S MECHANICAL RESONANCE
*
*
*
* FINE ACTUATOR CONSTANTS:
*   MF:    MASS (KG)
*   KFF:   CURRENT TO TORQUE CONSTANT (NT/AMP)
*   KXCF:  SPRING CONSTANT BETWEEN THE COARSE AND FINE ACTUATORS (NT/M)
*   KVCF:  VELOCITY"                                          "(NT/M/SEC)
*   MUF:   COEFFICIENT OF KINETIC FRICTION
*   G:     ACCELLERATION DUE TO GRAVITY
*   AFPOS: POSTION - ANALOG SERVO
*   AFVEL: VELOCITY - ANALOG SERVO
*   AFACC: ACCELLERATION - ANALOG SERVO
*   DFPOS: POSTION - DIGITAL SERVO
*   DFVEL: VELOCITY - DIGITAL SERVO
*   DFACC: ACCELLERATION - DIGITAL SERVO
```

```
*   E( ):  NUMERATOR OF THE COARSE ACTUATOR'S MECHANICAL RESONANCE
*   F( ):  DENOMINATOR OF THE COARSE ACTUATOR'S MECHANICAL RESONANCE
*
*
* DIGITAL CONTROLLER CONSTANTS:
*   FS:    SAMPLE FREQUENCY (HZ)
*   CDELAY: DIGITAL CONTROLLER COMPUTATION DELAY (SEC)
*   BITS:  NUMBER OF BITS IN THE DAC/ADC
*   VSPP:  PEAK TO PEAK VOLTAGE INPUT LEVEL INTO THE ADC
*   MAXCOF: LARGEST COEFFICIENT OF THE DIFFERENCE EQUATION SO THAT
*          THE QUANTIZATION OF THE COEFFICIENTS CAN BE PERFORMED.
*   A( ):  COEFFICIENTS IN THE COMPENSATOR DIFFERENCE EQUATION
*   B( ):  "                                                  "
*   R( ):  COMPENSATOR HISTORY
*   U( ):  "                  "
*   J( ):  COEFFICIENTS IN THE COMPENSATOR DIFFERENCE EQUATION
*   H( ):  "                                                  "
*   X( ):  COMPENSATOR HISTORY
*   Y( ):  "                  "
*   QCOMPF:QUANTIZATION LEVEL FOR THE FINE ACTUATOR'S DIGITAL
*          COMPENSATION.  DERIVED BY OBSERVING THE AMPLITUDE OF THE
*          I/O ON THE ANALOG COMP.
*   QCOMPC:QUANTIZATION LEVEL FOR THE COARSE ACTUATOR'S DIGITAL
*          COMPENSATION.  DERIVED BY OBSERVING THE AMPLITUDE OF THE
*          I/O ON THE ANALOG COMP.
*   QCOEFF:QUANTIZATION OF THE COEFFICIENTS IN THE FINE DIGITAL
*          COMPENSATOR'S DIFFERENCE EQUATION.
*   QCOEFC:QUANTIZATION OF THE COEFFICIENTS IN THE COARSE DIGITAL
*          COMPENSATOR'S DIFFERENCE EQUATION.
*
*
* FLAGS:
*   FDOUT: USED IN PROGRAMMING THE DIGITAL CONTROLLER COMPUTATION
*          DELAY. FDOUT=1 MEANS TO OUTPUT CONTROL SIGNAL.
*          FDOUT=0 MEANS TO CALCULATE THE CONTROL SIGNAL.
*
*
*****************************************************************************
*
*
*
*
*
INITIAL SEGMENT
*
*
*
*
*
```

```
*
FIXED   FDOUT,BITS,NUMFS, ...
        NUMFS,FSCONT,FSCOMP, ...
        NUMDEL,DECONT,DECOMP, ...
        NUMBIT,BTCONT,BTCOMP,BITTAB
*
CONST   KFC=7.5,MC=0.2,KVC=1.8,KXC=0.0,MUCS=0.0,MUCK=0.0, ...
        G=9.806,LVH=12.5,LVL=-12.5,RC=6.0,LC=3.0D-3, ...
        KPC=2.93,WCI=164.91,WCZ=1452.5,WCP=2446.1, ...
        KQ=1.5D6,KFF=0.3,MF=0.003,KVCF=0.3, ...
        KXCF=193.0,MUF=0.0,RF=10.0,LF=2.0D-4, ...
        KPF=1.27,WFI=1374.3,WFZ=12128.1,WFP=20344.5, ...
        KAPS=2.5D4,TRPICH=2.0D-6, ...
        KAMP=1.0D3,ULMVAC=3.5D1,LLMVAC=-3.5D1,RSC=1.0, ...
        RSF=1.0,ULMVAF=1.25D1,LLMVAF=-1.25D1,RADRUN=50.0, ...
        VSPP=5.0,MAXCOF,7.5, ...
        NUMFS=1,NUMDEL=1,NUMBIT=4, ...
        FQVOLT=2.0D-1,CQVOLT=7.0D-1
*
INCON   DCOMPT=0.0,DPOERL=0.0,FDOUT=0, ...
        FSCONT=1,FSCOMP=0, ...
        DECONT=0,DECOMP=0, ...
        BTCONT=1,BTCOMP=0
*
ARRAY   A(2),B(3),C(3),D(3),E(3),F(3),R(2),U(2),J(2),H(3),X(2),Y(2), ...
        FSTAB(1),DELTAB(5),BITTAB(6)
TABLE   A(1-2)=1.7124285,-0.71242853, ...
        B(1-3)=2.0184915,-3.6218616,1.6117352, ...
        J(1-2)=1.9600518,-0.96005176, ...
        H(1-3)=4.9003688,-9.6700780,4.7700309, ...
        C(1-3)=1.0,4523.88,1.279D10,D(1-3)=1.0,4272.56,1.141D10, ...
        E(1-3)=1.0,553.0,1.91D8,F(1-3)=1.0,503.0,1.579D8, ...
        R(1-2)=2*0.0,U(1-2)=2*0.0, ...
        X(1-2)=2*0.0,Y(1-2)=2*0.0, ...
        FSTAB(1)=6.0D4, ...
        DELTAB(1-5)=1.0D-9,4.0D-6,12.0D-6,24.0D-6,36.0D-6, ...
        BITTAB(1-6)=17,16,12,8,1,1
*
*
METHOD RKSFX
       DELT=2.0D-7
       FINTIM=6.0D-2
*
*
* INITIALIZE FOR THE FIRST RUN HERE.  THE INITIALIZATION FOR SUBSEQUENT
* RUNS IS PERFORMED IN THE TERMINAL SECTION.
       IF(KSIM.EQ.1) THEN
         IF(NUMFS.EQ.1) CALL ENDRUN
         FS=FSTAB(1)
         CDELAY=DELTAB(1)
```

```
        BITS=BITTAB(1)
      ENDIF
*
*
*
*
*
* ASSIGN VARIABLE VALUES FOR THE TIME RESPONSE RUN
*
*
*
* TOTAL MASS SUPPORTED BE THE COARSE ACTUATOR SERVO
      MT=MC+MF
* ACTUATOR BEMF CONSTANTS
      KBEMFC=KFC
      KBEMFF=KFF
* ACTUATOR TIME CONSTANTS
      TC=LC/(RC+RSC)
      TF=LF/(RF+RSF)
*
*
      W=2.0*PI*RADRUN
*
* DEFINE QUANTIZATION LEVELS:
*   FINE'S A/D, DIFFERENCE EQUATION, D/A CONVERTER
      QCOMPF=FQVOLT/(2.0**BITS)
*   FINE'S COEFFICIENTS
      QCOEFF=2.0*3.6218616/(2.0**BITS)
*   COARSE'S A/D, DIFFERENCE EQUATION, D/A CONVERTER
      QCOMPC=CQVOLT/(2.0**BITS)
*   COARSE'S COEFFICIENTS
      QCOEFC=2.0*9.6700780/(2.0**BITS)
*
*
      CALL PRINT
      DELS=1.0/FS
*
*
*****************************************************************************
*****************************************************************************
*
*
*
*
*
DERIVATIVE SEGMENT
*
*
*
*
```

```
* MASTER ACTUATOR ELECTRONICS FOR THE ANALOG SERVO
*
*
*
*
* DEFINE THE TRACK CHARACTERISTICS
* RADIAL RUNOUT SIGNAL
      F1=75.0D-6*SIN(W*TIME)
      F2=10.0D-6*SIN(2.*W*TIME)
      F3=1.0D-6*SIN(3.*W*TIME)
      F4=5.0D-7*SIN(4.*W*TIME)
      F5=1.0D-7*SIN(5.*W*TIME)
      F6=5.0D-8*SIN(6.*W*TIME)
      F7=8.0D-8*SIN(7.*W*TIME)
      F8=4.0D-8*SIN(8.*W*TIME)
      F9=1.0D-8*SIN(9.*W*TIME)
      F10=5.0D-9*SIN(10.*W*TIME)
      POSD=F1+F2+F3+F4+F5+F6+F7+F8+F9+F10
*
*
* DEFINE THE EQUATIONS FOR THE ELECTRONICS:
*
* POSITIONAL ERROR SIGNAL
      POSERF=KQ*(POSD-AFPOSR)
* ELECTRONIC COMPENSATION - ANALOG VERSION
      COMP1=ZEROPL(0.0,WFI,0.0,POSERF)
      COMP2=ZEROPL(0.0,WFZ,WFP,WFP*COMP1/WFZ)
      COMPT=KPF*RSF*COMP2
* POWER AMPLIFIER MODEL
      VERFM2=COMPT-IMF*RSF
      VERFA2=KAMP*VERFM2
      VBKFM2=KBEMFF*AVERER
      IMFP=(VERFA2+VBKFM2)/(RF+RSF)
      IMF=REALPL(0.0,TF,IMFP)
*
*
*
*
*
*
* SLAVE ACTUATOR ELECTRONICS
*
*
*
* RELATIVE POSITION SENSOR
      V1C=-KAPS*APORER
* ANALOG COMPENSATION
      CV1C=ZEROPL(0.0,WCI,0.0,V1C)
      CV2C=ZEROPL(0.0,WCZ,WCP,WCP*CV1C/WCZ)
```

```
      VSC=KPC*RSC*CV2C
*
* CURRENT AMP
      VERRCS=VSC-ISC*RSC
      VERCAS=KAMP*VERRCS
      VBAKCS=KBEMFC*ACVEL
      ISCP=(VERCAS-VBAKCS)/(RC+RSC)
      ISC=REALPL(0.0,TC,ISCP)
*
* EQUATIONS OF MOTION
*
*
*
*
*  FIRST DEFINE THE EQUATIONS FOR THE ANALOG SERVO.
*
*
* MECHANICAL EQUATIONS OF MOTION FOR THE COARSE ACTUATOR
      ACACC=(1/MT)*(KFC*ISC-KFF*IMF-KVC*ACVEL-KXC*ACPOSR ...
          -KXCF*APORER-KVCF*AVERER)
      ACVEL=INTGRL(0.0,ACACC)
      ACPOS=INTGRL(0.0,ACVEL)
      ACPOSR=TRNFR(2,2,0.0,E,F,F(3)*ACPOS/E(3))
*
* MECHANICAL EQUATIONS OF MOTION FOR THE FINE ACTUATOR
      AFACC=(1/MF)*(KFF*IMF+KVCF*AVERER+KXCF*APORER)
      AFVEL=INTGRL(0.0,AFACC)
      AFPOS=INTGRL(0.0,AFVEL)
      AFPOSR=TRNFR(2,2,0.0,C,D,D(3)*AFPOS/C(3))
*
* DEFINE PHYSICAL RELATIVE ERRORS BETWEEN ACTUATORS.
      APORER=ACPOSR-AFPOSR
      AVERER=ACVEL-AFVEL
      AACRER=ACACC-AFACC
*
*
*
*
*
*
*
*
*  SECONDLY -  DEFINE THE EQUATIONS FOR THE DIGITAL SERVO.
*
*
*
* RADIAL RUNOUT SIGNAL IS THE SAME AS THE ANALOG SERVO USES.
*
* DEFINE THE TRACKING ERROR SENSOR SIGNAL
      DPOSER=KQ*(POSD-DFPOSR)
```

```
      QFEV16=QNTZR(FQVOLT/(2.**16),DPOSER)
      QFEV14=QNTZR(FQVOLT/(2.**14),DPOSER)
      QFEV12=QNTZR(FQVOLT/(2.**12),DPOSER)
      QFEV10=QNTZR(FQVOLT/(2.**10),DPOSER)
      QFEV8=QNTZR(FQVOLT/(2.**8),DPOSER)
*
*  THE DIGITAL CONTROLLER WILL USE DPOSER AS THE INPUT
*  THE DIGITAL CONTROLLER'S OUTPUT IS DCOMPT
*
* CURRENT AMP
      DERFM2=DCOMPT-DIMF*RSF
      DERFA2=KAMP*DERFM2
      DBKFM2=KBEMFF*DVERER
      DIMFP=(DERFA2+DBKFM2)/(RF+RSF)
      DIMF=REALPL(0.0,TF,DIMFP)
*
*
*  SLAVE ACTUATOR ELECTRONICS
*
* DEFINE THE RELATIVE POSITIONAL ERROR SIGNAL
      DV1C=-KAPS*DPORER
      QCEV16=QNTZR(CQVOLT/(2.**16),DV1C)
      QCEV14=QNTZR(CQVOLT/(2.**14),DV1C)
      QCEV12=QNTZR(CQVOLT/(2.**12),DV1C)
      QCEV10=QNTZR(CQVOLT/(2.**10),DV1C)
      QCEV8=QNTZR(CQVOLT/(2.**8),DV1C)
*
*  THE DIGITAL CONTROLLER WILL USE DV1C AS THE INPUT
*  THE DIGITAL CONTROLLER'S OUTPUT IS DVSC
*
* CURRENT AMP
      DVRRCS=DVSC-DISC*RSC
      DVRCAS=KAMP*DVRRCS
      DVBKCS=KBEMFC*DCVEL
      DISCP=(DVRCAS-DVBKCS)/(RC+RSC)
      DISC=REALPL(0.0,TC,DISCP)
*
*
*
* MECHANICAL EQUATIONS OF MOTION FOR THE COARSE ACTUATOR
      DCACC=(1/MT)*(KFC*DISC-KFF*DIMF-KVC*DCVEL-KXC*DCPOS ...
          -KXCF*DPORER-KVCF*DVERER)
      DCVEL=INTGRL(0.0,DCACC)
      DCPOS=INTGRL(0.0,DCVEL)
      DCPOSR=TRNFR(2,2,0.0,E,F,F(3)*DCPOS/E(3))
*
* MECHANICAL EQUATIONS OF MOTION FOR THE FINE ACTUATOR
      DFACC=(1/MF)*(KFF*DIMF+KVCF*DVERER+KXCF*DPORER)
      DFVEL=INTGRL(0.0,DFACC)
      DFPOS=INTGRL(0.0,DFVEL)
```

```
      DFPOSR=TRNFR(2,2,0.0,C,D,D(3)*DFPOS/C(3))
*
* DEFINE PHYSICAL RELATIVE ERRORS BETWEEN ACTUATORS.
      DPORER=DCPOSR-DFPOSR
      DVERER=DCVEL-DFVEL
      DACRER=DCACC-DFACC
*************************************************************************************
*************************************************************************************
*
*
*
*
SAMPLE SEGMENT
*
*
*
*
*  THE SAMPLING SEGMENT IS USED FOR THE DIGITAL SERVO.
* THIS SEGMENT IS ENTERED UPON EACH DIGITAL SERVO SAMPLING INSTANT.
* EACH SENSORS OUTPUT VOLTAGE IS SAMPLED AND A CONTROL SIGNAL IS THEN
* GENERATED AS A FUNCTION OF THE POLE-ZERO LOCATIONS OF THE PARTICULAR
* COMPENSATOR.  THIS SEGMENT IS THEN EXITED AND REENTERED AFTER A
* PREPROGRAMED AMOUNT OF TIME WHICH IS REPRESENTATIVE OF TYPICAL
* DELAYS ENCOUNTERED IN HARDWARE IMPLIMENTATION.
* THIS WILL BE WHEN THE PRECALCULATED CONTROL SIGNAL WILL BE INPUTTED
* TO THE PLANT.
*
*
* DETERMINE IF THIS SAMPLE TIME IS FOR THE CONTROL SIGNAL CALCULATION
* OR THE OUTPUT OF THE CONTROL SIGNAL.
      IF(FDOUT.EQ.0) THEN
* MODEL THE QUANTIZATIONS
*    ADCS
        QDPOSR=QNTZR(QCOMPF,DPOSER)
        QDV1C=QNTZR(QCOMPC,DV1C)
*    COEFFICIENTS
        QA1=QNTZR(QCOEFF,A(1))
        QA2=QNTZR(QCOEFF,A(2))
        QB1=QNTZR(QCOEFF,B(1))
        QB2=QNTZR(QCOEFF,B(2))
        QB3=QNTZR(QCOEFF,B(3))
        QJ1=QNTZR(QCOEFC,J(1))
        QJ2=QNTZR(QCOEFC,J(2))
        QH1=QNTZR(QCOEFC,H(1))
        QH2=QNTZR(QCOEFC,H(2))
        QH3=QNTZR(QCOEFC,H(3))
* CALULATE THE CONTROL SIGNALS:
*   FINE CIMPENSATION
        PCOMPT=QNTZR(QCOMPF,QA1*R(1)+QA2*R(2)+ ...
               QB1*QDPOSR+QB2*U(1)+QB3*U(2))
```

```
        R(2)=R(1)
        R(1)=PCOMPT
        U(2)=U(1)
        U(1)=QDPOSR
*   COARSE CIMPENSATION
        PDVSC=QNTZR(QCOMPC,QJ1*Y(1)+QJ2*Y(2)+ ...
              QH1*QDV1C+QH2*X(1)+QH3*X(2))
        Y(2)=Y(1)
        Y(1)=PDVSC
        X(2)=X(1)
        X(1)=QDV1C
        DELS=CDELAY
        FDOUT=1
      ELSE
        DCOMPT=PCOMPT
        DVSC=PDVSC
        DELS=1.0/FS-CDELAY
        FDOUT=0
      ENDIF
*****************************************************************************
*****************************************************************************
*
*
*
*
*
DYNAMIC SEGMENT
*
*
*
*
*
*
*
*
*
*
*
*
* DEFINE ERROR VALUES
*
*
      APOERR=(ACPOSR-AFPOSR)/TRPICH
      ADEERR=(POSD-AFPOSR)/TRPICH
*
*
      DPOERR=(DCPOSR-DFPOSR)/TRPICH
      DDEERR=(POSD-DFPOSR)/TRPICH
*
*****************************************************************************
```

```
**************************************************************************
*
TERMINAL SEGMENT
*
      CALL PRINT
*
*  PERFORM RUNS WITH DIFFERENT SAMPLING FREQUENCIES:
      IF(FSCOMP.EQ.0) THEN
        IF(NUMFS.EQ.1) THEN
          FSCOMP=1
          GO TO 20
        ENDIF
        FSCONT=FSCONT+1
        FS=FSTAB(FSCONT)
        IF(FSCONT.EQ.NUMFS) FSCOMP=1
        CALL RERUN
        GO TO 10
      ENDIF
*
*  PERFORM RUNS WITH DIFFERENT AMOUNTS OF COMPUTATION DELAYS:
20    IF(DECOMP.EQ.0) THEN
        IF(NUMDEL.EQ.1) THEN
          DECOMP=1
          GO TO 30
        ENDIF
        DECONT=DECONT+1
        CDELAY=DELTAB(DECONT)
        IF(DECONT.EQ.NUMDEL) DECOMP=1
        CALL RERUN
        GO TO 10
      ENDIF
*
*  PERFORM RUNS WITH DIFFERENT NUMBER OF BITS:
30    IF(BTCOMP.EQ.0) THEN
        IF(NUMBIT.EQ.1) THEN
          BTCOMP=1
          GO TO 10
        ENDIF
        CDELAY=DELTAB(1)
        BTCONT=BTCONT+1
        BITS=BITTAB(BTCONT)
        IF(BTCONT.EQ.NUMBIT) BTCOMP=1
        CALL RERUN
        GO TO 10
      ENDIF
*
10      DCOMPT=0.0
        DPOERL=0.0
        DV1CL=0.0
        DVSC=0.0
```

```
        FDOUT=0
        R(1)=0.0
        R(2)=0.0
        U(1)=0.0
        U(2)=0.0
        X(1)=0.0
        X(2)=0.0
        Y(1)=0.0
        Y(2)=0.0
*
PAGE (50)
*RINT 5.0D-5,ADEERR,DDEERR,APOERR,DPOERR
*RINT 5.0D-5,QA1,QA2,QB1,QB2,QB3,QJ1,QJ2,QH1,QH2,QH3
*RINT BITS,QCOMPF,QCOEFF,QCOMPC,QCOEFC
*RINT 4.0D-5,DPOERL,DCOMPT,DIMF,DFACC,DFVEL,DFPOSR
PRINT FS,CDELAY,BITS
*
SAVE (S1) 5.0D-5,ADEERR,APOERR
*AVE (S2) 5.0D-5,POSERF,COMPT
*AVE (S3) 5.0D-5,V1C,VSC
SAVE (S4) 5.0D-5,DDEERR,DPOERR
*AVE (S5) 1.0D-4,DPOSER,DCOMPT
*AVE (S6) 1.0D-4,DV1C,DVSC
*AVE (S7) 1.0D-12,QFEV16,QFEV14,QFEV12,QFEV10,QFEV8, ...
*                 QCEV16,QCEV14,QCEV12,QCEV10,QCEV8
GRAPH (GXA/S1,DE=IBM3279,PO=2.5,1,RU=2) ...
      TIME(LO=0.0,SC=0.006,NI=10,LE=7,UN=SEC), ...
      APOERR(LO=-50,SC=10,UN=TRACKS,NI=10,LI=11,LE=7)
GRAPH (GXB/S4,DE=IBM3279,PO=2.5,1,RU=2,OV) ...
      TIME(LO=0.0,SC=0.006,NI=10,LE=7,UN=SEC), ...
      DPOERR(LO=-50,SC=10,UN=TRACKS,NI=10,LI=21,LE=7,PO=7,0)
GRAPH (GXC/S4,DE=IBM3279,PO=2.5,1,RU=3,OV) ...
      TIME(LO=0.0,SC=0.006,NI=10,LE=7,UN=SEC), ...
      DPOERR(LO=-50,SC=10,UN=TRACKS,NI=10,LI=31,LE=7,AX=OMIT)
LABEL (GXA) POSITIONAL ERROR BETWEEN THE FINE AND THE COARSE ACTUATORS.
LABEL (GXA) 10 DEGREE PHASE MARGIN.  BITS=ANALOG,16,12.   FS=60KHZ
GRAPH (G0A/S1,DE=IBM3279,PO=2.5,1,RU=2) ...
      TIME(LO=0.0,SC=0.006,NI=10,LE=7,UN=SEC), ...
      ADEERR(LO=-2,SC=0.4,UN=TRACKS,NI=10,LI=11,LE=7)
GRAPH (G0B/S4,DE=IBM3279,PO=2.5,1,RU=2,OV) ...
      TIME(LO=0.0,SC=0.006,NI=10,LE=7,UN=SEC), ...
      DDEERR(LO=-2,SC=0.4,UN=TRACKS,NI=10,LI=21,LE=7,PO=7,0)
GRAPH (G0C/S4,DE=IBM3279,PO=2.5,1,RU=3,OV) ...
      TIME(LO=0.0,SC=0.006,NI=10,LE=7,UN=SEC), ...
      DDEERR(LO=-2,SC=0.4,UN=TRACKS,NI=10,LI=31,LE=7,AX=OMIT)
LABEL (G0A) POSITIONAL ERROR BETWEEN THE FINE ACTUATOR AND THE TRACK.
LABEL (G0A) 10 DEGREE PHASE MARGIN.  BITS=ANALOG,16,12.  FS=60KHZ
END
STOP
```

LIST OF REFERENCES

1. Bartolina, R. "High Density Optical Recording Using Laser Diodes," RCA Engineer, pp. 20-27, May/June 1982.
2. Laub, L. "Optics of Reflective Video Disks," IEEE Transactions on Consumer Electronics, pp. 258-265, August 1976.
3. Bell, A. "Optical Data Storage Technology Status and Prospects," Computer Design, pp. 133-146, January 1983.
4. Meng, B. "Optical Disks Slip on Compatibility," Digital Design, pp. 28-37, January 1986.
5. Ohr, S. "Magneto-Optics Combines Erasability and High-Density Storage,"Electronic Design, pp. 93-100, July 1985.
6. IBM. Dynamic Simulation Language Reference Manual, San Jose, California: IBM, 1984.
7. Ogata, K. Modern Control Engineering. New Jersy: Prentice-Hall, 1970.
8. Franklin, G., and Powell, D. Digital Control of Dynamic Systems. Massachusetts: Addison-Wesley, 1981.